Unsaturated Zone Hydrology for Scientists and Engineers

James A. Tindall, Ph.D.

United States Geological Survey, National Research Program
Department of Geography and Environmental Sciences, University of Colorado Denver

James R. Kunkel, Ph.D., P.E.

Knight Piésold, LLC, Denver, Colorado;
Department of Geology and Geological Engineering, Colorado School of Mines

with

Dean E. Anderson, Ph.D.

United States Geological Survey, National Research Program

PRENTICE HALL
Upper Saddle River, New Jersey 07458

10

Contaminant Transport

INTRODUCTION

Numerous environmental management problems involve the transport and reactions of dissolved chemicals that are either native to the soil, added deliberately to the soil surface, or are accidentally spilled. The design of optimum application rates and application timing of fertilizer, domestic waste (sewage sludge), wastewater irrigation, herbicide, and low-level radioactive waste (disposal) depends on methodologies that maximize the degradation or retention of these chemicals within the unsaturated zone, while minimizing their mobility. Increased public awareness of the contamination of ground water by agricultural, industrial, and municipal chemicals (Pye, Patrick, and Quarles 1983) has focused considerable attention on solute transport, creating a heightened awareness and increased research in this area (Van Genuchten and Jury, 1987).

Transport of chemicals through the unsaturated zone depends on many factors: ion exclusion; ion exchange; volatilization; dissolution and precipitation; chemical and biological transformation; biodegradation; adsorption; diffusion; dispersion and volumetric water content; unsaturated hydraulic conductivity; and the matric potential of the medium (see figure 10.1). The investigation of transport through the unsaturated zone evolved primarily within the domain of soil science (i.e., soil physics), but, because of its importance and its complexity, has enlarged to encompass the fields of hydrology; hydrogeology; geochemistry, agronomy, agricultural engineering, geology, and environmental science. Due to its diversity, research has expanded to include: areas of mathematical approaches to solve flow and transport equations; theoretical investigations concerning homogeneous media through laboratory studies; the effects of preferential pathways and macropores on flow; fractal flow of solutes; field experiments with inherent heterogeneity; laboratory experiments focusing on exchange chromatography; radiation-scanning tomography; and the influence of biological, hydrodynamic, and geochemical processes during unsaturated flow conditions. This is not a complete list, but serves to illustrate the broad scope of research currently being conducted in the area of contaminant transport within unsaturated soils.

10.1 PHYSICAL PROCESSES AND MOVEMENT OF SOLUTES

Many texts treat the unsaturated zone as if it were in static equilibrium. Because soil is a dynamic system, however, it is seldom in equilibrium. This is because conditions continually change due to physical, chemical, and atmospheric influences or disturbances. For

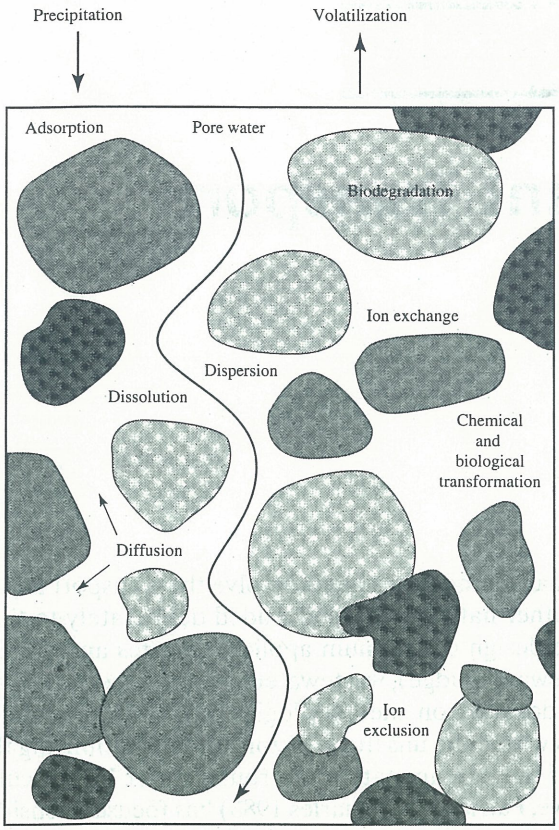

Figure 10.1 Schematic showing various processes that occur in the unsaturated zone

convenience in modeling, flux, and calculations of transport, the assumption of equilibrium conditions allows easier determination of these parameters. Disturbances that take place within the unsaturated zone normally will quickly dissipate as a system moves toward equilibrium. Earlier, we discussed the potential and thermodynamics of water within the unsaturated zone, the chemical properties of that water, and unsaturated water flow (chapters 4, 5, and 8). This section briefly outlines the physical processes that concern the concepts of water and solute flow in the unsaturated zone.

The flow of a solute in soils involves both movement and accumulation. Solute movement may be described as the change of position of water (solute) over a given time within the unsaturated-soil matrix. The accumulation of a solute usually refers to the change in mass of solute at a given volume of the matrix for a specific time period. This is usually caused by recharge events such as rainfall or irrigation, spills, and intentional dumping. However, the volume at a specific location can decrease by evaporation, drainage, advective flow, and/or plant uptake. The driving force for advective flow is the hydraulic gradient. During equilibrium conditions no fluid movement takes place because the potential within the soil matrix is the same at each point (i.e., hydraulic heads are static), but concentrations must also be in equilibrium to prevent diffusive flow of mass. Thus, the sum of static forces, $\Sigma F^s = 0$. As equilibrium changes during disturbance or other influencing factors, the sum of static forces is not zero, and we can say that this becomes the driving force for advective transport. To give more detail, Newton's second law of motion describes force, F, as

$$F = ma \tag{10.1}$$

where F is force in N (kg m s^{-2}), m is mass in kg, and a is acceleration in m s^{-2}. When more than one force is acting on the fluid, they can be added in the proper order so that the sum of

all forces acting on the fluid simultaneously is the vector sum, or resultant force ΣF. If the vector sum is zero, acceleration of the fluid is zero and the body is at mechanical equilibrium. The sum of forces can be separated into two types of forces: drag forces (dynamic), F^d, and static forces, F^s, such that $\Sigma F = \Sigma F^s + \Sigma F^d$. Static forces are always present, but drag forces occur only when static forces cause a body to move. These are the reaction forces associated with movement and may be written as $\Sigma F^s = -\Sigma F^d$. The conditions for static equilibrium can also be expressed in terms of potential, ψ_h (called hydraulic potential). This is expressed mathematically as

$$\frac{\Sigma F^s}{m} = -\frac{\partial \psi_h}{\partial z} \tag{10.2}$$

where ψ_h is the sum of both the pressure potential, ψ_p, and gravitational potential, ψ_g (see chapter 4), and z is the vertical direction; the minus sign indicates that movement is taking place from higher to lower potential. The driving force (hydraulic gradient) can also be written in terms of force per-unit volume as $= -\partial p_h/\partial z$ or per-unit weight $= -\partial H/\partial z$ where ψ_h is in J kg^{-1}, p_h is in J m^{-3} = Pa, and H is in J N^{-1} = m.

The rate of water movement through the unsaturated zone is typically referred to as a flux density, q. Often, the term "flux" (the volume of water divided by time) will be used when "flux density" is actually meant. Flux density is the amount of water (solute) passing through a perpendicular plane of unit area in direction z during a specific time interval. This volume or mass is divided by the area of the plane and the magnitude of the time interval—that is, the mass of solute/(area * time). The flux density is normally expressed on a volume basis, but is also expressed on a mass and weight basis. This becomes more apparent later in this chapter, in the discussion of the continuity equation.

We have mentioned both water flux and solute flux. Water flux is aptly described by Darcy's law (discussed in chapter 7); solute flux entails the movement of solutes (or chemicals) of various kinds with water. To obtain the solute flux, we multiply the water flux or flux density q by the dissolved concentration C of solute in solution, expressed as mass of solute per volume of soil solution. While this gives the general case qC (hereafter referred to as J), it is only an approximation because q is averaged over many soil pores, and does not represent actual water-flow paths that must meander around individual soil particles and various air pathways. There is an extra motion involved, described as hydrodynamic dispersion, D_H, which must be added to J to describe the motion of the solute relative to the average motion, so that $J + D_H =$ total flux. This is a simplified equation for solute flux. A more-detailed discussion regarding hydrodynamic dispersion and other parameters that influence solute flux is given in the following pages.

10.2 TYPES OF FLUID FLOW

When fluid flow takes place within the unsaturated zone, we consider only the water or solute within the zone of interest. When investigating the flow of infiltrating water, there are always two fluids present within the system: the fluid introduced and the fluid that is already present. The fluid present will almost always have a different ion concentration and activity level than the introduced fluid. Thus, we can think in terms of dispersion and mixing of fluids. Generally, there are two types of flow that are possible when two or more fluids occupy the same space within the soil matrix; these are miscible and immiscible flow, commonly referred to as "miscible displacement" and "immiscible displacement." In the case of miscible displacement, the fluids are completely soluble in each other, indicating that interfacial tension between the fluids is zero and there is no distinct fluid–fluid interface; this is the case with hydrodynamic dispersion. For immiscible displacement, the fluids do not mix and there is both interfacial

tension and a distinct interface between the fluids, indicating a pore- or capillary-pressure difference across the fluid–fluid interface.

For unsaturated-zone transport studies, the case of miscible displacement is the most common. As an example, if we investigate the hydraulic parameters of a field site, it is normal procedure to apply a tracer (usually conservative, such as a bromide) in recharge water. The infiltrating recharge water miscibly displaces the soil water already present. The two fluids initially can be separated by an abrupt interface, but due to hydrodynamic dispersion and diffusion, this interface immediately transforms into a transition zone between the two fluids. In comparison to the entire matrix domain of consideration, the transition zone is relatively small.

The most common occurrence of immiscible displacement in the unsaturated zone is when air fills the void space not occupied by water. This is a special case of the simultaneous flow of two immiscible fluids, with air being the non-wetting fluid. Various types of two-fluid flow occur in the engineering field. Examples of these are the flow of oil, water, and gas in oil reservoirs during production and secondary recovery operations (immiscible displacement), and injection of solvents during the secondary recovery process (miscible displacement).

10.3 BREAKTHROUGH CURVES, PISTON FLOW, AND HYDRODYNAMIC DISPERSION

A breakthrough curve is a graphical representation (or plot) of outflow concentration versus time or cumulative water drainage during an experiment. Much of the literature dealing with solute transport in the unsaturated zone reports the use of breakthrough curves in great detail—that is, mass-transfer studies in sorbing porous media (Van Genuchten and Wierenga 1976), miscible displacement in soils (Nielsen and Biggar 1962), and many others. The breakthrough curve indicates the relative tracer distribution of the effluent, with respect to the column or area of the soil matrix under consideration as it relates to either pore volume, time, or both. It is also a very useful way to illustrate the physical meaning of the advection–dispersion equation in one-dimensional form, as well as for comparing results from a model to data collected in the field or laboratory—that is, a plot of the modeled values versus experimental data. Examination of a breakthrough curve can indicate how aggregated the soil is, the presence of macropores or preferential flow paths, or presence of adsorption sites. A typical breakthrough curve is shown in figure 10.2. For an ideal medium, a C/C_0 would reach 0.5 at $V/V_0 = 1$. However, this rarely happens in normal conditions due to the effects of mechanical dispersion and molecular diffusion which cause spreading of the curve. Because of these effects, the tracer begins to appear in the effluent at the outflow end of the column at time t_1 (initial breakthrough), before the arrival of water traveling at velocity t_2 (average velocity; see figure 10.2).

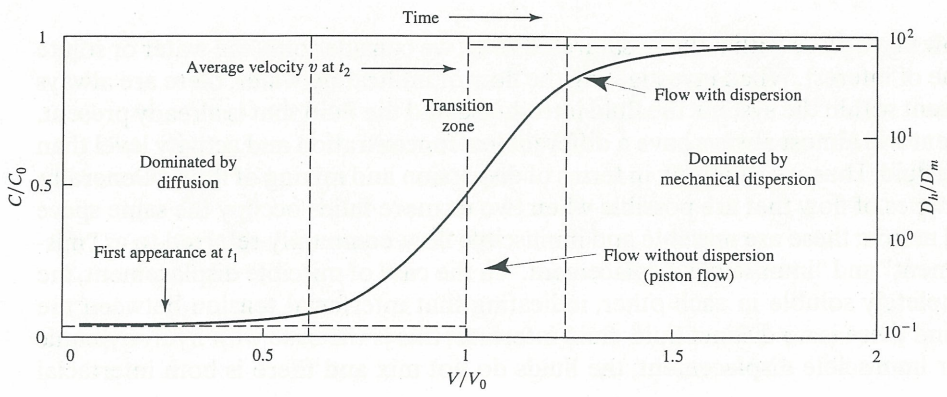

Figure 10.2 The longitudinal dispersion of a typical breakthrough curve, illustrating the effects of molecular diffusion and mechanical dispersion, velocities, and other parameters based upon both time and pore volumes of fluid passing through the column. t_1 represents the time of first appearance of the solute, and t_2 represents the time at which the solute would reach the midpoint at average velocity, discounting anion exclusion (i.e., by piston flow).

Additionally, the drier the soil, the greater the volume of effluent required for $C/C_0 = 1$ and the more tailing that occurs, but the sooner the effluent would break through. This happens due to discontinuity of the number of macropores as water content decreases (see figure 10.3). The overall number of macropores decreases, making less pore-space available for transport as water films around the particles decrease in thickness and length of continuous flow. As long as macropores are present (and because they fill fastest) effluent appears at an earlier breakthrough time and significant tailing occurs due to diffusion into areas of immobile (stagnant) water or intra-aggregates. Initially, these stagnant areas are bypassed, but as time proceeds, diffusion into them increases.

Piston Flow

Piston flow refers to total displacement of the original solution with the incoming solute or tracer, without mixing. This is a direct result of the "piston" (sharp wetting front) displacing the total amount of solution in the column (see figure 10.2). In a strict sense, piston flow is a special case of immiscible displacement in which the solute moves into an area and displaces not by mixing, but by pushing out the original solution and replacing it. This happens due to the properties of the medium and of the incoming and original solutions. These properties include temperature, viscosity, solubility, concentration, and other chemical and physical parameters. Since no mixing takes place during piston flow, the solute pushes out the original concentration, dependent on the total amount of incoming solute. As the total amount of incoming solute increases, more of the original solution is displaced; this is an additive effect. Also, because no mixing occurs, the displacement relies on advective velocity and no diffusion takes place. An example of this is the displacement of water by air, or oil by water. Since both components or liquids are immiscible and advective velocity overcomes any effects due to diffusion, we can expect a very steep front on the breakthrough curve during piston flow. However, since both the radius of the soil pores and the diameter of individual soil particles are not constant—and changes occur in the hydrodynamic dispersion, water content, and chemical-diffusion coefficient—it is highly unlikely that pure piston flow occurs under typical immiscible displacement or any other soil condition.

Hydrodynamic Dispersion

Hydrodynamic dispersion is a non-steady, irreversible process (i.e., the initial tracer distribution cannot be obtained by reversing the flow) in which the tracer mass mixes with the

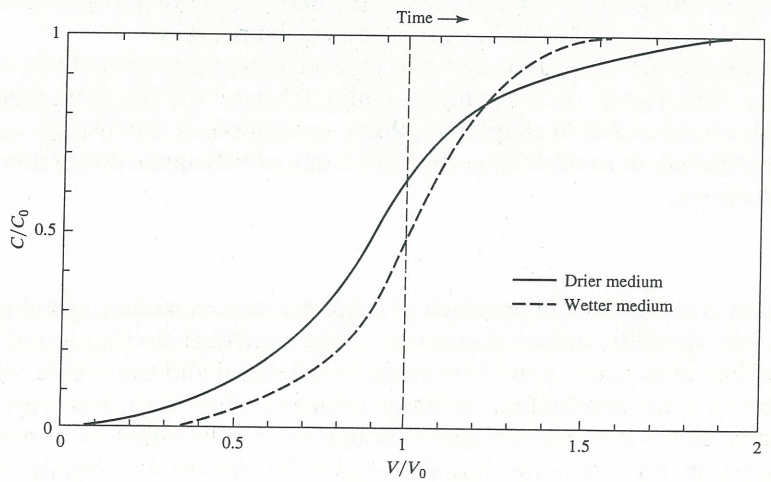

Figure 10.3 The shift of a breakthrough curve based on the water content of the medium

nonlabeled portion of the solution. This is due to the presence of flow through a complicated system of pathways within the soil matrix. Hydrodynamic dispersion consists of two parts: **(1)** mechanical dispersion (sometimes referred to as convection) and **(2)** molecular diffusion. These two conditions are usually artificially separated, but in actuality are totally inseparable in form because both occur together; the dependence of each on different parameters can vary due to changes in physical and chemical conditions, however. As an example: mechanical dispersion is more prominent at high-water content and greater-flow velocities because it is here that contaminant particles mix more freely with water within soil pores, as that water meanders around individual particles. Molecular diffusion predominates at low-water content and low-flow velocity since at this stage, chemical phenomena associated with a tracer or contaminant continue, even though mechanical dispersion due to water movement has ceased. Molecular diffusion alone takes place at the molecular level, in the absence of motion (both in a soil and/or solution); dispersion occurs at the pore level. Hydrodynamic dispersion is also generally associated with early breakthrough of the contaminant.

The causes of hydrodynamic dispersion are: **(1)** the range in pore size causes solutes to arrive at the end of a soil column (used for an example) at different times; **(2)** transverse diffusion into pores (especially stagnant areas) of some of the solute, while direct flow through other pores causes solutes to arrive at different times; and **(3)** molecular (chemical) diffusion ahead of the wetting front as it varies with time.

Soil structure affects hydrodynamic dispersion and the resultant shape of the breakthrough curve in numerous ways. As particle size increases or the soil is aggregated, the graphic representation of the breakthrough curve has more tailing due to diffusion into stagnant regions, but the effluent appears at the end of the column sooner due to larger pore size. However, to get $C/C_0 = 1$, a larger volume of effluent would be required, due to diffusion into both the stagnant areas and into the tortuous path of large aggregates. Smaller-particle sizes yield a more even distribution in pore size, which means there is less stagnant water, so the effluent appears at a later time, and requires less volume for $C/C_0 = 1$ than for a soil with large aggregates (see figure 10.4).

The symmetry of a breakthrough curve is due to the contribution of longitudinal dispersion and the narrow range in pore-water velocity distribution. This usually means the medium is more uniform in texture and pore geometry. In such circumstances, it can be assumed that no interaction takes place between the solute and the solid. However, due to tortuosity of path, volumetric water content, and other parameters previously mentioned, we do not normally expect a symmetrical breakthrough curve. When using extracted soil cores (or blocks) to run tracer experiments, initiation of the breakthrough curve on the y-axis usually indicates flow along the interface between the extracted core and the encasement material. This can bias results, so it must be corrected (see figure 10.5).

The basic approaches used to represent hydrodynamic dispersion have been described empirically by mathematics such as Hagen–Pouiselle's law (discussed in chapter 6) and by modeling, which is discussed in chapter 13. When using models, one usually conducts a field or laboratory experiment to determine the effects of hydrodynamic dispersion by analysis of breakthrough curves.

Mechanical Dispersion

Most dispersion is caused by the presence of solids through meandering soil pores of different sizes that vary spatially, and are dependent on the statistical distribution of velocity of the liquid. Dispersion takes place in two directions, longitudinal and transverse, with the greater amount occurring in the longitudinal direction (along the flow line). Transverse dispersion is smaller in scope, unless flow velocity slows enough for it to be equal-to, or greater-than longitudinal dispersion. At this point, however molecular diffusion normally dominates. The

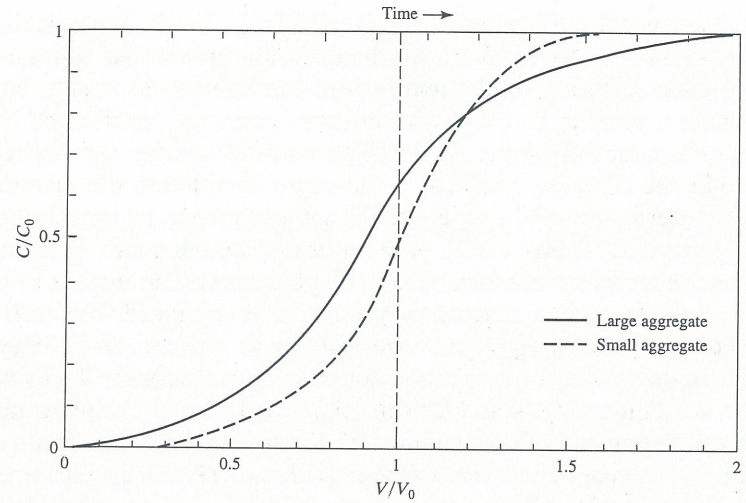

Figure 10.4 The shift of a breakthrough curve based on aggregate size

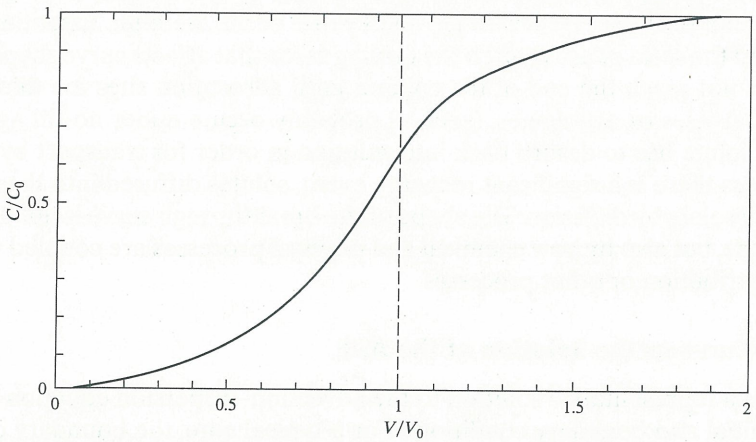

Figure 10.5 A typical breakthrough curve using a constant flux input

movement of the solute in each pore-channel depends on the deviation of path, length of path, and pore size. With larger pores, we obtain a more rapid and wider range in liquid velocities through the soil. The hydrodynamic-dispersion flux is written in the same form as that for molecular diffusion (Bear 1972), and can be expressed by

$$J_H = -D_H \frac{dC}{dz} \tag{10.3}$$

where D_H is the hydrodynamic dispersion coefficient (L^2T^{-1}), C is the concentration (M L^{-3}), and z is the vertical distance (m). This coefficient is considered proportional to pore-water velocity, v, that is, q/θ (Biggar and Nielsen 1967; Bear 1972), and has been expressed as $D_H = \alpha v$, where α is the dispersivity (cm). The dispersivity depends on the length of path over which the water flux and solute diffusion is averaged. It is also an important calibration tool for dispersion in many models.

Molecular Diffusion

At low pore-water velocities, solute transport is dominated by diffusion. Molecular diffusion is best described by Fick's first law:

$$J_D = -D_0 \frac{dC}{dz} \tag{10.4}$$

where D_0 is the molecular-diffusion coefficient (L^2T^{-1}). Thermodynamically, the gradient in chemical potential is the driving force for the diffusion process. As water content decreases in a soil, molecular diffusion predominates over mechanical dispersion, since dispersion is dependent on flow velocity. In a soil with uniform pore-size distribution but low hydraulic conductivity, molecular diffusion is predominant as flow velocity approaches zero.

The larger the diffusion coefficient, the more completely the incoming solute mixes with stagnant water in immobile zones and as a consequence, its appearance in the effluent is delayed (Biggar and Nielsen 1962). When a breakthrough curve shifts to the left it is because of incomplete mixing and lack of fluid displacement. The further to the left the curve shifts, the smaller the volume of resident water that is displaced. This lack of displacement can be caused by: **(1)** large aggregate size causing an abundance of immobile (stagnant) water present in the medium (i.e., pore-water velocity is zero); **(2)** the exclusion of a solute due to solute–solid interactions; and **(3)** sometimes by increased solute concentration, which can cause incomplete mixing of the solute with the soil water and/or anion exclusion.

A breakthrough curve is shifted to the right due to: **(1)** the displacing fluid or its solutes are retained, either by precipitation or exchange; **(2)** chemical reaction of the solute or solid; and **(3)** exchange of the solute with the solid phase of the medium. Essentially, adsorption of the solute to the solid phase is often the driving force that affects curve shape. As a result, the tracer does not reach the end of the column until adsorption sites are filled. In the case of large soil particles or aggregates, (such as probably occurs under no-till agricultural conditions), the solute has to desorb back into solution in order for transport by mobile water to occur. Unless there is a significant recharge event, solutes diffused into these aggregates are transported solely by diffusion. The shape of the breakthrough curve is not determined by retention alone, but also by how chemical and physical processes are coupled with microscopic velocity distribution or other processes.

Relation of a Breakthrough Curve to the Solution of the ADE

To arrive at a representative solution to the advection–dispersion equation (ADE), we need to know initial and boundary conditions. For a typical core, the boundary conditions would be as follows: *Top Boundary* $C(0, t) = 0$ for $t < 0$; $C(0, t) = C_0$ for $t > 0$; *Initial Condition* $C(x, 0) = 0$; *Bottom Boundary* (semi-infinite media) $C(0, t) = 0$ for $t \leq 0$. With these boundary and initial conditions, a solution can be obtained for the advection–dispersion equation

$$D_z \frac{\partial^2 C}{\partial z^2} - v_z \frac{\partial C}{\partial z} = \frac{\partial C}{\partial t} \tag{10.5}$$

where D_z is the hydrodynamic dispersion coefficient in the longitudinal direction (assumed vertical, z, in this case) (L^2T^{-1}), C is solute concentration (ML^{-3}), v is the average linear ground water velocity LT^{-1}, and t is time (T). The solution for the ADE, given for the above-listed boundary and initial conditions is

$$\frac{C(t)}{C_0} = \frac{1}{2}\left[\operatorname{erfc}\left(\frac{z - vt}{2\sqrt{D_z t}}\right) + \exp\left(\frac{vz}{D_z}\right)\operatorname{erfc}\left(\frac{z + vt}{2\sqrt{D_z t}}\right)\right] \tag{10.6}$$

where erfc is the complimentary error function. When D_z, z, or t is large, the second term on the right-hand side of equation 10.6 is negligible. With this solution, we can compute the shape of a typical breakthrough curve for a medium for which the solution is appropriate.

A General Solution for Dispersion of a Displacing Solute Front

At this point we assume a column of saturated soil to which we will apply a solution with concentration, C_0, of bromide. Within the column (initially) there is no bromide; however, at

$x_1 < 0$ a bromide solution is applied to the end of the column, yielding a boundary-value problem such that

$$\frac{\partial C}{\partial t_1} = D\left(\frac{\partial^2 C}{\partial x_1^2}\right) \tag{10.7}$$

Using the previous discussion, the initial conditions for the column are $f(u) = C(x_1, t_1) = C_0$ for $x_1 < 0$ and $t_1 = 0$; also, $f(u) = C(x_1, t_1) = 0$ for $x_1 > 0$ where $t_1 = 0$. The limit as x_1 approaches infinity is expressed as $\lim C(x_1, t_1) = 0$ for $0 < x_1 < \infty$ and $0 < t_1 < \infty$. If one sets $C(x_1, 0) = C_0$ and institutes the initial conditions for $x_1 < 0$, then equation 10.7 can be expressed mathematically as

$$C(x_1, t_1) = \frac{1}{2\sqrt{\pi D t_1}} \int_{-\infty}^{0} C_0 \exp\left[\frac{-(x_1 - u)^2}{4Dt_1}\right] du \tag{10.8}$$

To solve this equation we need to develop an error function, erf. To begin, we must change the variable of integration from u to $(x_1 - u)/[2(Dt_1)^{0.5}]$ (this is the square root of the negative exponent of e). The next step is to determine the limits of integration by letting $u = 0$ and $u = -\infty$, in order to determine the upper limit such that $x_1/[2(Dt_1)^{0.5}]$, with the lower limit as infinity. For equation 10.8 we must change du to $d(x_1 - u)[(Dt_1)^{0.5}]$ and from the relation

$$d\left[\frac{x_1 - u}{2\sqrt{(Dt_1)}}\right] = -\frac{du}{2\sqrt{Dt_1}} \tag{10.9}$$

we must multiply du in equation 10.8 by $-[2(D_t D_1)^{0.5}]^{-1}$ and must also multiply the complete integral by $-2(Dt_1)^{0.5}$, to avoid changing the value. Upon completing these steps we obtain

$$C(x_1, t_1) = -\frac{2\sqrt{Dt_1}}{2\sqrt{\pi D t_1}} \int_{\infty}^{x} \frac{1}{2\sqrt{Dt_1}} C_0 \exp\left[\frac{-(x_1 - u)^2}{4Dt_1}\right] d\left[\frac{(x_1 - u)}{2\sqrt{Dt_1}}\right] \tag{10.10}$$

The last term on the right-hand side of the equation disappears upon integration and, as before, we need to assign a dummy variable to it, denoted by β, that, upon limit interchange, yields

$$C(x_1, t_1) = \frac{1}{\sqrt{\pi}} \int_{x_1/(2\sqrt{Dt_1})}^{\infty} C_0 \exp(-\beta^2)\, d\beta. \tag{10.11}$$

This will give an erf in the form

$$C(x_1, t_1) = \frac{1}{2} C_0 \left[\frac{2}{\sqrt{\pi}} \int_0^{\infty} \exp(-\beta^2)\, d\beta - \frac{2}{\sqrt{\pi}} \int_0^{x_1/(2\sqrt{Dt_1})} \exp(-\beta^2)\, d\beta\right] \tag{10.12}$$

where the error function, erf, is typically written as

$$\text{erf}(z) = \frac{2}{\sqrt{\pi}} \int_0^{z} \exp(-\beta^2)\, d\beta \tag{10.13}$$

The typical properties associated with the erf are $\text{erf}(-z) = -\text{erf}(z)$, $\text{erf}(0) = 0$, and $\text{erf}(\infty) = 1$. The values associated with $\text{erf}(z)$ range from 0 to +1 for $\text{erf}(z)$ and 0 to −1 for $-\text{erf}(z)$. Using the property $\text{erf}(\infty) = 1$ in equation 10.12 we obtain

$$C(x_1, t_1) = \frac{1}{2} C_0 \left(1 - \text{erf}\left[\frac{x_1}{2\sqrt{Dt_1}}\right]\right) \tag{10.14}$$

This equation is for the moving-coordinate system; for the fixed-coordinate system we write

$$\frac{C(x, t)}{C_0} = \frac{1}{2}\left(1 - \text{erf}\left[\frac{x - vt}{2\sqrt{Dt_1}}\right]\right) \tag{10.15}$$

In addition to the standard error function, erf, there is also erfc, the complementary error function. It can be determined by $\text{erfc}(z) = 1 - \text{erf}(z)$. For values of $\text{erf}(z)$ and $\text{erfc}(z)$, see appendix 3.

Although this form is mathematically adequate in describing what is happening in a soil, it is not easily used to plot a breakthrough curve because it does not reflect the relation. The form is easily changed by introducing the Darcy velocity (discussed in chapter 7) and the pore-volume concept. For example, consider a soil column of fixed length, L. The Darcy velocity (also called the flux, q) is simply the quantity of flow, Q (L^3/T), divided by the cross-sectional area, A (L^2). However, in a soil, a particle of water moves faster than the bulk water standing over the soil. Consequently, the average linear velocity is written as $q = (QA^{-1}/\theta)$, where θ is the liquid-filled phase of the soil. The pore volume, PV, of the medium can be written as $PV = \theta V_t$ where V_t is the total volume of the column. For a given duration, a number of pore volumes, N_{pv}, will pass through the column, which is written as $Npv = Qt/PV$, and can be rewritten as $N_{pv} = Qt/\theta V_t$. We divide both sides by the area, A; by substituting LA for V_t and using $q = Q/A$, we have $N_{pv} = qt/L$, which lets us express $C(x, t)/C_0$ in terms of PV. Now, by letting $L = x$, we can rewrite equation 10.15 as

$$\frac{C(x,t)}{C_0} = \frac{1}{2}\left(1 - \text{erf}\left[\frac{(1 - N_{pv})}{2\sqrt{\frac{DN_{pv}}{qL}}}\right]\right) \tag{10.16}$$

Also, equation 10.16 can be written in terms of the erfc function since erfc = 1 − erf; simply substitute erfc into the equation where appropriate. If the reader wishes to find the solution for the dispersion of a "slug" (i.e., a volume of fluid per area of x_0/L) in a similar fashion to that described above, it yields

$$\frac{C(x,t)}{C_0} = \frac{1}{2}\left(\left[\text{erf}\frac{1 + \frac{x_0}{L} - N_{pv}}{2\sqrt{\frac{DN_{pv}}{qL}}}\right] - \left[\text{erf}\frac{1 - N_{pv}}{2\sqrt{\frac{DN_{pv}}{qL}}}\right]\right) \tag{10.17}$$

Determining the Error Function

Essentially, there are two ways to calculate the error function: (1) from tables of error functions and (2) from tables of related probability integrals, which are easier to find and are more common. We can write the normal probability integral as

$$N(z) = \frac{1}{\sqrt{2\pi}}\int_0^z \exp\left(-\frac{w^2}{2}\right) dw \tag{10.18}$$

Using equation 10.18, one can substitute $w/\sqrt{2}$ for β in equation 10.13 such that

$$\text{erf}(z) = \frac{2}{\sqrt{2\pi}}\int_0^{\sqrt{2}z} \exp\left(-\frac{w^2}{2}\right) dw \tag{10.19}$$

Consequently $\text{erf}(z) = 2N(\sqrt{2}z)$ or $2N(1.414z)$. As a result, $N(z)$ is simply the area under the curve which from standard rules of calculus can be written for this case as

$$f(w) = \frac{\exp\left(-\frac{w^2}{2}\right)}{\sqrt{2\pi}} \tag{10.20}$$

QUESTION 10.1

Using the relation $\text{erf}(z) = 2N\sqrt{2}z$, find erf 0.90.

QUESTION 10.2

What is z when $\text{erf}(z) = 0.797$?

Calculating the Displacing Front of a Breakthrough Curve

In order to calculate points on the breakthrough curve we need to know the number of pore volumes that have eluted through the column, N_{pv}, D, q, and L. We begin by using the definition of the error function (equation 10.13) and substituting $w^2/2$ for β^2 (as before) from the definition of the probability; then equation 10.16 can be rewritten as

$$\frac{C(x,t)}{C_0} = \frac{1}{2} - \frac{1}{\sqrt{2\pi}} \int_0^{(1-N_{pv})/\sqrt{2DN_{pv}/qL}} \exp\left(-\frac{w^2}{2}\right) dw \tag{10.21}$$

With this equation, we plot a breakthrough curve; however, to determine D in the equation the derivative must first be obtained (we show later that there is a simpler way to obtain D). To save time and space, a few steps are skipped and the derivative dq/dp is expressed as

$$\frac{dq}{dp} = -\frac{\sqrt{\frac{2DN_{pv}}{qL}} - \left(\frac{1}{2}\right)\frac{(1-N_{pv})\left(\frac{2D}{qL}\right)}{\sqrt{\frac{2DN_{pv}}{qL}}}}{\frac{(2DN_{pv})}{qL}} \tag{10.22}$$

Letting the number of pore volumes equal one (1) and substituting, we may write

$$\left.\frac{d\left[\frac{C(x,t)}{C_0}\right]}{dp}\right|_{N_{pv}=1} = \left[2\sqrt{\frac{\pi D}{qL}}\right]^{-1} \tag{10.23}$$

Now, we may set the left side equal to S and solve for D (the dispersion coefficient), which is expressed as

$$D = \frac{qL}{4\pi S^2} \tag{10.24}$$

In summary, we know both L and q from experimental measurement where $q = (Q/A)/\theta$. Consequently, to determine the diffusion coefficient, D, we need to measure the slope, S, at $N_{pv} = 1$ of the breakthrough curve; measure $C(x,t)/C_0$ versus N_{pv}, which is set equal to the derivative of the left-hand side of the equation 10.23; and solve for D.

QUESTION 10.3

You are running a column experiment in the laboratory. The column measures 125-cm height by 50-cm diameter. Determine D given that $Q = 2810$ cm hr^{-1}, $\theta = 0.45$ (water-filled porosity), and S (slope of C/C_0) at $N_{pv} = 1$.

QUESTION 10.4

How would you find the derivative of $C(x, t)/C_0$ with respect to N_{pv}?

Calculating the Concentration in a Moving Slug of Fluid for a Breakthrough Curve

By rewriting equation 10.17 in terms of the normal probability integral we obtain

$$\frac{C(x,t)}{C_0} = \sqrt{2\pi}^{-1} \int_0^{[1+(x_0/L)-N_{pv}]/\sqrt{2DN_{pv}/qL}} \exp\left(-\frac{w^2}{2}\right) dw - \sqrt{2\pi}^{-1} \int_0^{[(1-N_{pv})/\sqrt{2DN_{pv}/qL}]} \exp\left(-\frac{w^2}{2}\right) dw \tag{10.25}$$

This will allow one to find a moving front (or slug) of fluid. Without working out the derivation, the diffusion coefficient (D) for this equation can be determined, after Corey, Nielsen, and Kirkha (1967) such that

$$D = \frac{qL\left(\frac{x_0}{2L}\right)^2}{2\left(1+\frac{x_0}{2L}\right)z^2} \tag{10.26}$$

where x_0 is the volume (mL) of the slug, V_s, added to the medium. Thus, $x_0 = V_s/A\theta$, where A is the cross-sectional area of interest. The value for z may be determined by

$$z = \frac{\left(\frac{x_0}{2L}\right)}{\sqrt{2D\frac{(1+x_0)/2L}{qL}}} \tag{10.27}$$

or in evaluating the maximum $C(x, t)/C_0$ by changing the limit on the second integral from $-z$ to z, adding both integrals, and dividing by 2 so that

$$\frac{1}{2}\left(\frac{C(x,t)}{C_0}\right)_{\max} = \sqrt{2\pi}^{-1} \int_0^z \exp\left(-\frac{w^2}{2}\right) dw \tag{10.28}$$

Thus, to find D, measure $C(x, t)/C_0$ at its maximum value on the breakthrough curve, divide by two, and set it equal to the right-hand side of equation 10.28. As a result, when the maximum value of $[C(x, t)/C_0]$ is divided by two, we go to the table of normal probability functions to find z; this allows us to solve equation 10.26. Once D is obtained, equation 10.25 can be used to plot the breakthrough curve. We discuss procedures for determining D through experimental methods later in this chapter.

Thus far, we have considered only dispersion as the mixing process and have neglected diffusion. In discussing this parameter we assume that the viscosity and density of all fluids within the system are the same, and that the dispersion coefficient is independent of solute concentration. However, the discussion has served to introduce miscible-displacement mathematics. Later, in question 10.7, the student is asked to derive the ADE. Considering the answer to the question (in one dimension), the solution can be expressed as

$$\frac{C(x,t)}{C_0} = \frac{1}{2}\left[\operatorname{erfc}\left(\frac{1-N_{pv}}{2\sqrt{\frac{DN_{pv}}{qL}}}\right) + \exp\left(\frac{qL}{D}\right)\operatorname{erfc}\left(\frac{1+N_{pv}}{2\sqrt{\frac{DN_{pv}}{qL}}}\right)\right] \tag{10.29}$$

As before, D can be found by equating the slope of the breakthrough curve at $N_{pv} = 1$ to the derivative of equation 10.29, with respect to N_{pv} evaluated at $N_{pv} = 1$. This is done in the same method as before, by converting equation 10.29 to the normal probability integral to find that

$$D = \frac{qL}{4\pi S^2} \tag{10.24}$$

Similar to previous solutions, once D is obtained, known values of q and L can be substituted into equation 10.29 and one can plot $C(x, t)/C_0$ versus the number of pore volumes, N_{pv}. For a soil that has a low-flow velocity, a diffusion model can easily fit the experimental data. For a high-flow velocity, a dispersion model fits better. This is logical, since D depends on fluid velocity. In this case, D is described by the diffusion coefficient in the diffusion model, and the dispersion coefficient in the dispersion model; however, remember that the two are essentially inseparable. Some of the original research evaluating this topic (Nielsen and Biggar 1962) indicates that for soils with a wide range of microscopic-pore velocities (typical in the unsaturated zone), the use of an average-flow velocity in the model can cause deviations between the experimental curve of the data versus the theoretical curve of the model. This is primarily due to: ion adsorption and exchange; rate of diffusion; pore geometry; chemical reaction; precipitation; incomplete mixing of solute with solution; aggregate size, as well as other physical and chemical factors. All of these parameters affect the dispersion coefficient D and thus, can affect the appearance of the first detectable concentration, the shape of the breakthrough curve, whether the breakthrough curve is shifted left or right, and/or the outcome of the modeled solution.

The mathematical models presented here have made several simplifying assumptions. Despite assumptions, however, using mathematical or analytical models for comparison to experimental data can provide information and insight about a soil. If the models accurately predict the results of an experiment, one can reasonably assume that the hypothesis used for the model works well for both the medium of interest and the solute being investigated. However, solutions for a specific soil or medium type are not always readily transferable to another chemical solution or medium.

Figure 10.6 shows a comparison of a numerical solution using the United States Geological Survey program VS2DT (Healy 1990) versus an analytical solution. Using a soil column of 35-cm length, water flowing into the column is maintained at a concentration of C_0 for 160 s, after which the concentration is set to zero for an additional 320 s. Figure 10.6 shows that the numerical results of VS2DT produces a good match, with analytical results at a distance of 8 cm for the column inlet at all times for steady water flow, and both first-order decay and linear sorption for three different cases of decay and sorption.

QUESTION 10.5

What is the derivative to equation 10.29?

Calculation of the Dispersion Coefficient (*D*)

To simulate transport through soil practically, the effective dispersion coefficient D should be determined—usually in the longitudinal direction. The dispersion coefficient is often calculated for a homogeneous medium and normally, determination of D is accomplished with the use of packed laboratory columns and intact cores for the medium of interest by "trial and error." Once the solute concentration of the resident solution in the column is known, a feed solution of the same relative concentration, but containing a different solute, is leached

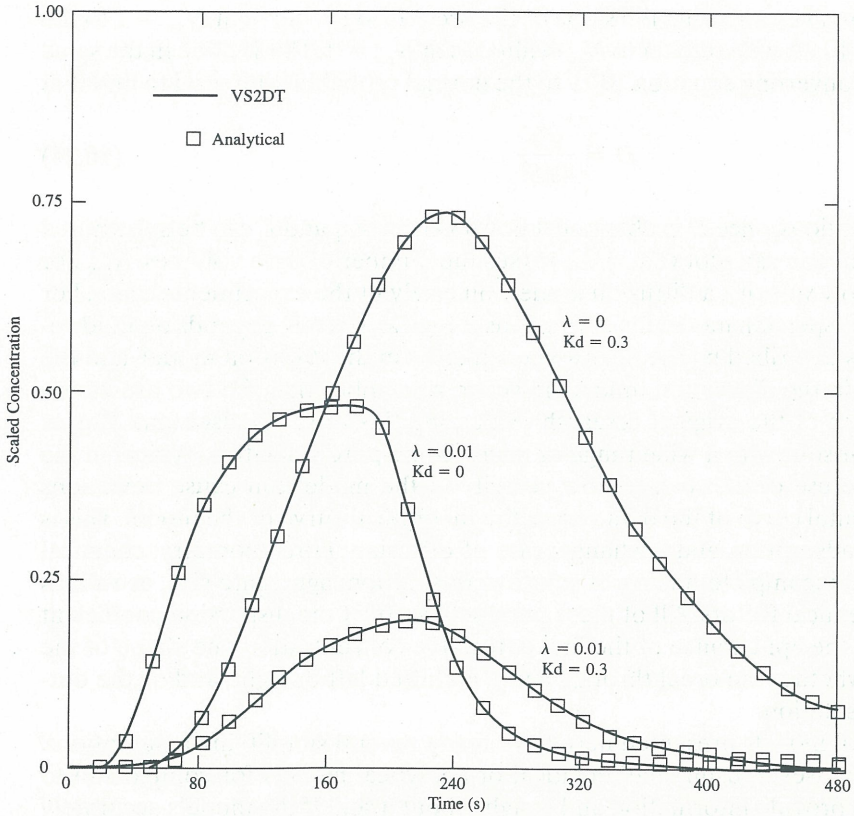

Figure 10.6 Analytical and numerical (VS2DT) results at a distance of 8 cm from a column inlet (data from: Healy 1990)

through the column. The dispersion coefficient is then determined as a function of time, distance, and concentration. When using packed columns, they should be uniformly packed so as to avoid layering, to ensure homogeneity. This helps prevent macroscopic variations in water content and pore-water velocity, which can result in additional spreading. Uniform packing also allows the use of a constant "effective" pore-water velocity for the experiment. Viscosity and density differences between resident and feed solutions during mixing are usually avoided in this experiment, because these differences can lead to fingering. As a result, low concentrations of a conservative tracer (i.e., bromide or chloride) do not affect the density and the viscosity of the solvent. Biggar and Nielsen (1964) show that fingering dominates for a density difference of 3.4×10^{-3} g cm^{-1} and a viscosity difference of 0.003 cP, obscuring the effect of molecular diffusion.

There are also other factors to consider in the determination of D. One is gravity segregation, discussed in detail by Rose and Passioura (1971b). However, this is more important in cases of saturated flow and saltwater intrusion, in which contaminated salt/water intrudes horizontally into a fresh-water aquifer. Since permeability k decreases rapidly during the desaturation process, gravity segregation is of little consequence in unsaturated-flow conditions. The reader is referred to Scheidegger (1974) for an in-depth discussion of gravity segregation. A major factor to consider is apparatus-induced dispersion. This is critically important when short columns are used under unsaturated-flow conditions. In the event of layering caused by insufficient mixing during column preparation, D can be as much as 40 percent less than obtained with a one-layer equation. This is because mixing is assumed to occur in the medium only, but in actuality it occurs in the "dead-volume" inside the column, but outside the medium. Thus, packing to reduce the "dead-volume" and obtain homogeneity is

crucial. Also, by measuring concentration with depth as well as in the effluent, we obtain a more accurate D than by simply measuring concentration in the effluent alone. Measurements of concentration within the medium can be obtained from samples collected using suction lysimeters, or by measuring electrical sensitivity at a point in the medium with a conductivity probe if using salts such as sodium chloride.

The dispersion coefficient is often determined as a function of position at a certain time using an analytical inverse solution to the ADE. It can also be determined for varying time at a given depth. One method for determining D was given in equation 10.24; in this section we discuss other methods to calculate D. The one-dimensional ADE (equation 10.5) was used by Fried and Combarnous (1971). Assuming a longitudinal dispersion coefficient, an approximate solution to equation 10.5 can be written as equation 10.15. For a given time, the solution follows a normal distribution $1 - N[(x - \mu)/\sigma]$, with a mean displacement $\mu = vt$ and standard deviation $\sigma = (2Dt)^{0.5}$. The term $N[\ ]$ is the probability-density function (PDF) for a normal distribution with values $N[-1] = 0.16$ and $N[1] = 0.84$, as suggested by Lapidus and Amundson (1952). The width of the transition zone, 2σ, can be determined by plotting C/C_0 versus x (depth) such that

$$2\sigma = x_{0.16} - x_{0.84} = \sqrt{8D_L t} \tag{10.30}$$

where $x_{0.16}$ and $x_{0.84}$ are the positions for which C/C_0 is equal to 0.16 and 0.84 respectively. The longitudinal dispersion coefficient can be calculated by

$$D_L = \frac{(x_{0.84} - x_{0.16})^2}{8t} \tag{10.31}$$

For concentrations at a certain position as a function of time, we have

$$D_L = \frac{1}{8}\left[\frac{x - vt_{0.16}}{\sqrt{t_{0.16}}} - \frac{x - vt_{0.84}}{\sqrt{t_{0.84}}}\right]^2 \tag{10.32}$$

While Fried and Combarnous (1971) discuss how the transverse-dispersion coefficient can be determined, very little other research has been done to that end.

Rose and Passioura (1971a) used the Brenner number, B ($B = vL/D$; L is column length) and determined D by plotting $C_e = [(C - C_i)/(C_0 - C_i)]$ versus $\ln PV$ on probability paper where C_e is the exit concentration (dimensionless) and PV (pore volume) $= (vt/L)$. Nearly straight lines for particular values of B were obtained. Due to this linear relation we have

$$\text{erfc}^{-1}(2C_e - 1) = -m \ln PV - \beta \tag{10.33}$$

where m is the slope and β is the intercept. Rose and Passioura (1971a) also developed the following relation for $16 < B < 640$:

$$\log B = 0.1139(\log m)^3 - 0.3504(\log m)^2 + 2.3623(\log m) + 0.4732 \tag{10.34}$$

By plotting $-\ln PV$ versus $\text{erfc}^{-1}(2C_e - 1)$, the slope m and the intercept β can be determined. The Brenner number B can be obtained from equation 10.34; D can then be obtained using the relation $B = vL/D$. Van Genuchten and Wierenga (1986) use a slightly simpler version of equation 10.34.

Another method for obtaining D is by curve-fitting or least-squares analysis of the effluent curve. One of the more popular programs for determining D is called CXTFIT by Toride, Leij, and Van Genuchten (1995). These researchers use a nonlinear, least-squares inversion method to determine the dispersion coefficient, the retardation factor (R), and first-order degradation constants. This type of program is most useful on column-breakthrough experiments involving concentrations at fixed locations at different times, or for a specific time at different locations.

Additional methods for obtaining D involve the calculation of D from concentration versus distance curves, and the Boltzmann transformation. To obtain D in a concentration versus distance scenario, we simply section laboratory columns at specific distances or determine the solute concentration in situ in the field. The resulting equation for this method, given by Van Genuchten and Wierenga (1986), is $D = R/4\pi t\, S^2$, where R is the retardation factor (the complete form is shown later, in equation 10.93) and S is the slope of the experimental curve where the solute concentration is 0.50, or by calculation of the slope (β) $D = R/4\beta^2 t$. Note that in expression $R = vt/x_0$, x_0 is the value (distance) of x where the relative effluent concentration equals 0.5, and v is the average pore-water velocity. In using the Boltzmann transformation to transfer the partial-differential equation into an ordinary equation, we assume the dispersion coefficient to be dependent mainly on water content because of the relatively low velocity, the small value of the Peclet number, and the rapidly changing water content during infiltration.

The process of dispersion depends on several things: water content; molecular diffusion; velocity; viscosity; density; and hydraulic conductivity. To determine the influence of pore-water velocity and particle size, data are commonly analyzed by plotting D_L/D_0 versus $\mathcal{P}$ (the Peclet number) where $\mathcal{P} = vd/D_0$ on log–log paper. For such cases, d is a characteristic pore-size or particle-size dimension similar to that used in scaling (see chapter 16). Using the Peclet number, Bear (1979) designates the following dispersion regimes: (1) molecular diffusion is dominant when $\mathcal{P} < 0.4$; (2) molecular diffusion and mechanical dispersion are of the same order for $0.4 < \mathcal{P} < 5$ and thus, additive; (3) major mechanical dispersion occurs with some molecular diffusion in the range $5 < \mathcal{P} < 1000$—there is interference in these effects and they cannot be added; (4) mechanical dispersion is dominant for $1000 < \mathcal{P} < 1.5 \times 10^5$ with negligible molecular diffusion; and (5) mechanical dispersion occurs when the flow regime is out of the domain of Darcy's law ($\mathcal{P} > 1.5 \times 10^5$). As a note of caution, however, if we use experimental values for D, the solute front will exhibit additional spreading when solving the ADE by numerical methods. This computational artifact is called numerical dispersion and is most prone to occur directly around the front when using high values for P.

10.4 NONREACTIVE SOLUTES

Typical investigations of solute transport involve the movement of a conservative tracer through a medium that is both isotropic and homogeneous. A conservative tracer is one that does not react or interact with the medium, and which is completely miscible in the pore-water solution. The most commonly used conservative tracers are chloride and bromide (generally as KBr, and KCl or NaCl). If we assume no source or sink terms, the conservation of mass at a large scale (or what is termed a macroscopic scale) may be mathematically described as

$$\frac{\partial\, \theta C}{\partial t} = -\nabla \cdot [J_H + J_v C] = -\nabla \cdot J_s \tag{10.35}$$

where θ is the volumetric water content (unitless), C is solute concentration (ML^{-3}), t is time (T), J_H is flux due to hydrodynamic dispersion that includes both dispersive and diffusive fluxes ($ML^{-2}T^{-1}$), Jv is the volumetric-flux of the influent (L^3T^{-1}), J_s is the total-flux of the solute ($ML^{-2}T^{-1}$), and $\nabla \cdot$ (pronounced nabla dot) is the divergence (L^{-1}).

Based on Fick's first law, the autonomous flux J_D is given in equation 10.3. However, hydrodynamic dispersion is written as

$$D_H(v, \theta) = \alpha v + D_0(\theta) \tag{10.36}$$

where α is the dispersivity (L), sometimes called the mass-transfer coefficient; v is the average advective pore-water velocity expressed as v, or q/θ where q is the Darcy flux (LT^{-1}); θ is

the volumetric water content; and D_0 is as described in equation 10.3 written here as a function of water content (θ). The left term on the right-hand side of equation 10.36 is often termed the mechanical-dispersion coefficient (D_m). Rewriting equation 10.3 and substituting equation 10.36, we obtain

$$J_D = -\theta D_H \frac{\partial C}{\partial z} \tag{10.37}$$

where D_H is the hydrodynamic-dispersion coefficient (L^2T^{-1}) and z is the vertical distance (L). D_H now represents the random effects of both molecular diffusion and mechanical dispersion.

By using the relation between Darcy's law and pore-water flux ($J_v = v\theta$), we can substitute equation 10.37 into equation 10.35 to obtain the one-dimensional transport equation for steady-state conditions; here we assume that v (average velocity) and θ are constant with depth, z:

$$\frac{\partial \theta C}{\partial t} = \frac{\partial}{\partial z}\left[\theta D_H(v, \theta)\frac{\partial C}{\partial z} - v\theta C\right] \tag{10.38}$$

We shall now drop the "H" on D_H and refer to it simply as D. Because θ is constant, the equation may be simplified to equation 10.5 by dividing through by θ:

$$\frac{\partial C}{\partial t} = D\frac{\partial^2 C}{\partial z^2} - v\frac{\partial C}{\partial z} \tag{10.5}$$

This is a linear, parabolic, second-order partial differential equation in which both v and D are independent of z and t (Risken 1984). For anisotropic, multi-dimensional flow, equation 10.5 can be rewritten

$$\frac{\partial C}{\partial t} = \frac{\partial}{\partial z_i}\left[D_{ij}\frac{\partial C}{\partial z_j}\right] - \frac{\partial v_i C}{\partial z_i} \tag{10.39}$$

where D_{ij} is the dispersion tensor and i, j are direction indices (Smith 1985).

Equation 10.5 is most useful for laboratory investigations in which packed columns are used to control: soil heterogeneity; structural differences; cracking; shrinking; swelling; and biological activity. For these conditions, equation 10.5 can be used to describe most of the phenomena represented in figure 10.1 (Bresler 1973a; Cho 1971; Cushman 1982; Robbin Jurinak, and Wagenet 1980 a, b; Van Genuchten and Cleary 1982).

10.5 SORPTION REACTIONS

When pesticides and other organic chemicals are applied to soils, the solutes do not act as a conservative tracer due to electrical-charge differences between the exchange sites in the soil matrix and the applied contaminant. For example, most soils found in the United States have a negative net charge; thus, the application of a pesticide or other organic compound would display reactive properties—that is, normally, the contaminant would be strongly bound to soil particles in the upper profile. However, many types of soil in various parts of the world contain variably charged soils (Sumner 1992) such as hydrous oxides and aluminum and iron sesquioxides, almost all of which exhibit ion-exclusion and adsorption phenomena. In the process of anion exclusion, negatively charged anions are repulsed from the negatively charged surfaces of soil particles, which results in more rapid flux of the anions. Consequently, breakthrough curves that exhibit anion exclusion are generally shifted left, that is, initial breakthrough occurs earlier than if no anions were present. While this phenomenon is commonly associated with the application of a conservative tracer like potassium bromide onto net-negative soils, it is also seen with the application of various reactive contaminants to variably charged soils, where the contaminant and soil can have a net positive charge.

Generally, a tracer (or chemical) that is applied intentionally to the soil is present in a single liquid, non-sorbed phase. Assuming the processes of adsorption and desorption apply, equation 10.35 can be written as

$$\frac{\partial}{\partial t}[\theta C + C_s] = -\nabla \cdot [J_D + J_v C] \tag{10.40}$$

where C_s is the concentration ($\mathrm{M\,L^{-3}}$) of the adsorption–precipitation phase. Equation 10.40 can be rewritten as

$$\frac{\partial}{\partial t}[\theta C + C_s] = \frac{\partial}{\partial z}\left[D\theta \frac{\partial C}{\partial z}\right] - \frac{\partial v\,\theta C}{\partial z} \tag{10.41}$$

There are three common types of adsorption isotherms for which the ADE has been written: **(1)** linear; **(2)** Freundlich; and **(3)** Langmuir. Gupta and Greenkorn (1974) give the following expressions for the ADE with regard to each isotherm.

Linear:

$$\left[1 + \frac{K_1}{\theta}\right]\frac{\partial C}{\partial t} = D\frac{\partial^2 C}{\partial z^2} - v\frac{\partial C}{\partial z} \tag{10.42}$$

Freundlich:

$$\left[1 + \frac{nK_2}{\theta}C^{n-1}\right]\frac{\partial C}{\partial t} = D\frac{\partial^2 C}{\partial z^2} - v\frac{\partial C}{\partial z} \tag{10.43}$$

Langmuir:

$$\left[1 + \frac{a}{\theta(1 + bC)^2}\right]\frac{\partial C}{\partial t} = D\frac{\partial^2 C}{\partial z^2} - v\frac{\partial C}{\partial z} \tag{10.44}$$

where a, b, K, and n are empirical constants. The amount of chemical adsorbed in mass-per gram of soil in a solution with a known equilibrium concentration (C) in mass per volume, can be calculated by $S = KC^n$, where K is the adsorption coefficient and S can be expressed as the source/sink term. The exponent n may be taken as: **(1)** 1.0 if a linear isotherm is expected; **(2)** 0.87 if a nonlinear isotherm is likely (0.87 is an average of 26 pesticides as reported by Lyman, William, and Rosenblatt 1990); or **(3)** any value that has empirical basis. For case 3, we consider measured values for similar compounds to that being investigated. Scientists typically investigate linear isotherms as a first choice because of simplicity. However, for accuracy, nonlinear isotherms are preferred.

Due to the source/sink term, S, there is a retardation factor, R, involved in the ADE. The retardation factor is affected by soil-bulk density, volumetric water content, soil-adsorption characteristics, and other parameters; we describe it in the following paragraphs. Initially, we write $(S\rho_b/\theta)$ which yields ($\mathrm{ML^{-3}}$), however, when multiplying by the volume, $\nabla x\,\nabla y\,\nabla z$, we are left with total-mass adsorbed. The retardation factor for a volume basis is expressed by

$$\left(\frac{\rho_b}{\theta}\frac{\partial S}{\partial t}\Delta x\,\Delta y\,\Delta z\right) = MT^{-1} \tag{10.45}$$

Substitution into equation 10.5 gives

$$\frac{\rho_b}{\theta}\frac{\partial S}{\partial t} + \frac{\partial C}{\partial t} = D\frac{\partial^2 C}{\partial z^2} - \frac{v\,\partial C}{\partial z} \tag{10.46}$$

Because $S = KC^n$, application of the chain rule (and assuming $n = 1$) yields

$$\frac{\partial S}{\partial t} = \frac{K\,\partial C}{\partial t} \tag{10.47}$$

Substituting equation 10.47 into equation 10.46, we obtain

$$\frac{\rho_b}{\theta}\frac{K\,\partial C}{\partial t} + \frac{\partial C}{\partial t} = D\frac{\partial^2 C}{\partial z^2} - \frac{v\,\partial C}{\partial z} \tag{10.48}$$

This can now be rewritten in terms of one dependent variable, as

$$\frac{R\,\partial C}{\partial t} = D\frac{\partial^2 C}{\partial z^2} - \frac{v\,\partial C}{\partial z} \tag{10.49}$$

where

$$R = \frac{\rho_b}{\theta}K + 1 \tag{10.50}$$

R (retardation coefficient) is dimensionless. Thus, equation 10.49 is the ADE for one-dimensional flow at steady state with assumption of reaction between solute and solid phases. To obtain the slope of the exchange isotherm, we plot dS/dC. An exchange isotherm, in which all parameters are typically held constant (except concentration), is the amount of solute sorbed to the medium versus the amount of solute in concentration. This also includes the physical and chemical parameters of both the soil and solution. Note that in the consideration of a binary system, the amount of solute adsorbed S (usually written as μg adsorbed/g medium), and the solution concentration C (μg/mL or ML^{-3}), are fitted to the Freundlich equation, $S = KC^n$, to determine the adsorption coefficient, K, and the parameter, n.

A principal difficulty in using the ADE for either analytical determination or numerical modeling is that it is often difficult to obtain values for the parameters used in the equation. The simplest method for obtaining these various parameters is to utilize regression equations obtained from experimental data in log–log form. For a wide variety of pesticides and other chemicals, Kenaga and Goring (1980) give the following equation to calculate the adsorption coefficient:

$$\log K_{oc} = -0.55 \log S_w + 3.64 \tag{10.51}$$

where S_w (water solubility) is reported in mg L^{-1}. In this instance, -0.55 represents the a constant and 3.64 represents the b constant. Other equations reported by Kenaga and Goring (1980), mainly for pesticides, are

$$\log K_{oc} = 0.681 \log BCF(f) + 1.963 \tag{10.52}$$

and

$$\log K_{oc} = 0.681 \log BCF(t) + 1.886 \tag{10.53}$$

where $BCF(f)$ is the bioconcentration factor due to flowing-water tests and $BCF(T)$ is the bioconcentration factor using model ecosystems. Regression equations for other applications are listed in Table 10.1 and in chapter 15. The adsorption coefficient, K (from the Freundlich equation: $S = KC^n$), can be estimated from K_{oc} from the expression $K = K_{oc}$(percent oc)/100, where K_{oc} = (μg adsorbed/g organic carbon)/(μg/mL solution). The adsorption coefficient K is not the same as K_{oc}. The adsorption coefficient K_{oc} is the extent to which an organic chemical partitions itself between the solution and solid phases in either unsaturated or saturated soil; K_{oc} is largely independent of soil properties and can be thought of as the ratio of the amount of chemical adsorbed per-unit weight of organic carbon (oc) in a soil at assumed equilibrium.

QUESTION 10.6

Estimate K_{oc}, K, and S for dicamba. Assume a water solubility of 0.04 mg L^{-1}, organic carbon content of 2 percent, and a solution concentration, C, of 10 mg L^{-1}.

TABLE 10.1 Regression Equations for the Estimation of K_{oc}

Eq. No.	Equation*	No.†	r^2	Chemical classes represented
1	$\log K_{oc} = -0.54 \log S + 0.44$ (S in mole fraction)	10	0.94	Mostly aromatic or polynuclear aromatics, two chlorinated
2	$\log K_{oc} = -0.557 \log S + 4.277$ (S in μ moles/L)	15	0.99	Chlorinated hydrocarbons
3	$\log K_{oc} = -0.544 \log K_{ow} + 1.377$	45	0.74	Wide variety, mostly pesticides
4	$\log K_{oc} = 0.937 \log K_{ow} - 0.006$	19	0.95	Aromatics, polynuclear aromatics, triazines and dinitroaniline herbicides
5	$\log K_{oc} = 0.94 \log K_{ow} + 0.02$	9	††	*s*-Triazines and dinitroaniline herbicides
6	$\log K_{oc} = 1.029 \log K_{ow} - 0.18$	13	0.91	Variety of insecticides, herbicides, and fungicides
7	$\log K_{oc} = 0.0067 (P - 45N) + 0.237$	29	0.69	Aromatic compounds: ureas, 1,3,5-triazines, carbamates, and uracils

Sources: 1. Karickhoff, Brown, and Scott 1979; 2. Chiou, Peters, and Freed 1979; 3. Kenaga and Goring 1978; 4. Brown and Flagg 1981; 5. Brown, D. S. (personal communication); 6. Rao and Davidson 1980; 7. Hance 1969

*K_{oc} = soil (or sediment) adsorption coefficients; S = water solubility; K_{ow} = octanol–water partition coefficient; P = parachor; N = number of sites in molecule which can participate in the formation of a hydrogen bond

†= number of chemicals used to obtain regression equation

†† Not given

QUESTION 10.7

Derive Richard's equation and then, beginning with Fick's first law of diffusion, derive the general ADE (commonly referred as the solute-transport equation) for one-dimensional, steady-state flow.

10.6 EQUILIBRIUM CHROMATOGRAPHY

Most solute-transport studies involve solute interaction with the solid phase, and for a majority of these studies, the solution is obtained numerically by utilizing experimentally, exchange isotherms that are determined. For most studies, it is assumed that steady-flow conditions prevail and only two different ionic (cations) species are present during miscible displacement; equilibrium chromatography is in this category. Following Bolt (1982), it is convenient to express the adsorbed concentration S (which depends on the liquid concentration of a specific species of interest) in moles-of-charge per volume of soil ($mol_c\ m^{-3}$) while C is expressed in moles-of-charge per volume of solution ($mol_c\ m^{-3}$). To simplify the calculation, we assume concentration is constant during ion exchange. If we neglect effects due to dispersion and diffusion, a step-change in concentration occurs at the concentration front, mathematically expressed as $J_v t/\theta$; this is, actually the penetration depth. Because we assume the concentration is constant during ion exchange and thus, time t, depends only upon C for such, we rewrite equation 10.40 as

$$\left(\frac{dS}{dC} + \theta\right) - \frac{\partial C}{\partial t} = -J_v \frac{\partial C}{\partial x} \tag{10.54}$$

For this case, dS/dC is the differential capacity of the exchanger for the exchanging ion, J_v is the volumetric-water flux (LT^{-1}), and other parameters are as previously explained. The

$\partial C/\partial x$ term must be finite (assume negligible dispersive flux) to solve equation 10.54. Using the chain rule of calculus and rewriting equation 10.54, we obtain

$$\left(\frac{\partial x}{\partial t}\right)_C = \left(\frac{J_v}{\frac{dS}{dC} + \theta}\right) \tag{10.55}$$

Should the concentration profile exhibit a jump (i.e., the condition of the finite term is violated), the conservation of mass is expressed as

$$\left(\Delta \frac{dS}{dC} + \theta \Delta C\right) dx = \Delta C \, dV_i \tag{10.56}$$

where V_i is the input volume per unit area of the soil column. This also requires that equation 10.55 be rewritten such that

$$\left(\frac{dx}{dt}\right)_{\Delta C} = \frac{J_v}{\left(\frac{\Delta S}{\Delta C} + \theta\right)} \tag{10.57}$$

Following our previous assumptions, the position for a specific concentration (both dS/dC and θ are homogeneous with respect to location and $dV_i = J_v dt$) is found by integration of equation 10.55 so that

$$x_C = \int_0^t \left(\frac{J_v}{\frac{dS}{dC} + \theta}\right) dt = \frac{V_i - V_0(C)}{\left(\frac{dS}{dC} + \theta\right)} \tag{10.58}$$

where $V_0(C)$ is the volume of solution applied to the column, at the instant that the concentration at $x = 0$ reaches C. For a step-type displacement, $V_0 \equiv 0$. For the adsorbed and liquid phase, the average depth (position) of the concentration front is given by

$$x_p = \frac{\int_{C_i}^{C_0} x_c \left(\frac{dS}{dC} + \theta\right) dC}{\int_{C_i}^{C_0} \left(\frac{dS}{dC} + \theta\right) dC} \tag{10.59}$$

Thus, with the use of equilibrium chromatography we determine the propagation in the adsorbed phase. In order to investigate the shape of the solute front, equation 10.58 is differentiated ($V_0 = 0$) such that

$$\left(\frac{\partial x}{\partial C}\right)_{V_i} = -\frac{V_i \frac{dS'}{dC}}{\left(\frac{dS}{dC} + \theta\right)^2} \tag{10.60}$$

Based on the previous discussion, three types of ion exchange are of concern here. These include linear ($dS'/dC = 0$), favorable or convex isotherm ($d^2S/dC^2 < 0$), and unfavorable ($dS'/dC > 0$). In the case of linear exchange, $\partial x/\partial C = 0$ for any applied volume that indicates the initial profile is not altered during fluid flow through the soil. However, in the case of favorable exchange, there is a minor problem: according to equation 10.54, the slope of the solute front is negative ($\partial C/\partial x < 0$), but by using equation 10.60, we see that $\partial C/\partial x > 0$, implying that the solute front migrates faster at high-concentration than at low-concentration—physically impossible in the case of a step front. Thus, the rate of propagation should be

calculated using equation 10.57. Also, if the particular case of interest is not a step change, a sharpening effect typically occurs until a step front is actually established. Equation 10.60 indicates that for an unfavorable exchange at a C of interest, the concentration front flattens with increasing V_i; this produces solute spreading, or in simple terms, a decrease in the concentration gradient.

10.7 MATHEMATICAL MODELING OF TRANSPORT PHENOMENA IN SOILS

In the previous sections we discussed the basic physical processes and movement of solutes, the types of fluid flow that occur in the unsaturated zone, breakthrough curves, and nonreactive and reactive solutes. We now attempt to simplify the basic equations given thus far, with separate discussions of the various equations used for longitudinal dispersion, dispersion of a displacing front and a pulse, and various solutions and numerical calculations of these simple models, prior to discussing general solutions to the ADE.

Assuming that a fluid with an input concentration of C_0 is displacing another fluid of equal density and viscosity, there are basically two coordinate systems. One system is the moving-coordinate system of the fluid (Lagrangian method); the other, a fixed-coordinate system of the medium that allows physical measurement at specific points (Eulerian method). Without the fixed-coordinate system, it is difficult to measure between points within the moving fluid. For simplification purposes we also assume a coordinate system with space-coordinate x_1 and a time-variable of t_1. The transformation to the moving-coordinate system would be $x = x_1 + vt_1$ and $t = t_1$ where v is the velocity of the moving fluid, which also happens to be the velocity of the fixed-coordinate system. This allows for a fixed plane in the moving (x_1, t_1) system. Since the plane moves at velocity v and initially was at the sharp boundary (or interface) between the displacing and displaced fluid, the plane must always be $x_1 = 0$ in the moving-coordinate system. We determine $C(x_1, t_1)$ by the inverse such that $x = x_1 - t_1$ and $t_1 = t$ yields $C(x, t)$. By assuming dispersion in a capillary tube (linear flow), we have

$$q = -D\left(\frac{\partial C}{\partial x_1}\right) \tag{10.61}$$

where all parameters are as previously discussed. Also, following the rationale and considering the area, as stated in the solution of question 10.7 (at the end of the chapter), longitudinal dispersion is given as

$$\frac{\partial C}{\partial t_1} = D\left(\frac{\partial^2 C}{\partial x_1^2}\right) \tag{10.62}$$

which has the initial condition $C(x_1, t_1) = f(x_1)$ for $t_1 = 0$. The general solution for the dispersion equation is expressed as

$$C(x_1, t_1) = \frac{1}{2\sqrt{\pi D t_1}} \int_{-\infty}^{\infty} f(u) \exp\left[\frac{-(x_1 - u)^2}{4Dt_1}\right] du \tag{10.63}$$

This general solution is valid for $-\infty < x_1 < \infty$. By treating u as a dummy variable of integration that disappears when the definite integral involving u is evaluated,

$$f(u) = [C(x_1, 0)]_{x=U} = C(u, 0) \tag{10.64}$$

This is the formulated initial condition. As a final-boundary condition, we have $C(\infty, t_1) = 0$ for t_1 (finite) and $C(x_1, \infty) = 0$ for finite x_1. Consequently, $C(x_1, 0) =$ the concentration in the capillary tube at time $t_1 = t = 0$ and at $x_1 = x$ for which $x_1 = x$ is the starting position in the capillary tube of the fluid pulse that moves with dispersion; $C(x_1, t_1)$ depends on $C(x_1, 0)$.

QUESTION 10.8

Beginning with the longitudinal-dispersion equation 10.62, derive equation 10.63, the general solution of the one-dimensional dispersion equation.

10.8 FURTHER SOLUTIONS TO THE ADE: INITIAL AND BOUNDARY CONDITIONS

To obtain a solution to the ADE, we must select the appropriate initial and boundary conditions of the given transport problem, necessary and sufficient to guarantee a unique solution to the transport equation. Three types of boundary conditions are normally used in solute transport. These are: **(1)** the Dirichlet condition (boundary condition of the first kind), in which the value of a dependent variable is specified at every point of a boundary—sometimes referred to as a constant head or constant pressure boundary; **(2)** the Neumann condition, boundary condition of the second kind; in which the gradient of the pressure and gradient of the piezometric head are imposed on the boundary—sometimes called a constant-flux boundary; and **(3)** the Cauchy condition (boundary condition of the third kind), a mixed boundary condition in which the state variable of piezometric head and its gradient are imposed on the boundary. Also, a solution to the ADE has to consider the necessary source functions and constitutive relations. In addition to the initial and boundary conditions we also have to consider the types of concentrations the posed problem deals with. The typical concentrations used in transport phenomena are: time-averaged; volume or spatial averaging; and flux-averaged concentration. Mathematically, the time-averaged concentration C is expressed as

$$\overline{C}_t(x, y, z, t_0) = \frac{1}{\Delta t}\int_{t_0-(\delta t/2)}^{t_0+(\delta t/2)} C(x, y, z, t)\, dt \tag{10.65}$$

The spatial-averaged concentration (microscopic in this instance) is expressed as

$$\overline{C}_v(x_0, y_0, z_0, t) = \lim_{\Delta\, \delta v} \frac{\int_{\Delta v_L} C\, dv}{\int_{\Delta v_L} dv} \tag{10.66}$$

where C_v is the volume-averaged concentration, Δv is the soil volume of interest, Δv_L is the volume of the liquid phase in the Δv, dv is the (microscopic) differential-volume element, and δv is the representative elementary volume; all measured in L^3. The coordinates x_0, y_0, and z_0 are positions that are fixed at the center of the medium of interest. A representative elementary volume (REV) was defined for soil by Lauren et al. (1988) as a rule-of-thumb requiring a measurement area to contain at least 30 peds in cross-section, in order to be representative of a soil. This represents an estimate based on a morphological soil-structure analysis; the sample volume is primarily a function of soil structure, not the type of extraction device used to obtain an in-situ sample. The flux-averaged concentration (at a position of interest), $\overline{C}_f$, is expressed as

$$\overline{C}_f(t) = \frac{J_s}{J_v} \tag{10.67}$$

where the flux-averaged concentration represents the mass of solute per-unit volume of fluid passing through a specific cross-section for a specific time interval. Often, solute-flux distribution is of greater interest than pore-fluid concentrations (Parker and Van Genuchten 1984b). The basic relation between flux-averaged and volume-averaged concentrations is

expressed as

$$\overline{C_f} = \overline{C_v} - \frac{D}{v}\frac{\partial \overline{C_v}}{\partial x} \tag{10.68}$$

It is important to be able to distinguish between volume-and flux-averaged concentrations during an experiment as well as during data analysis. Most research typically expresses concentrations during transport as volume-averaged concentrations denoted by C, and not necessarily by $\overline{C_v}$.

We use a column of soil as an example for selecting initial and boundary conditions. To solve the ADE for transport through our column, we need to select the inlet and exit boundary conditions and initial condition; following Van Genuchten and Alves (1982), we write the initial condition as $C(x,t) = f(x)$ for $x > 0$ and $t = 0$ where $f(x)$ is an arbitrary function. The boundary condition at $x = 0$ for the Dirichlet problem is expressed as $C(x,t) = g(t)$ for $x > 0$ and $t > 0$. For the Cauchy problem (third type), the boundary condition is expressed as:

$$\left(-D\frac{\partial C}{\partial x} + vC\right)\Big|_{x\downarrow 0} = vg(t) \quad t > 0 \tag{10.69}$$

For this expression, $g(t)$ is also an arbitrary function that describes the concentration of the influent.

Continuing to use our column as an example, the exit-boundary conditions can be described for a column of finite length or a column of semi-infinite length. For the finite-length column, the exit-boundary condition that must be satisfied is

$$\left(-D\frac{\partial C}{\partial x} + vC\right)\Big|_{x\uparrow L} = vC_z \quad t > 0 \tag{10.70}$$

where C_z is the concentration at the exit, which we assume equals $C|_{x\uparrow L}$. As a result $[\partial C/\partial x](x,t) = 0$ for $x\uparrow L$ and $t > 0$. For a semi-infinite column the exit-boundary condition can be expressed as $[\partial C/\partial x](x,t) = 0$ for $x \to \infty$ and $t > 0$.

Analytical solutions for both conditions are similar. A mathematical solution for the Cauchy problem yields a conservation of mass-type equation and is therefore preferred for the inlet-boundary condition. A transition zone develops when the fluid moves through the soil column, that results in a fluid-concentration variance from the influent concentration. This occurs because the influent is not well mixed, which results in a boundary layer outside the medium. Thus, a certain amount of time is required for equilibrium to be achieved. Although the initial-boundary conditions given for the Dirichlet problem (first type) imply equal concentrations in both the medium and influent, this is not the case at first because the influent solution can only be injected at a specific rate. As a result, we have a displacement experiment which involves a step change in concentration such that $(g(t) < 0) = 0$ and $g(t > 0) = C_0$, and a Cauchy-type condition should be used as

$$\left(-D\frac{\partial C}{\partial x} + vC\right)\Big|_{x\downarrow 0} = vC_0 \tag{10.71}$$

where C_0 is the influent concentration. We are also aware that a discontinuity in C across the inlet boundary increases with increasing D/v. Solutions that are subject to first-type boundary conditions generally lead to flux-averaged concentrations, while solutions subject to the third-type (mixed or Cauchy) lead to volume-averaged concentrations.

Using this basic information we determine several analytical solutions for various inlet- and exit-boundary conditions. If we assume an infinite system $(-\infty < x < \infty)$, a solution for the general ADE (equation 10.5) can be obtained (by making a coordinates-transformation

so that $\xi = x - vt$ and $\tau = t$) which will transform equation 10.5 into

$$\frac{\partial C}{\partial \tau} = D\frac{\partial^2 C}{\partial \xi^2} \tag{10.72}$$

which has the original boundary and initial conditions of $C = C_i$ for $x > 0$ and $t < 0; x \to \infty$ and $t > 0$; also, $C = C_0$ for $x < 0$ and $t < 0; x \to -\infty$ and $t > 0$. These must be transformed as well. If we use an alternative transformation, then

$$\xi = \frac{x - vt}{\sqrt{4Dt}} \tag{10.73}$$

which yields an ordinary differential equation, such that

$$\frac{d^2 C}{d\xi^2} + 2\xi\frac{dC}{d\xi} = 0 \tag{10.74}$$

This equation has transformed initial and boundary conditions where $C = C_i$ for $\xi \to \infty$ and $C = C_0$ for $\xi \to -\infty$ with the solution

$$\overline{C} = \frac{(C - C_i)}{(C_0 - C_i)} = \frac{1}{2}\operatorname{erfc}\xi \tag{10.75}$$

We need to remember that coordinate transformation is not always convenient, and may not work for other types of boundary conditions.

Van Genuchten and Alves (1982) and Carslaw and Jaeger (1959) have shown that Laplace transforms can be an efficient tool for solving equation 10.5. Table 10.2 gives some analytical solutions for several inlet-and exit-boundary conditions.

TABLE 10.2 Analytical Solutions for Various Inlet and Exit Boundary Conditions (R assumed constant)

Inlet boundary condition	Exit boundary conditions	Analytical solution for selected boundary conditon
$\left(-D\frac{\partial C}{\partial x} + vC\right)\Big\|_{x=0} = vC_0$ case 1	$\frac{\partial C}{\partial x}(L, t) = 0$	$c = 1 - \sum_{m=1}^{\infty} \frac{\frac{2vL}{D}\beta_m\left[\beta_m \cos\left(\frac{\beta_m x}{L}\right) + \frac{vL}{2D}\sin\left(\frac{\beta_m x}{L}\right)\right]\exp\left[\frac{vx}{2D} - \frac{v^2 t}{4DR} - \frac{\beta_m^2 Dt}{L^2 R}\right]}{\left[\beta_m^2 + \left(\frac{vL}{2D}\right)^2 + \frac{vL}{D}\right]\left[\beta_m^2 + \left(\frac{vL}{2D}\right)^2\right]}$ $\beta_m \cot(\beta_m) - \frac{\beta_m^2 D}{vL} + \frac{vL}{4D} = 0$
$C(0, t) = C_0$ case 2	$\frac{\partial C}{\partial x}(L, t) = 0$	$c = 1 - \sum_{m=1}^{\infty} \frac{2\beta_m \sin\left(\frac{\beta_m x}{L}\right)\exp\left[\frac{vx}{2D} - \frac{v^2 t}{4DR} - \frac{\beta_m^2 Dt}{L^2 R}\right]}{\left[\beta_m^2 + \left(\frac{vL}{2D}\right)^2 + \frac{vL}{2D}\right]}$ $\beta_m \cot(\beta_m) + \frac{vL}{2D} = 0$
$\left(-D\frac{\partial C}{\partial x} + vC\right)\Big\|_{x=0} = vC_0$ case 3	$\frac{\partial C}{\partial x}(\infty, t) = 0$	$c = \frac{1}{2}\operatorname{erfc}\left[\frac{Rx - vt}{2\sqrt{DRt}}\right] + \sqrt{\frac{v^2 t}{\pi DR}}\exp\left[-\frac{(Rx - vt)^2}{4DRt}\right]$ $-\frac{1}{2}\left(1 + \frac{vx}{D} + \frac{v^2 t}{DR}\right)\exp\left(\frac{vx}{D}\right)\operatorname{erfc}\left[\frac{Rx + vt}{2\sqrt{DRt}}\right]$
$C(0, t) = C_0$ case 4	$\frac{\partial C}{\partial x}(\infty, t) = 0$	$c = \frac{1}{2}\operatorname{erfc}\left[\frac{Rx - vt}{2\sqrt{DRt}}\right] + \frac{1}{2}\exp\left(\frac{vx}{D}\right)\operatorname{erfc}\left[\frac{Rx + vt}{2\sqrt{DRt}}\right]$

Sources: Data from Brenner (1962); Cleary and Adrian (1973); Lindstrom (1976); and Lapidus and Amundson (1952) for cases 1 through 4, respectively.

TABLE 10.3 Solutions for C_x in Terms of the Peclet Number ($\mathcal{P}$) and Pore Volume, N_{pv} for the Analytical Solutions in Table 10.2

Case	Relative concentration of effluent upon exit from column
1	$C_x(N_{pv}) = 1 - \sum_{m=1}^{\infty} \dfrac{2\beta_m \sin(\beta_m) \exp\left[\dfrac{\mathcal{P}}{2} - \dfrac{\mathcal{P}N_{pv}}{4R} - \dfrac{\beta_m^2 N_{pv}}{\mathcal{P}R}\right]}{\beta_m^2 + \dfrac{\mathcal{P}^2}{4} + \mathcal{P}}$ $\mathcal{P}\beta_m \cot(\beta_m) - \beta_m^2 + \dfrac{P^2}{4} = 0$
2	$C_x(N_{pv}) = 1 - \sum_{m=1}^{\infty} \dfrac{2\beta_m \sin(\beta_m) \exp\left[\dfrac{\mathcal{P}}{2} - \dfrac{\mathcal{P}N_{pv}}{4R} - \dfrac{\beta_m^2 N_{pv}}{\mathcal{P}R}\right]}{\beta_m^2 + \dfrac{\mathcal{P}^2}{4} + \dfrac{\mathcal{P}}{2}}$ $\beta_m \cot(\beta_m) + \dfrac{\mathcal{P}}{2} = 0$
3	$C_x(N_{pv}) = \dfrac{1}{2}\operatorname{erfc}\left[\sqrt{\dfrac{\mathcal{P}}{4RN_{pv}}}(R - N_{pv})\right] + \sqrt{\dfrac{\mathcal{P}N_{pv}}{\pi R}} \exp\left[-\dfrac{\mathcal{P}}{4RN_{pv}}(R - N_{pv})^2\right] - \dfrac{1}{2}\left(1 + \mathcal{P} + \dfrac{\mathcal{P}N_{pv}}{R}\right) \operatorname{erfc}\left[\sqrt{\dfrac{\mathcal{P}}{4RN_{pv}}}(R + N_{pv})\right]$
4	$C_x(N_{pv}) = \dfrac{1}{2}\operatorname{erfc}\left[\sqrt{\dfrac{\mathcal{P}}{4RN_{pv}}}(R - N_{pv})\right] + \dfrac{1}{2}\exp(\mathcal{P}) \operatorname{erfc}\left[\sqrt{\dfrac{\mathcal{P}}{4RN_{pv}}}(R + N_{pv})\right]$

Source: Data from Van Genuchten and Wierenga (1986).

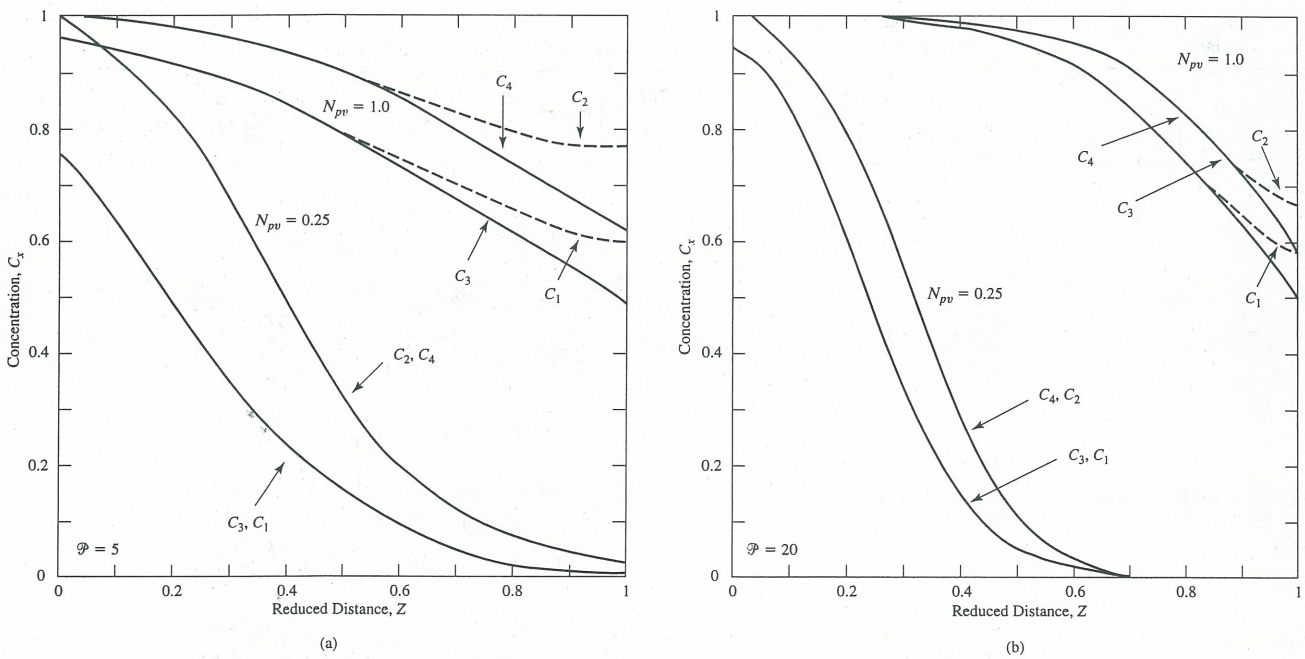

Figure 10.7 (a) A calculated concentration distribution for $R = 1$ and $\mathcal{P}$-value (Peclet number) of 5; (b) A calculated concentration distribution for $R = 1$ and $\mathcal{P}$-value for 20. N_{pv} refers to pore volume. These curves were obtained using the analytical solutions in table 10.3; C_1–C_4 refer to case 1 through case 4. Notice how solutions for C_1 and C_2 (dashed lines) deviate from remaining solutions.

We can rewrite equation 10.5 to reflect the Peclet number, $\mathcal{P}$, as one of its parameters. (The Peclet number and its effect on transport is discussed in detail in chapter 13.) The rewritten equation is expressed as

$$R\frac{\partial\left(\frac{C-C_i}{C_0-C_i}\right)}{\partial\left(\frac{vt}{L}\right)}=\frac{1}{\mathcal{P}}\frac{\partial^2\left(\frac{C-C_i}{C_0-C_i}\right)}{\partial\left(\frac{x}{L}\right)^2}-\frac{\partial\left(\frac{C-C_i}{C_0-C_i}\right)}{\partial\left(\frac{x}{L}\right)} \tag{10.76}$$

where $\mathcal{P}=vL/D$. Table 10.2 lists analytical expressions for $\overline{C}|_{(x/L)=1}=C_x$ where C_x is the exit concentration. The cases listed in table 10.3 correspond to the same initial and boundary conditions listed by case in table 10.2; the expressions listed in table 10.3 also involve the number of pore volumes (N_{pv}) along the column, which are expressed as vt/L.

Differences between the various boundary conditions on the concentration profiles are illustrated in figure 10.7a, b. Notice that at small t, the use of a first-type boundary condition (relative to other types) results in significant differences. Also, as solute concentration begins to increase at the column exit, a difference between the solutions for the finite and semi-infinite cases occurs. This is because the concentration at the inlet and outlet is not continuous nor is it likely to be. Generally, these solutions can predict solute concentration in a homogeneous media and can also be used to determine transport parameters such as D. As a general rule, the semi-infinite solution is favored.

10.9 NUMERICAL SOLUTIONS OF EQUILIBRIUM EXCHANGE

In the preceding sections, we discussed some fundamentals of solute transport, both with and without dispersion. In doing this, we obtained explicit expressions for the position of a solute front with approximate analytical solutions. This section focuses on numerical techniques that are normally required to solve the ADE because of the nonlinearity associated with exchange isotherms. An explicit finite-difference method was used by Lai and Jurinak (1971; 1972) to solve the ADE for nonlinear adsorption. The conditions assume use of a binary-exchange system for one-dimensional, steady-state flow and monovalent exchange. These authors introduce two dimensionless variables: $X_k=C_k/C_T$ and $Y_k=S_k/S_T$, which correspond to the solute-concentration in the liquid and adsorbed-phase, respectively. Lai and Jurinak (1972) obtain the following mathematical expression:

$$\frac{\partial X_k}{\partial t}=D(X_k)\frac{\partial^2 X_k}{\partial x^2}-v(X_k)\frac{\partial X_k}{\partial x} \tag{10.77}$$

where $D(X_k)$ represents the dispersion coefficient and $v(X_k)$ represents the velocity coefficient; both were adapted according to the following mathematical expressions

$$D(X_k)=\frac{D}{1+\left(\frac{\rho_b S_T}{\theta C_T}\right)f'(X_k)}$$
$$v(X_k)=\frac{v}{1+\left(\frac{\rho_b S_T}{\theta C_T}\right)f'(X_k)} \tag{10.78}$$

where $f'(X_k)=dY_k/dX_k$ and the denominator of equations 10.78 are simply the retardation factor R (as previously described), which depends on X_k because of nonlinearity in the exchange process.

For one-dimensional, steady-state conditions of multi-component equilibrium exchange in both homogeneous and layered media, Rubin and James (1973), showed that multiple fronts and plateau zones occur during multi-species transport problems. They used a varying total solute concentration in the liquid phase C_T. Using chromatography in a similar approach, Valocchi, Street, and Robert (1981) developed an analytical approach for multi-species transport of exchanging solutes. By including hydrodynamic dispersion and assuming electrolyte concentrations are not constant, the governing equation is

$$\theta \frac{\partial C_k}{\partial t} + \rho_b \frac{\partial S_k}{\partial t} = \theta D \frac{\partial^2 C_k}{\partial x^2} - J_v \frac{\partial C_k}{\partial x} \quad k = 1, 2, \ldots, n \tag{10.79}$$

and

$$\begin{aligned} C_T &= \sum_{k=1}^{n} C_k \\ S_T &= \sum_{k=1}^{n} S_k \end{aligned} \tag{10.80}$$

where C_T is the total-solute concentration in the liquid phase (variable) and S_T is the total-solute concentration in the adsorbed phase (assumed constant since it usually equals CEC). The exchange coefficient assumes an associated valence with the adsorbed species v_k, with a valence for the exchanging species j_k. Thus, the exchange coefficient is expressed as

$$K_{jk} = \left(\frac{Y_j}{X_j}\right)^{v_k} \left(\frac{X_k}{Y_k}\right)^{v_j} \tag{10.81}$$

where X and Y are dimensionless concentrations. The exchange coefficient, K_{jk}, is important because it affects the shape of the solute front. Equation 10.81 is a generalized solution; the use of activity coefficients makes it more accurate. However, in order to obtain a solution to the ADE, the number of dependent variables must be reduced. This is achieved by expressing S_k in terms of C_k, and by using the $n - 1$ independent-equilibrium expressions in combination with the second equation of equation 10.80. This leads to a multi-component exchange isotherm for a species k such that

$$S_k = F_k(C_1, C_2, \ldots, C_n) \quad k = 1, 2, \ldots, n \tag{10.82}$$

Substitution of equation 10.82 into equation 10.79 yields a set of n transport equations such that

$$\begin{aligned} \theta \frac{\partial C_k}{\partial t} + \rho_b \sum_{k=1}^{n} f_{jk} \frac{\partial C_j}{\partial t} &= D\theta \frac{\partial^2 C_k}{\partial x^2} - J_v \frac{\partial C_k}{\partial x} \\ f_{jk} &= \frac{\partial F_k}{\partial C_j} = \frac{\partial S_k}{\partial C_j} \end{aligned} \tag{10.83}$$

Equation 10.83 is easily solved by the Galerkin finite-element method. In many transport problems, the solute front is assumed to travel at a rate proportional to $t^{1/2}$; however, for a concave isotherm, $K_{jk} < 1$, the profile (front) of X_k generally travels at a rate proportional to t, which is similar to dispersion under Fick's law. In the case of a convex isotherm, $K_{jk} > 1$, the X_k front becomes steeper with distance traveled in the medium; both Helfferich (1962) and Brunauer (1945) discuss many different types of isotherms. Normally, ion exchange is influenced or induced by dispersion because of the mixing across the solute front as it passes through the medium. Because of nonlinear exchange, the retardation factor R is not constant, however. By assuming an effective, constant value for R, the effective velocity of the solute front is expressed as

$$v_e = \frac{v}{R} = \frac{dx_p}{dt} \tag{10.84}$$

where x_p is the equivalent depth of penetration of the solute front. This provides a way to calculate a constant value for R which may be used in cases where small or trace quantities of species are present in solution, for which linear exchange is almost always assumed. Generally, a constant R can be used with reasonable predictability if dispersion is negligible.

Various approaches are used for obtaining numerical solutions to the ADE. A popular approach used by Robbins, Jurinak, and Wagenet (1980a) is to use separate subroutines in the computer program to calculate cation exchange, complexation, and precipitation/dissolution. There are numerous computer packages on the market that facilitate the simulation of equilibrium chemistry, that involve various components and reactions (see chapter 13 for a list of such models). However, the authors and other researchers (Jennings, Kirkner, and Theis 1982) suggest direct insertion of these parameters (exchange, complexation, etc.) into the main transport-equation being used, which has been the methodology discussed thus far—that is, the inclusion of R. This is because convergence problems arise when the ADE and the model describing exchange, complexation, and so on (equilibrium chemistry), are combined. Jennings, Kirkner, and Theis (1982) express the dependency of solid-phase concentration to various quantities such that $S = f(C, S_T, t, x, \partial C/\partial t)$, which can easily be solved by the Galerkin finite-element method (Pinder and Gray, 1977; Kirkner, Jennings, and Theis 1985).

Abriola (1987) discusses various research which has been performed on contaminant-transport modeling. Generally, we carefully consider the type of chemical reaction when choosing the numerical-solution technique to be used for the problem. For example, Rubin (1983) described six broad classes of chemical reactions that occur during contaminant transport; each has its own mathematical expression unique to the reactions taking place.

10.10 NONEQUILIBRIUM CONDITIONS

In addition to instantaneous equilibrium, which is generally assumed between a solute in the liquid and adsorbed phase (both of which occur due to the exchange isotherm), two kinds of nonequilibrium exist in transport studies. These include physical and chemical nonequilibrium. As was discussed in chapter 8, liquid flow in the vadose zone is primarily by water films, which may be periodically discontinuous.

In contrast to physical nonequilibrium, chemical nonequilibrium is caused by kinetic-adsorption and exchange processes. Often, these processes are not instantaneous and the typical approach for a solution is to combine the ADE with a rate equation for chemical adsorption within the medium of interest. The physical constituents of a medium (clay, organic matter, sand, etc.) have a wide variety of exchange sites that are generally classified as type 1 (instantaneous) and type 2 (time-dependent). A rough approximation of first-order kinetics as applied by Selim, Davidson, and Mansell (1976a) expresses the general sorption rates for these phenomena as

$$\frac{\partial S_1}{\partial t} = \frac{\theta}{\rho_b} k_1 C - k_2 S_1 \tag{10.85}$$

where S_1 is the concentration of the sorbed solute (ML^{-1}) and k_1 and k_2 are the forward-rate reaction coefficients. This equation can also be written for backward reactions. For equilibrium conditions, the concentration of the sorbed solute can be expressed as

$$S_1 = \frac{\theta}{\rho_b} \frac{k_1}{k_2} C = K_1 C \tag{10.86}$$

and the sorbed concentration for all sites is $S = S_1 + S_2 = (K_1 + K_2)C = KC$. For time-dependent sites we write

$$\frac{\partial S_2}{\partial t} = \alpha(K_2 C - S_2) \tag{10.87}$$

where α is the first order rate coefficient (T^{-1}). Substitution into equation 10.5 (the normal ADE) yields

$$\left(1 + \frac{Kf\rho_b}{\theta}\right)\frac{\partial C}{\partial t} + \frac{\rho_b}{\theta}\frac{\partial S_2}{\partial t} = D\frac{\partial^2 C}{\partial x^2} - v\frac{\partial C}{\partial x} \tag{10.88}$$

where f is $S_1/S = K_1/K$, and the equation for the sorbed solute is expressed as

$$\frac{\partial S_2}{\partial t} = \alpha[(1 - f)KC - S_2] \tag{10.89}$$

and for a one-site model, $f = 0$ and the first term on the left-hand side of equation 10.88 drops out; also, S_2 is expressed simply as S; this also follows for equation 10.89.

A positive distinction between the physical and chemical nonequilibrium is not usually possible. As a result, Cameron and Klute (1977) conceived a "black box"-approach for describing the sorption process. Basically, they described two types of sites that are the same as those discussed for each of the models presented here; instantaneous and time-dependent, in which sorption of the time-dependent reaction is described kinetically and takes into account both the physical and chemical nonequilibrium conditions. Cameron and Klute (1977) divided their sites into two types expressing equilibrium (S_1) and kinetics (S_2), where exchange between ions in sorbed and liquid phases is via Freundlich (S_1) and kinetic (S_2) processes. Their solutions to the ADE involve Laplace transforms, and they were able to model atrazine, phosphorus, and silver transport successfully.

Nkedi-Kizza et al. (1983) fitted both a first-order reversible kinetic model and a diffusion-controlled model utilizing breakthrough curves. How fast equilibrium is achieved through the ion-exchange process is determined by two mechanisms: solute supply of the influent to the liquid–solid interface, and the nature of the exchange reaction. According to Helfferich (1962), the ion diffusion to the exchange sites is the rate-limiting step, even in cases of chemical nonequilibrium and when no immobile water is present. The physical nonequilibrium model is characterized by instantaneous equilibrium at mobile sites and diffusion-controlled equilibrium at immobile exchange sites, which is described by equation 10.111, later. For time-dependent sites, the kinetic nature of the exchange process is described by equations 10.88–89. If we express both models in dimensionless terms, they are the same and have nearly identical breakthrough curves.

Dependent on the physical parameters and phenomena being measured, the ADE can be generalized to include most equilibrium phenomena of interest in unsaturated zone hydrology. This includes: adsorption; precipitation; dissolution; radioactive decay; and additional chemical reactions. The following expression of the ADE was presented by Parker and Van Genuchten (1984a)

$$\frac{\rho_b}{\theta}\frac{\partial S}{\partial t} + \frac{\partial C}{\partial t} = D\frac{\partial^2 C}{\partial z^2} - v\frac{\partial C}{\partial z} - \mu_w C - \frac{\mu_s \rho_b}{\theta}S + \gamma_w + \frac{\gamma_s \rho}{\theta} \tag{10.90}$$

where μ_w and μ_s are rate constants based on first-order decay in the liquid and solid phase (T^{-1}) and γ_w ($ML^{-3}T^{-1}$) and γ_s (T^{-1}) are rate constants for zero-order production in the liquid and solid phases.

A category of reactions that are classified as chemical nonequilibrium are those of the radioactive-decay chain. Considering the transport of a single radionuclide species, the governing equation for two-dimensional transport in a variably saturated media is expressed as

$$\frac{\partial}{\partial x_i}\left(D_{ij}\frac{\partial C}{\partial x_j}\right) - \frac{\partial}{\partial x_i}(v_i C) = \frac{\partial}{\partial t}[\phi S_w C + \rho_s(1 - \phi)C_s] - qC^* + \lambda[\phi S_w C + \rho_s(1 - \phi)C_s] \tag{10.91}$$

where D_{ij} is the apparent hydrodynamic-dispersion tensor, C is solute concentration, v_i is the Darcy velocity, ρ_s is particle density, ϕ is effective porosity, C_s is the adsorbed concentration,

λ is the first-order decay coefficient, and C^* is the solute concentration in the injected fluid. By assuming that the relation between adsorbed and solution concentration is described by a linear-equilibrium isotherm equation 10.91 can be expressed as

$$\frac{\partial}{\partial x_i}\left(D_{ij}\frac{\partial C}{\partial x_j}\right) - \frac{\partial}{\partial x_i}(v_i C) = \frac{\partial}{\partial t}[\phi S_w R C] - qC^* + \lambda \phi S_w R C \tag{10.92}$$

where S_w is the water-phase saturation expressed as a percentage (also referred to as θ in some publications) and R, the retardation factor, is expressed as

$$R = 1 + \frac{\rho_s(1-\phi)k_d}{\phi S_w} = 1 + \frac{\rho_b k_d}{\phi S_w} \tag{10.93}$$

By expanding the convective and mass-accumulation terms of equation 10.92 and by using the continuity equation of fluid flow, and assuming that the time derivative of $(\rho_b k_d)$ is negligible, equation 10.92 reduces to

$$\frac{\partial}{\partial x_i}\left(D_{ij}\frac{\partial C}{\partial x_j}\right) - v_i\frac{\partial C}{\partial x_i} = \phi S_w R\left(\frac{\partial C}{\partial t} + \lambda C\right) + q(C - C^*) \tag{10.94}$$

The term $q(C - C^*)$ is zero in cases where q corresponds to the specific discharge of a pumped well because $C \equiv C^*$. The hydrodynamic dispersion tensorial components can be computed by the method of Scheidegger (1961) such that

$$D_{11} = \frac{D_L(v_1)^2}{|v|} + \frac{D_T(v_2)^2}{|v|} + D^0 \tag{10.95}$$

$$D_{22} = \frac{D_L(v_2)^2}{|v|} + \frac{D_T(v_1)^2}{|v|} + D^0 \tag{10.96}$$

$$D_{12} = D_{21} = (D_L - D_T)\frac{v_1 v_2}{|v|} \tag{10.97}$$

where the subscripts L and T of D refer to longitudinal and transverse dispersion and D^0 (apparent molecular-diffusion coefficient) $= \phi\tau D_m$, where D_m is the free-water molecular-diffusion coefficient and τ is evaluated using the relation of Millington and Quirk (1961), such that $\tau = \phi^{4/3}S_w^{10/3}$.

For the transport of a chain of decaying-solute species, the following equation can be used

$$\begin{aligned}\frac{\partial}{\partial x_i}\left(D_{ij}\frac{\partial C_l}{\partial x_j}\right) - v_i\frac{\partial C_l}{\partial x_i} &= \phi S_w R_l\left(\frac{\partial C_i}{\partial t} + \lambda_l C_l\right) + q(C_l - C_l^*) \\ &\quad - \sum_{m=1}^{M}\phi S_w \xi_{lm} R_m \lambda_m C_m, \quad l = 1, \ldots, n_c\end{aligned} \tag{10.98}$$

where the subscript l denotes the chemical component, n_c is the number of components in the chain, ξ_{lm} is the mass fraction of the parent component m transforming to the daughter component l, and M is the number of parents transforming to l. For radioactive decay, λ_l is related to the half-life by $\lambda_l = ln\ 2/(t_{1/2,l})$. Initial and boundary conditions associated with equation 10.98 can be expressed as

$$C_l(x_1, x_2, 0) = C_{l0} \tag{10.99}$$

$$C_l(x_1, x_2, t) = \overline{C}_l \quad \text{on} \quad B_1 \tag{10.100}$$

$$D_{ij}\frac{\partial C_l}{\partial x_j}n_i = q_{Cl}^D \quad \text{on} \quad B_2 \tag{10.101}$$

$$D_{ij}\frac{\partial C_l}{\partial x_j}n_i - v_i n_i C_l = q_{Cl}^T \quad \text{on} \quad B_3 \tag{10.102}$$

For a decaying source, the prescribed concentration, $\overline{C}$, or prescribed contaminant flux, q_{Cl}^T, is time-dependent and governed by Bateman's equation:

$$\frac{d\overline{C_l}}{dt} = -\lambda_l C_l + \sum_{m=1}^{M} \xi_{lm}\lambda_m \overline{C_m} \quad \text{where} \quad \overline{C_l}(t=0) = \overline{C_l^0} \tag{10.103}$$

For an n_c-member chain, the general solution of equation 10.103, subject to the prescribed concentration at $t = 0$, is expressed as

$$\begin{aligned}\overline{C_l} = \overline{C_l^0}\, e^{-\lambda_l t} + \xi_{l,l-1}\lambda_{l-1}\overline{C_{l-1}^0} \sum_{m=l-1}^{l} \frac{e^{-\lambda_m t}}{\prod_{\substack{k=l-1 \\ k\neq m}} l(\lambda_k - \lambda_m)} \\ + \cdots + \xi_{l,l-1}\lambda_{l-1}\xi_{l-1,l-2\ldots}\,\xi_{21}\lambda_1\overline{C_l^0} \cdot \sum_{m=1}^{l} \frac{e^{-\lambda_m t}}{\prod_{\substack{k=1 \\ k\neq m}} l(\lambda_k - \lambda_m)}\end{aligned} \tag{10.104}$$

where l ranges from 1 to n_C, and $\overline{C_l^0}$ $(l = 1, \ldots, n_c)$ are initial source concentrations of components 1 through n_C, and λ_1 $(l = 1, \ldots, n_C)$ are source-decay coefficients. Equation 10.104 assumes a step release of dissolved contaminants at the source—that is, all waste material begins to dissolve at $t = 0$ and distribution is allowed to proceed continuously at a uniform rate. If we wish to perform a pulse release of duration T of the contaminant, equation 10.104 must be modified by multiplying the right-hand side by $f = [U(t) - U(t - T)]$ where $U(t - T)$ is the Heaviside unit function, defined by

$$U(t-T) = \begin{pmatrix} 1, t \geq T \\ 0, t < T \end{pmatrix} \tag{10.105}$$

The use of the equations for chained-decay transport in this section makes some major assumptions on their adequate use. These assumptions presuppose that the air phase is static—that is, water is the only flowing fluid phase; flow of the fluid phase is considered isothermal and governed by Darcy's law; the fluid is only slightly compressible and homogeneous; and the medium is also homogeneous. Also, solute transport is governed by Fick's law and adsorption and decay are described by a linear-equilibrium isotherm and a first-order decay constant. For the case of a straight three-member chain, an analytical solution can be found

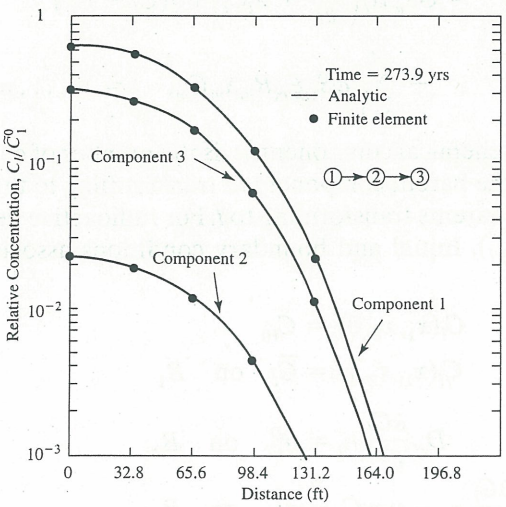

Figure 10.8 Simulated concentration profiles for the case of straight chain radionuclide decay, showing comparison of analytical and finite element solutions (data from Huyakorn et al. 1992)

TABLE 10.4 Parameter values for one-dimensional transport of three-member radioactive-decay chains

	Radionuclide properties			
Component l	$t_{1/2}$ yrs	λ_l yrs^{-1}	R_l	C_l^0
1	433	0.0016	9352	1
2	15	0.0462	9352	0
3	6540	0.0001	9352	0

in Coats and Smith (1964). Using both analytical and numerical solutions, the transport of a chain of three radionuclides released from a source located at $x = 0$ in a confined porous medium reservoir, is shown in figure 10.8. The properties used for transport calculation for the three radionuclides are listed in table 10.4.

10.11 COMBINED EFFECTS OF ION EXCHANGE AND DISPERSION

In chapter 7 we discussed how hydraulic conductivity could be calculated through a layered soil by summing the resistance associated with each layer. Using a similar idea and analytical techniques, the physical-dispersion effects for an unsaturated soil can be combined into one dispersion length (L_D). This was done by Bolt (1982), who attempted to include ion exchange as well. Frissel, Poelstra, and Reiniger (1970) showed that a column-averaged L_D value could be used. Assuming constant L_D, equation 10.49 can be used, and if one also assumes a linear exchange (dS/dC) is constant and can be divided through by R, the analytical solution for the resulting equation can be used, the basic ADE.

For favorable exchange, the solute front in the liquid phase generally lags behind the solute front in the adsorbed phase. In terms of effective retarded velocity (v_r), equal to the right-hand side of equation 10.57 at steady-state, solutes at low concentration will travel at velocities less than v_r, while those at high concentration will travel at velocities greater than v_r. With time, a steady front will be formed with respect to the moving coordinate, steady-state. For steady-state, the propagation of the solute front is expressed as

$$\left(\frac{\partial x}{\partial t}\right)_C = \frac{J_v}{(dS/dC) + \theta}\left[1 - L_D \frac{\partial(\partial C/\partial x)}{\partial C}\right] \tag{10.106}$$

for which Bolt (1982) determined (analytically) the adsorbed and liquid concentrations.

For unfavorable exchange, the ADE must be solved numerically to describe the solute front. This is due to the lack of development of a steady front with respect to the moving coordinate, because dispersion, diffusion, and ion exchange cause high concentrations to travel slower than low concentrations.

10.12 MOBILE AND IMMOBILE REGIONS IN SOILS

Due to the structure of soil, pockets of air are generally present within soil pores regardless of water content. It is well known, that after purging a medium with carbon dioxide and then saturating it from bottom to top, there is entrapped air that is virtually impossible to remove. The description of mobile and immobile regions within a medium has been widely used, in direct relation to this phenomena. The concept of mobile and stagnant areas of transport was

first used by Coats and Smith (1964) later expanded on by Van Genuchten and Wierenga (1976), and has been widely used and explained by numerous other scientists since then. The concept is simple—wetted-pore space is represented by two different water contents: a mobile-water content θ_m, through which water flows; and an immobile water content $\theta_{im} = \theta_s - \theta_m$, in which water is stagnant and does not flow, but which can be pushed out at various times due to high-recharge events. The concentration of solute under these conditions is represented by the same subscripts. As we might suspect, a solute in the mobile phase is transported via advection and dispersion due to water flow, while the solute in the immobile (stagnant) area is transported via diffusion processes that are typically rate-limited.

Normally, as aggregate size increases (as in a well-structured clay) and velocity of flow decreases, the amount of immobile water will increase. The concept of mobile and immobile water not only applies to structured soils, but also to other media types according to De Smedt and Wierenga (1979a, b, 1984), who applied this argument to glass beads (an unstructured system); it was discovered that concentration of the effluent was accurately predicted only when accounting for both types of water content. Without use of the immobile phase, a very high dispersion coefficient is needed in order to fit the experimental data with the ADE. However, Philip (1968a, b) discovered that only during initial stages of the diffusion process was transient diffusion different for mobile and immobile regions. Philip (1968) also found that during initial infiltration, the dimensionless cumulative-diffusive flux obeyed a $t^{1/2}$ time law for the mobile region and the immobile region obeyed a $t^{3/2}$ time law, but shortly after the initiation of the diffusive process, the cumulative-diffusive flux of both regions again obeyed a $t^{1/2}$ time law. Consequently, he argued that dead-end porosity is inconsequential and that there is an unwarranted distinction between the two regions of flow; other researchers (Smiles et al. 1978b; Warrick, Biggar, and Nielsen 1971; Kirda, Nielsen, and Biggar 1974) agree with Philip, but only for non-aggregated media. This is due primarily to the presence of macropores and preferential pathways in various soils found to be significant in transporting herbicides and other chemicals (White 1985; Edwards et al. 1990; Delin and Landon 1993; Tindall and Vencill 1993, 1995).

Such disagreements are not uncommon due to spatial variability of the medium used by the researchers, as well as the physical, chemical, and biological characteristics of both the medium and the chemical being studied. The above argument is similar to the determination by various researchers, as to whether or not the dispersion coefficient D is either velocity-dependent or velocity-independent. Smiles and Philip (1978a) found no dependence of D on v during infiltration of KCl into a mixture of kaolinite and sand. Pfannkuch (1963) reported that D was independent of v but in order for this to be true, the Peclet number, $\mathcal{P}$, was less than one (i.e., $\mathcal{P} = vd/D_e$). Watson and Jones (1982) found D to be dependent on v, but they used high $\mathcal{P}$ numbers ($P > 35$), whereas the previous researchers were using $\mathcal{P} < 1$. This is plausible since dispersion is the more active process at higher pore-water velocities, and diffusion is more prevalent at low pore-water velocities.

Aggregated Soils

In the earlier section on breakthrough curves we discussed how aggregated media affects the shifting and shape of a typical breakthrough curve. Water flow through media with large aggregates is complex; it is directly related to both immobile and mobile regions within the medium, and the amount of preferential flowpaths within the medium (preferential flowpaths and macropores are discussed in the next section). As a result, there has been considerable recent attention to the transport of industrial and agricultural chemicals through aggregated media, because chemicals and water applied to them can be lost due to bypass, preferential flow, or macropore flow. Not only is flow different, but chemical and microbiological effects on the applied (or spilled) chemical to the medium can be quite different than

in less-structured media; this applies particularly to inter- versus intra-aggregate pore space within the medium.

Because of these processes, the resulting source/sink terms are more complex, for which the ADE must be modified significantly to explain and describe exchange inside the solid (aggregate) particles. Within aggregated media, we normally need to distinguish the difference between micropores and macropores. Micropores are located inside the aggregates, through which flow is a diffusive process; macropores are located between the aggregates, through which flow is advective (sometimes called dispersive, viscous, or convective). When pore-water volume increases during rainfall or other recharge events, advective flow can completely dominate the system. It is within such systems that the definition of mobile versus immobile regions plays a major role in formulation of the ADE and its solution.

Passioura (1971) and Passioura and Rose (1971) obtained the following simplified form of the ADE to describe flow and transport in aggregated media

$$\frac{\theta_{im}}{\theta_{mo}}\frac{\partial C_{im}}{\partial t} + \frac{\partial C_{mo}}{\partial t} = D_{mo}\frac{\partial^2 C_{mo}}{\partial x^2} - v_{mo}\frac{\partial C_{mo}}{\partial x} \tag{10.107}$$

where the subscripts *mo* and *im* refer to mobile and immobile phases, respectively. The immobile phase inside the aggregate is treated as a distributed sink and D_{mo} is the diffusion coefficient of the mobile-liquid phase. The concentration of the chemical in both phases for equation 10.107 is not usually known, so we have to resort to a simpler form of the ADE (equation 10.5), that uses an effective dispersion coefficient D. This entails a combination of advective dispersion in the mobile phase of the aggregated media, and the stagnant phase within the aggregate. If one assumes steady-state, then the implication is that

$$\frac{\partial C_{mo}}{\partial x} = \frac{\partial C}{\partial x} \tag{10.108}$$

Following this assumption, Passioura (1971) developed the following expression for the dispersion coefficient within an aggregate

$$D_{im} = \frac{\theta_{im}}{\theta_T}\frac{v^2 a^2}{15 D_{eim}} \tag{10.109}$$

where θ_T is the total-volume fraction (air and water) and the subscript e denotes effective-dispersion coefficient. The diffusion coefficient for intra-aggregate (macropore) flow can be expressed by

$$D_{mo} = D_{emo} + v_{mo}a \tag{10.110}$$

where v is aggregate pore-water velocity and a is aggregate radius. Measurement of a strict θ in either phase is not easy to obtain; however, θ_{im} can be considered to be the water content at matric potentials less than 7–10 kPa (Rose and Passioura 1971a; Tindall and Vencill 1995). Thus, after obtaining θ_T and that for the immobile phase (based on matric potential), the water content for the mobile phase can be determined by difference.

For aggregated media, flow is also primarily in the void space between aggregates. For large-aggregate sizes, unsaturated flow is more likely to be discontinuous than for small-particle sizes. The flow in large aggregates can become discontinuous at higher-water contents due to entrapped air. Because of aggregate size, the influent solute will not reach all sorption sites immediately, and instantaneous exchange cannot occur. Mobile and immobile flow regions occur within an aggregated soil, where the immobile region is within the aggregates. This results in advective flow in the mobile regions (between aggregates) and diffusive flow within the aggregates, which causes the concentration within the immobile region to lag behind that in the mobile region; this is true for both the liquid and adsorbed phase. As one might suspect,

the greatest number of adsorption sites is within the aggregate, and after an initial-recharge event, flow through the medium becomes a reversible, diffusion-controlled event between the mobile and immobile regions. For a mobile–immobile region medium, considering physical nonequilibrium, Van Genuchten and Wierenga (1976) expressed the ADE as

$$\theta_{mo}\frac{\partial C_{mo}}{\partial t} + \theta_{im}\frac{\partial C_{im}}{\partial t} + \rho_b f\frac{\partial S_{mo}}{\partial t} + \rho_b(1-f)\frac{\partial S_{im}}{\partial t} = \theta_{mo}D\frac{\partial^2 C_{mo}}{\partial x^2} - \theta_{mo}v_{mo}\frac{\partial C_{mo}}{\partial x} \quad (10.111)$$

This equation was modified after Coats and Smith (1964), where f is the fraction of sorption sites in direct contact with the mobile region of the liquid, and m and im subscripts refer to mobile and immobile regions. Equation 10.111 is exactly the same as equation 10.107, but with the sorption terms. For transfer in the liquid phase between the two regions we write

$$\theta_{im}\frac{\partial C_{im}}{\partial t} + \rho_b(1-f)\frac{\partial S_{im}}{\partial t} = \alpha(C_m - C_{im}) \quad (10.112)$$

where α is the mass-transfer coefficient with units T^{-1}. Other processes within the medium correspond to these same types of parameters. An excellent example is anion exclusion, in which the volume of exclusion is basically equivalent to the immobile region expressed above.

The presence of aggregates in soil causes limited accessibility of fluid to adsorption and exchange sites; this is generally due to physical nonequilibrium, where it is often appropriate to utilize an effective-dispersion coefficient for aggregates of particular shapes or sizes, since it allows omission of the source-sink term describing mass transfer in the stagnant-liquid phase. Adsorption in mobile and immobile regions within the vadose zone have been treated by Van Genuchten and Wierenga (1976), Selim, Schulin, and Fluhler (1987), Bolt (1982), and others. Without longitudinal diffusion or dispersion, as in the previous equation, the ADE is written as

$$\theta_{mo}\frac{\left(\frac{\Delta S}{\Delta C} + \theta_{im}\right)}{\theta_{mo}}\frac{\partial C_{im}}{\partial t} + \theta_m\frac{\partial C_{mo}}{\partial t} + J_v\frac{\partial C_{mo}}{\partial x} = 0 \quad (10.113)$$

which is easily solved by using a transformation to obtain scaled variables and choosing a position-dependent time. Van Genuchten (1981) calls this solution a Goldstein J-function.

While the approach above is useful, the stagnant-phase effect can be described after Crank (1975) by an equivalent length parameter (L_r). For spherical aggregates with radius r, Crank's expression in the event of ion exchange is

$$\frac{\partial\left(\frac{dS}{dC} + \theta_{im}C_{im}\right)}{\partial t} = \frac{15}{r^2}\theta_{im}D(C_{mo} - C_{im}) \quad (10.114)$$

and

$$k_a = \frac{15D}{r^2}\frac{\theta_{im}}{\theta_{mo}} \quad (10.115)$$

where k_a is a rate constant (T^{-1}) for diffusion inside an aggregate, for which instantaneous chemical equilibrium is assumed. This allows the expression of L_r in terms of k_a. The primary advantage of this method is that all effects are taken into account by one value for a dispersion length that allows the ADE to be solved analytically.

Using a nonreactive solute, Scotter (1978) found that theoretical-breakthrough curves, in the presence of large channels, indicated a considerable amount of solute appeared in the effluent before one pore volume had leached through. Using Scotter's (1978) pore-geometry approach for cylindrical channels, Van Genuchten, Tang, and Guennelon (1984) developed

an analytical solution for transport through cylindrical macropores. In this instance, the cylindrical macropore represents the mobile phase and the surrounding medium represents the smaller pores or immobile-phase of liquid flow. Van Genuchten, Tang, and Guennelon (1984) also used fractions to represent adsorption sites in contact with the mobile and immobile phases, as well as separate retardation factors for each phase. During the initial or early-time, the medium surrounding a macropore is considered semi-infinite, and dispersion within the macropore can generally be ignored without loss in predictability. This approach is now widely accepted when describing solute transport in aggregated soils.

QUESTION 10.9

Assuming linear adsorption for both the mobile and immobile phase, write a general form of the ADE for reactive-solute transport.

Fractured Media

Interest in transport through fractured media has increased in recent years because of the desire to dispose of hazardous wastes in fractured bedrock. The formulation of the ADE for transport in fractured media is similar to that in aggregated media. For example, the macropore in aggregated soil becomes the fissure in fractured rock, which accounts for advective flow. Diffusive flow (or the immobile region) in fractured media is simply diffusion into the rock matrix rather than the aggregate, as in aggregated soils. Although some analytical solutions are available, most solutions are typically numerical.

The transport parameters and processes that need to be delineated within fractured media include: **(1)** advective flow and transport along the fracture length; **(2)** mechanical dispersion longitudinally along the fracture; **(3)** molecular diffusion from the fracture into the porous rock matrix; **(4)** molecular diffusion within the fracture itself (along the fracture axis); **(5)** adsorption onto the matrix face along the fracture; **(6)** adsorption within the porous rock matrix; and **(7)** radioactive (first-order) decay. As previously mentioned, diffusion of a chemical into an aggregate or rock matrix greatly reduces the transport time of the chemical, and allows for microbial decay, half-life degradation, and greater adsorption within the matrix. Tang, Frind, and Sudicky (1981) used the following equation for solute transport within a fractured media, using the general principles outlined so that

$$\frac{\partial C_{mo}}{\partial t} = \frac{D}{R_{mo}}\frac{\partial^2 C_{mo}}{\partial z^2} - \mu_b C_{mo} + \frac{\theta D_{eim}}{\partial x}\frac{\partial C_{im}}{\partial x}\bigg|_{x=b} - \frac{v}{R_{mo}}\frac{\partial C_{mo}}{\partial z} \tag{10.116}$$

where μ_b is the decay constant (T^{-1}), $2b$ is the mean fracture width (L), $R_{mo} = 1 + (\rho_b/\theta)(K_{dmo})$ is the retardation factor, K_{dmo} is the coefficient of distribution within the fracture, and θ is the unsaturated water content. Transport inside the porous rock can be described by

$$\frac{\partial C_{im}}{\partial t} = \frac{D_{eim}}{R_{im}}\frac{\partial^2 C_{im}}{\partial x^2} - \mu_b C_{im} \tag{10.117}$$

where D_{eim} is the effective-diffusion coefficient within the rock matrix, $R_{im} = 1 + (\rho_b/\theta)(K_{dim})$ is the retardation factor, z is the vertical direction on the x, y, z plane, x is the horizontal direction, and K_{dim} is the coefficient of distribution within the rock matrix. For both equations 10.116 and 10.117, linear adsorption is assumed. By using Laplace transforms, Tang, Frind, and Sudicky (1981) solved these equations analytically for both specific initial and boundary conditions. Rasmuson and Neretnieks (1981) and others have also investigated the transport of decaying radionuclides through fractured rock. Generally, it has been discovered that advective dispersion within fractures results in longer travel distances for

radionuclides, which has the effect of decreasing diffusion into the rock matrix; thus, movement is hinderered so that the radionuclide often decays before it reaches ground water. Consequently, matrix diffusion can prevent or reduce contamination of underlying aquifers with low-level, decaying radionuclides.

What has been termed a stratified approach was used by Neretnieks (1983) to determine transport of radionuclides through fractured rock; basically, this assumed flow through parallel channels of different size. This is analogous to Pouiselle's law, in which flow is assumed through a bundle of capillary tubes. For stratified flow, the width of the zone of dispersion, σ, is proportional to the distance traveled x instead of $x^{1/2}$, as in Fick's law of diffusion. Consequently, any increase in the observation distance yields a larger value for D if the ADE is used to describe transport in such media. The implication is that using Fick's law to extrapolate over large distances and times can have significant consequences, and error in some applications. Thus, for larger distance and residence times, the effects of stratified flow and matrix diffusion become major factors in comparison with the effects of hydrodynamic dispersion.

Layered Media

Transport of solutes through layered soil is a very important aspect of unsaturated zone hydrology because most natural systems (soil profiles) have a distinct stratification due to factors of profile development (see chapter 2). As a result, much research has been conducted on contaminant transport through layered soils and stratified aquifers. For example, many laboratory experiments are set up such that a loam-soil layer overlies a sand layer, or a sand or loam layer might overlay a clay layer so that there is a distinct discontinuity in characteristics. Typical experiments have investigated wetting fronts, water retention, and solute transport. By adding a short pulse of solute to the inlet end of layer one and measuring the effluent concentration at $z = L_1$, the time of solute travel can be determined for layer one. However, the travel time for the solute in underlying layer two cannot usually be measured directly because of the inability to apply a short pulse of solute to the inlet end of layer two. As a result, the concentration of the effluent is typically measured at $z = L_1 + L_2$ and time, $t = t_1 + t_2$.

To complicate matters further, each layer generally has different physical, chemical, and hydraulic properties; all of these affect sorption, microbial degradation, and subsequent transport of the chemical of interest. Thus, a different behavior in transport of the chemical should be expected in layered media. In cases where an overlying soil layer has significant advective transport compared to a minimal advective transport in the underlying layer, significant spreading and tailing of the solute front occurs when flow is parallel to stratification. In such cases, a large D is obtained if we use the generalized form of the ADE. It is naturally assumed that the media is heterogenous due to layering, and under such conditions Gillham et al. (1984) indicate that no Fickian dispersion would occur; but in the case of large transport times and nonuniform velocity fields, Fickian dispersion occurs (Gupta and Bhattacharya 1986). The latter case is generally expected, due to spatial variability of soils.

Sudicky, Gillham, and Frind (1985) investigated the transport of chloride in a thin sand layer between two silt layers that were water saturated. The solution was injected into the sand layer to investigate horizontal flow parallel to the silt layers; within the sand layer, advective flow occurred. From the sand to the silt layers, transverse diffusion occurred, and molecular diffusion occurred in the silt layers, which was transverse to the direction of flow. It is likely that complete mixing occurred in the sand, thus the general form of the ADE was

$$\frac{\partial C_{mo}}{\partial t} = D_T \frac{\partial^2 C_{mo}}{\partial y^2} - v \frac{\partial C_{mo}}{\partial x} \tag{10.118}$$

In this case, the diffusion from the sand to silt layers is transverse dispersion D_T, C_{mo} is the concentration of chloride in the sand layer, and the x direction is parallel to layering. The movement of the solute in the silt layers, for which there is no advective velocity, is represented by a diffusive form of the ADE such that

$$\frac{\partial C_{im}}{\partial t} = D_e \frac{\partial^2 C_{im}}{\partial y^2} \tag{10.119}$$

where C_{im} is the concentration of solute in the silt layers and D_e is the effective-diffusion coefficient for the silt. This is a clear case of a nonuniform-velocity field, exhibiting strong dispersion due to interlayer transport of the chemical.

By assuming a linear-exchange constant K_d, Starr, Gillham, and Sudicky (1985) used the same system with a reactive solute, ^{85}Sr. The general form of the ADE could not be used for the reactive solute due to poor performance at high-flow velocities; thus, neglecting D_L, transport in the sand layer was described by

$$\frac{\partial C_{mo}}{\partial t} = \frac{\theta_{im}}{\theta_{mo}} \frac{D_e}{R_{mo} b} \frac{\partial C_{im}}{\partial y}\bigg|_{y=b} - \frac{v}{R_{mo}} \frac{\partial C_{mo}}{\partial x} - \mu C_{mo} \tag{10.120}$$

where the width of the sand layer is $2b$ and other parameters are as previously discussed.

Marle et al. (1967) showed that depth-averaged moments can account for heterogeneity due to layering or stratification. Fischer et al. (1979) investigated transport in soil with depth h that was bounded by impermeable layers at $y = 0$ and $y = h$, and for which the magnitude of flow in the x-direction depends on y. For a moving-coordinate system, the transport equation is

$$\frac{\partial C}{\partial t} = D\left(\frac{\partial^2 C}{\partial \xi^2} + \frac{\partial^2 C}{\partial y^2}\right) - v' \frac{\partial C}{\partial \xi}$$
$$v' = v - \bar{v}; \qquad \xi = x - \bar{v}t \tag{10.121}$$

where ξ is the cartesian coordinates in a moving-coordinate system, and the overbar notation indicates a depth-averaged value such that

$$\bar{v} = \frac{1}{d}\int_0^h v\, dy \tag{10.122}$$

The spatial moments can be expressed as

$$m_p = \int_{-\infty}^{\infty} \xi^p C(\xi, y, t)\, d\xi \tag{10.123}$$

The operator defined by equation 10.123 is applied to the individual terms of equation 10.34. If one assumes that $C = 0$ and $\partial C/\partial \xi = 0$ for $\xi \to \pm\infty$, then

$$\frac{\partial m_p}{\partial t} = D\left[p(p-1)m_{p-2} + \frac{\partial^2 m_p}{\partial y^2}\right] + v' p m_{p-1} \tag{10.124}$$

Equation 10.124 is averaged over depth according to equation 10.122, resulting in

$$\frac{\partial \overline{m_p}}{\partial t} = Dp(p-1)\overline{m_{p-2}} + p\overline{v' m_{p-1}} \tag{10.125}$$

The depth-averaged moment m_p is sequentially solved for $p = 0, 1, 2, \ldots, n$ and using the theory of statistical moments, we can characterize solute concentration and distribution by determination of the variance, skewness, mean, and other parameters. For an example, the reader can read Marle et al. (1967), which shows how the moment method can be applied to multi-layered soil. Other researchers (Fried and Combarnous 1971; Guven et al. 1984; Guven and Molz 1986) have used the moment method with good results.

Because soils often do not consist of homogeneous layers with distinct physical and hydraulic characteristics, this strongly influences the parameters within the ADE, leaving a complicated case of solute transport; this is especially true if velocity varies both longitudinally and transversely. As a result, many models use a black-box type approach, where each layer is assumed to have homogeneous properties. This approach has been used with fair success with the pesticide root-zone model, PRZM, developed by the U.S. Environmental Protection Agency (Carsel et al. 1984).

In undisturbed, naturally structured, and layered media with existing macropores and flow channels, only partial displacement of resident soil-water and solutes by incoming solutions occurs. Intact cores in the laboratory are a common tool to address questions involving the characterization and predictability of solute transport in such media. Also, core size has a significant effect on results; generally, the larger the core, the more comparable the results are to collected field data. Since heterogeneity of field soils normally is large, the use of laboratory-measured hydrodynamic-dispersion coefficients is sometimes not appropriate with the typical core sizes used. Bouma (1979) and Bouma et al. (1979) indicate that field variability is strongly reduced by using cores with a volume of 10 L or larger. Tindall, Hemmen, and Dowd (1992) and Tindall and Vencill (1995) have obtained good agreement between laboratory- and field-transport parameters for herbicides using intact cores 28 L in size—that is, 15 cm diameter by 40 cm height.

10.13 PREFERENTIAL FLOW PATHS, MACROPORES, AND FINGERING

In 1980, it was discovered that more than 1,000 wells on eastern Long Island, New York, had been contaminated by the herbicide aldicarb (Baier and Moran 1981). It has been generally perceived that herbicides and many other chemicals have a long residence time within soils, and are strongly adsorbed. Due to adsorption as well as biological and chemical processes, it was commonly assumed that most chemicals would be permanently degraded or "bound" within the soil profile, thereby preventing ground water contamination. Since the early 1980s, researchers have increasingly reported the unexpected rapid movement of chemicals through the vadose zone to ground water. This can be due in part to the greater technological advances in measurement techniques of various chemicals; however, the governing processes through which contamination has occurred have not changed.

Field and laboratory experiments on adsorption and leaching suggest that agricultural and industrial chemicals have relatively limited mobility, and most chemical residues are confined to the surface horizon of soils. However, when scientists observed chemical residues that were at greater depths in the profile than expected (based on classical assumptions of solute transport), doubts arose about sampling and analysis techniques, and unexplained point-source contamination. Eventually, scientists rediscovered the principle of preferential flow.

Lawes, Gilbert, and Warington (1882) described preferential flow over 100 years ago. These scientists described the basic difference between matrix flow and preferential flow, and illustrated that matrix flow will predominate in less-structured media, while in structured media such as clays, preferential flow will dominate; the preponderance of one type of flow compared to the other will have significant impacts on solute transport. Despite the fact that large pores were recognized as conduits for rapid flow, it was not until the 1970s that soil physicists started to quantify the impact of preferential flow on solute transport and related recharge of ground water. Also, the fact that preferential flow can occur does not mean that preferential transport of the chemical will also occur.

Preferential flow is simply the nonideal behavior of water flow in soil. To inform the student, nonideal behavior has a wide variety of terms associated with it: preferential flow;

macropore flow; fingering; wetting-front instability; bypass flow; channeling; short-circuiting; partial displacement; subsurface storm flow; and others. All of these depict essentially the same phenomena. This section attempts to describe nonideal flow by three commonly used terms. Preferential flow is the general term used to describe the movement of water and related solutes through preferred flow paths in soils.

We describe a preferential flow path as a pathway of preferred flow that has a lower bulk density than the surrounding soil matrix rather than a crack or fauna tunnel; thus, it offers the least resistance to flow under specific field conditions. This implies that part of the soil matrix is "bypassed" when flow occurs, especially during significant recharge events (Tindall and Vencill 1995). The preferential flow path is considered a mesopore by some, ranging in size from 10–1,000 μm (Luxmoore 1981). Macropores are defined as large cracks, worm holes, fauna tunnels, and channels created from decayed roots, with a size range of $>$ 1,000 μm. However, for such large cracks to transport much fluid, the head (or pressure potential) within the medium has to exceed atmospheric potential. For example, when a large crack (larger than a micropore of 0–10 μm) within the profile is filled with air, water can enter the crack only if the potential within the matrix exceeds atmospheric potential. This is likely to happen only during significant runoff or recharge events, or in cases where a capillary fringe occurs directly above the crack. In this case, ponded water overcomes atmospheric potential, thereby forcing fluid into the crack where it can rapidly flow to deeper depths.

The pore sizes mentioned above for micro-, meso-, and macropores are based on the senior author's research, but are comparable to those of Luxmoore (1981). Various researchers have pore-classification scales describing these pore sizes (Luxmoore 1981; Jongerius 1957; Johnson and McClelland 1960; Everett 1972; Greenland 1977; Landon 1984); thus, it is no surprise that the need for standard pore-size classification was raised by Luxmoore (1981), who suggested the sizes listed above. While strict agreement on the pore sizes representing the various pathways of preferential flow has yet to occur, the effects of these pathways on ground water contamination are in mutual agreement.

The terms fingering, wetting-front instability, and partial-volume flow are applied differently than macropore flow; they are associated with layered soils, air compression, hydrophobic soils, and water redistribution following ponding. Fingering is not usually visible in the field (as is the case with macropores) but has become visible when using dyes to stain such areas and then excavating these areas (Starr, Gillham, and Sudicky 1986). Numerous laboratory and field studies have been conducted investigating fingering, using applied and theoretical approaches and involving both analytical- and numerical-modeling procedures (Miller and Gardner 1962; Hill and Parlange 1972; Baker and Hillel 1990).

Many of these experiments have been performed using a layer of fine-textured soil over a layer that is much coarser. Raats (1973) and Philip (1975a, b) used the Green and Ampt (1911) infiltration model to approximate fingering, a reasonable approach when using a uniform, coarse-textured initially dry soil. However, the underlying assumptions are that the soil is subject to one-dimensional absorption and the lack of entrapped air; in this instance, an initially dry soil will exhibit a sharp wetting-front rather than a diffuse front. Also assumed is that the soil is initially dry, so this approach is limited. Small amounts of initial wetness are sufficient to reduce instabilities that occur if the media is at an initially dry state (Diment and Watson 1983, 1985; Philip 1975a, b). This is because the distribution of initial wetness affects the pathways that the fingers would take; also, Glass et al. (1989) showed that fingers can repeatedly form in the same location during successive infiltration cycles in initially wet sands.

Hillel and Baker (1988) suggested that when a wetting front is characterized by a high value of suction, the front will not penetrate into a coarse-textured layer from a fine-textured

layer until the suction at the interlayer boundary falls to an effective water-entry suction ψ_e, which is characteristic of the sublayer. They concluded that if the sublayer conductivity, K_u, at its water-entry suction (expressed as $K_u(\psi_e)$), exceeds the flux through the top layer, Q_t, the pore-water velocity increases across the interlayer and only a small portion of the underlying layer conducts any water delivered to it, which results in fingering. Baker and Hillel (1990) proposed that fingering would not be initiated unless $K_u(\psi_e) > Q_t$, assuming steady-state flow, and that by using the quotient of these terms the wetted fraction, F, of the underlying layer could be predicted such that

$$F = \frac{Q_t}{K_u(\psi_e)} \tag{10.126}$$

Using a top layer of very fine sand overlying a layer of coarser texture, Baker and Hillel (1990) obtained good results with this model. Also, utilizing a linear regression of the relation between particle size and the effective suction of water entry ψ_e, then

$$\psi_{e(\text{pred})} = \frac{4370}{d_u} + 0.074 \tag{10.127}$$

where d_u is the median particle diameter (μm) of the underlying layer, and ψ_e is in cm. The conductivity (cm/s) is determined from the expression

$$K_u(\psi_e)_{\text{pred}} = 10^{[-(299/d_u)-0.916]} \tag{10.128}$$

By utilizing Darcy's law (see chapter 7) for the top-layer flux (Hillel and Baker 1988),

$$Q_t = K_t \frac{(H_0 + z_i + \psi_e)}{z_i} \tag{10.129}$$

If one assumes $K_t \approx K_{ts}$ (the saturated hydraulic conductivity of the top layer), then by substitution

$$F_{\text{pred}} = \frac{Q_t}{K_u(\psi_e)} = \frac{K_{ts}\left(H_0 + z + \left[\left(\frac{4370}{d_u}\right) + 0.074\right]\right)}{z_i(10^{[-(299/d_u)-0.916]})} \tag{10.130}$$

Generally, fingering is a nondeterministic process, unlike macropore flow. Upon wetting, the water or solute is (or is not) transported down the same finger as before, during subsequent recharge events. Hillel and Baker (1988) and Baker and Hillel (1990) suggest that particle size and θ are the common properties underlying the promotion and suppression of fingering. Despite this evidence, other properties such as particle-size distribution, initial-water content, hysteresis, and so on, need to be investigated since these parameters also appear to affect fingering.

The primary factors that cause nonideal transport of solutes are nonhomogenous physical and chemical media properties, and transport and sorption nonequilibrium. Preferential flow is usually a function of soil porosity that is separated into the portion of media occupied by gases and fluid, and more specifically, to the medium's ability to retain water at various matrix potentials (pressure or suction gradients). Pores can form naturally, especially in the upper profile, where microbiological processes are greatest. Other voids (such as cracks) can form during wetting and drying events and can further bifurcate, allowing possible connection with other cracks to form continuous channels and even peds. In agricultural and industrial settings in which no tillage or other type of surface-sealing activities take place, soil can have a high density of continuous macropores (Dick, Edwards, and Haghiri 1986). The mode of fluid flow is also dependent on initial water content of the media. Thus, edaphic, management, and meteorological factors ensure that both porosity and the potential for preferential flow are dynamic variables, both temporally and spatially.

QUESTION 10.10

Using a sublayer particle size, d_u, of 1000–2000 μm, determine the wetted fraction for this media. Assume the ponding depth H_0 is 1.0 cm, the layer thickness z_i is 5.8 cm, and the saturated conductivity K_{ts} is 2.0×10^{-3} cm/s. Also, ψ_e is 3.0 cm, $K_u(\psi_e)$ is 7.7×10^{-2} cm/s, and Q_t is 3.4×10^{-3}.

QUESTION 10.11

If the particle size d_u decreases, will the wetted fraction F increase or decrease?

Modeling Chemical Transport under Conditions of Preferential Flow

Chemical transport under nonideal conditions is dependent on pore-size distribution for which there are two general cases: **(1) Uniform distribution**—in the presence of a relatively narrow, uniform pore-size distribution (i.e., there is little variability); nonideality usually increases with a reduction in water content from saturation. With uniform saturated pores, dispersion is minimal. When such a medium desaturates, the pores empty slowly and fluid flow occurs mostly by thin water films attached to each particle. Thus, the pores become not only relatively "empty," but also the immobile domain. At a low-water content, much dispersion (diffusion in this case) is exhibited and the resulting breakthrough-curve shifts left. If the medium continues to desaturate, the emptiness of the pores results in a narrowly wetted pore-size distribution, and chemical transport becomes more ideal once again. As a result, nonideality might be compared to a bell-shaped curve: it increases as θ decreases from saturation, reaching a maximum value at some critical θ, then decreases as θ is further reduced. **(2) Nonuniform distribution**—generally, structured media have a wide range of pore sizes, many of which can be macropores. During saturated transport, nonideality is high because of pore-size distribution; however, as the macropores empty during desaturation, a narrowing of the effective porosity or pore-size distribution results. This reduces nonideality because the pores now conducting fluid are more uniform in size. It has been suggested that θ_{im} can be considered to be the water content at matric potentials less than about -7 to -10 kPa (Rose and Passioura 1971a, b; Tindall and Vencill 1995). Thus, the macropores transporting water empty at very low matric potentials near saturation; below this threshold, transport is via matrix flow and nonideality decreases as the soil desaturates. Despite this, there is a critical point at which further reduction in water content can create immobile regions and increased nonideality results, as in case 1.

In structured soils, chemical transport and fluid flow between the mobile and immobile regions are commonly determined by the use of Fick's law to describe physical, diffusive transfer (explicitly), by using empirical first-order mass-transfer expressions to obtain an average transfer; and implicitly, by using an effective-dispersion coefficient that includes a source/sink diffusion term, hydrodynamic dispersion, and axial diffusion. In this case, the lumped D replaces the usual hydrodynamic-dispersion coefficient.

Diffusion-based models that use Fick's law normally assume that aggregates have a spherical geometry. A similar type of model that utilizes a cylindrical geometry was developed by Van Genuchten, Tang, and Guennelon (1984) for predicting solute transport in media with macropores. A geometric description of the medium is required to develop the ADE for these model types. For mathematical simplicity, most of these models assume uniform-size aggregate structure, but for natural media these conditions do not usually exist. As a result, aggregate-size distribution and aggregate-shape variations have to be taken into account for these models to apply to a range and variety of cases. Rao, Jessup, and Addiscott (1981) showed that nonspherical aggregates can be represented by the use of equivalent-spherical

aggregates whose radii are such that the volume of the sphere is equal to the volume of the nonspherical aggregate. Rasmuson (1982) showed that one aggregate shape could be approximated with another by employing the same ratio of external-aggregate surface area to total porosity. Van Genuchten (1985) developed a geometry-dependent shape factor (f) that can be used to transform an aggregate of specific shape and size into an equivalent sphere that has similar diffusion characteristics to the original aggregate.

Both distribution and shape variations of aggregates must be described to extend diffusion-based models to field situations. Rao et al. (1980a, b) developed a method that works well, utilizing a range of aggregate sizes to compute an equivalent radius from the volume-weighted radii of each size-class; this was further validated by Nkedi-Kizza et al. (1982). A combination of the shape transformations used by Van Genuchten (1985) with the aggregate-size distribution of Rao, Jessup, and Addiscott (1981), for a soil that contains varying sizes of nonspherical aggregate, allows the transformation of the medium to one of equivalent, spherical aggregates of uniform size. With such an approach, the diffusion model can be extended to a variety of field situations. Many models are currently available that attempt to predict preferential transport of chemicals in the vadose zone. Cooney, Adesanya, and Hines (1983) found that aggregate-size distribution ranges of less than $\simeq$0.15 mm are narrow enough that the effects of nonuniform distribution can be ignored. Thus, the diffusion model used for predicting transport should be chosen carefully.

The physical mass-transfer model replaces the mechanistic description of diffusive transfer in the diffusion model, with a kinetic first-order mass-transfer expression. This no longer requires a description of the medium's structure because chemical transfer is now described by a mass-transfer coefficient, and is assumed to be a function of the difference in chemical concentration between the mobile and immobile regions. Coats and Smith (1964) performed early work on mass transfer in two-region flow, and subsequent expressions for the mass-transfer coefficient have been presented by Rao et al. (1980a, b), Raats (1984), and Park, Parker, and Valocchi (1986). Using these allows an independent determination of the mass-transfer coefficient and reduces its limitation on various soils.

The lumped (or effective-dispersion) model accounts for diffusive transfer between the mobile and immobile regions, implicitly. As the medium approaches equilibrium, the symmetry of the experimental breakthrough curve increases to a point at which asymmetry is very difficult to ascertain. At this point, nonequilibrium is evidenced by the increased dispersion. This model fits experimental data very well in such cases (Nkedi-Kizza et al. 1982; Lee et al. 1988). The diffusion and mass-transfer models have been compared by Rao et al. (1980b), Goltz (1986), and Miller and Weber (1986) and in all cases, the diffusion model gave similar results to the mass-transfer model. However, the increase in accuracy gained with the diffusion model does not justify the additional mathematical complexity or the larger number of parameters associated with it. As a result, the mass-transfer model is preferred by some researchers because of the major advantage it has in not requiring a description of soil structure.

Problems Encountered in Modeling Preferential Flow

The complex nature of soils and the formation of structured media—which can have large voids that may or may not be continuous—creates a lack of continuity. This lack of continuity causes problems in estimating chemical fluxes under preferential-flow conditions. At present, scientists have no way to describe the continuity of macropores or preferential flowpaths and thus, modeling is difficult. Generally, soil is treated with traditional physical concepts, including local equilibration of potentials and fluid flux that is proportional to the hydraulic gradient. In preferential flow, this is extremely important because, during wetting of soil that exhibits preferential flow characteristics, the wetting front penetrates the profile

to significant depths, thus bypassing the intervening pore-space in the general matrix. This decreases the residence time and solid-phase interaction of solutes and also reduces the effects of retardation, adsorption, and degradation, thereby increasing the potential of ground water contamination.

The use of drainage rates and tracers indicates preferential-flow behavior and sometimes supports the validity of a given model under certain conditions, but it is often difficult to extrapolate information gained in one experiment, to other initial and boundary conditions for different sites and experiments. Much of our knowledge is based upon parameters obtained from destructive sampling, which have been limited to small samples or small column studies. A "representative elementary volume" (REV) is used to describe a volume of medium over which water content and potential are usefully defined. Bouma (1979) and Bouma, Dekker, and Haans (1979) recommended an REV of 10 L to escape the effects of spatial variability.

Analysis of the problems of previous research in modeling flow through structured media suggests that new models will have to consider **(1)** the variety of pore sizes in which preferential flow takes place, since it takes place not only in non-capillary-sized pores; **(2)** the continuity of preferential-flow paths except under saturated conditions; **(3)** since not all large pores are effective in conducting fluid, what part of the pore is interacting with the adjacent matrix; **(4)** investigation of laminar-film flow and its effectiveness in flow in large pores; **(5)** the climatological and other local conditions that are important in preferential flow; **(6)** colloidal facilitated transport through larger pores and the local geochemical reactions that may result in improved structure within large pore walls (i.e., cutans); **(7)** the effects of hysteresis in preferential flow; **(8)** the influence of bounding macropores on matrix flux in desaturated conditions; **(9)** the change, with time, of the structure of preferential-flow paths and macropores, that continually develop in undisturbed media and in soils that support agricultural crops, and trees, and others.

Various models have been developed in an attempt to deal with the predictability of transport under preferential-flow conditions. To summarize, these include: diffusion models; mass-transfer models; effective-dispersion models; multi-region flow models; mechanistic; statistical; statistical–mechanistic models; transfer-function models (described in chapter 13); and numerical models (Steenhuis, Parlange, and Andreini 1990). However, all of these are based on physical parameters that can be measured in the laboratory or the field, to characterize medium behavior. Theoretically, these parameters should be characteristic of a given medium at the scale of the measured REV but only for a profile that is homogeneous and unstructured. As a result, the values obtained for the measured parameters are not applicable in structured soils because such media are both heterogeneous and layered/structured, which requires a very large number of parameter values. These are nearly impossible to obtain without altering the nature of the system, so we generally ignore the problem and make an "assumption" (all encompassing) that the parameter of interest can be used at a profile or hill-slope scale. Interestingly enough, there is little guidance in estimating the "real" parameters, or on how to obtain effective values for them. At present, the best we can do is to use conservative tracers and various isotopes (see chapter 13) as well as intact cores of representative size.

Currently, both uncertainty and risk are associated with the predictions of various models; these need to be further evaluated in experimental studies. Models should be developed at the scale of interest for which they are intended to be used, or developed at a smaller scale and modified for use at larger scales, using accurately collected data. The current trend appears to be to develop more complex models because of the computational ability of advanced computer systems (Jarvis 1994). However, simply increasing the complexity of model structure at the expense of adding more parameters (extremely difficult to measure and

identify), is not the best approach. For practical field- and regional-scale applications, models need to be developed for specific scales, and nondestructive measurement techniques must be developed that yield the necessary experimental information.

10.14 COLLOIDAL-FACILITATED TRANSPORT

The transport of contaminants to ground water via preferential pathways is of increasing concern as a major environmental problem in the U.S. Agricultural, industrial, and petroleum-derived chemicals may move to ground water as soluble constituents in soil water, or may be associated with soil-derived colloids that are capable of transporting such pollutants to the ground water. Pesticides, trace metals, and contaminant organics, that exhibit high adsorption and/or low water solubility, can move to ground water by this mechanism. The process is greatly exacerbated by the presence of preferential pathways.

Gaps exist in our current understanding of colloidal transport in soils and underlying geologic materials, a process likely ongoing for many years, that may explain the higher-than-expected concentrations of contaminants in ground water. Previous investigations have focused on homogeneous soil materials but have not fully accounted for the influence of aqueous and surface chemistry on colloid stability.

Previous investigations dealing with contaminant migration to subsurface environments have considered soil or ground water as a two-phase system, where contaminants could partition between the mobile-liquid phase and immobile-solid phase. Based on this approach, it was predicted that many contaminants would be relatively immobile because of low solubility or high-adsorption affinity for the solid phase. However, recent research suggests the existence of mobile–immobile conditions of the aqueous phase within soils, especially those containing large interconnecting systems of macropores. Thus, it is becoming increasingly evident that under certain (yet poorly defined) conditions, contaminant migration to and/or within ground water can be significantly enhanced by colloidal migration, where the colloidal phase itself is undergoing transport via preferential pathways (Rees 1987; Buddemeier and Hunt 1988; McCarthy and Zachara 1989). It has been suggested that radionuclides, organics (including PCBs, PAHs, and pesticides), and nonradioactive inorganic contaminants found in ground water may have migrated via colloidal-transport mechanisms, and currently, significant research efforts are focusing on this mechanism (Champ 1990; Nelson et al. 1985; Gschwend and Wu 1985; Jury, Elaboi, and Resketo 1986; Rees 1987; McDowell-Boyer, Hunt, and Sitar 1986; Buddemeier and Hunt 1988; Enfield, Bengtsson, and Lindquist 1989; Harvey et al. 1989; McCarthy and Zachara 1989; Ryan and Gschwend 1990; Penrose et al. 1990).

Colloidal-transport mechanisms have recently received considerable attention in popular scientific publications (Raloff 1990; McCarthy 1990; Jardine, Weber, and McCarthy 1990; Champ 1990; Looney, Newman, and Elzerman 1990; Gschwend 1990; Enfield and Kerr 1990). Fewer investigations have specifically addressed hydro-geochemical processes regulating the generation of stable colloidal suspensions (SCS) within soil, or the mechanisms operative in colloidal migration through the unsaturated zone. While a significant body of literature has addressed the theory and application of colloid stability and transport through well-defined, homogeneous media (Yao, Habibian, and O'Melia 1971; O'Melia 1980), the process governing the generation of SCS in intact soil and unconsolidated geologic materials has received less attention (McCarthy and Zachara 1989).

Colloid Migration

Qualitatively, the transport of colloids within soil is dependent on three fundamental processes: **(1)** generation of colloids; **(2)** stabilization of colloidal suspensions; and **(3)** unat-

tenuated transport—that is, the transport without aggregation, sorption, or filtration within the soil as in preferential pathways (McCarthy and Zachara 1989). The generation and transport of three general classes of colloidal material in soils has been identified: inorganic colloids, microorganisms, and organic molecules. These materials can be important in contaminant mobility, both as facilitator of transport to ground water, and as a source of ground water colloids capable of remobilizing contaminants within the subsurface.

Eluvial and illuvial processes—whereby clay and other inorganic colloids are transported vertically from surface soils and redeposited in lower strata—have long been recognized as important pedogenic processes (Jenny and Smith 1935). Clay migration within soil profiles previously has been evaluated using a number of radio-labeled clay suspensions. Bertrand and Sor (1962) examined the influence of rainfall intensity on soil structure, and migration of colloidal materials via application of ^{86}Rb labeled clays. ^{32}P (Kazo and Gruber 1962), ^{90}Sr (Von Reichenbach and Von der Bussche 1963), ^{60}CO (Toth and Alderfer 1960), and ^{59}Fe (Woolridge 1965; Coutts et al. 1968a, b) have also been utilized to examine lateral and vertical transport of soil particles.

Generation of colloidal clay and iron, aluminum, or mixed iron–aluminum colloidal soils is achieved through dispersion of the particles or dissolution of cementing agents. These particles are also formed by dissolution and transport of dissolved constituents, with subsequent reprecipitation of clays or soils. The stabilization of the colloidal suspensions is highly dependent on soil-solution chemistry, with counterion type and concentration as two of the most important variables. Traditionally, colloidal-suspension stability has been explained using DLVO theory (Sposito 1984; see chapter 3). Whether colloids are transported through the soil matrix or deposited within that matrix is usually related to molecular sieving, with the intent of colloidal aggregation related to sieving efficiencies. Similar discussions of coagulation and filtration theory with regard to water and waste-water treatment (Yao, Habibian, and O'Melia 1971; O'Melia 1980) emphasize the importance of chemical factors in particle-removal efficiency.

Clay illuviation and all colloidal transport through soils implicate the role of preferential flow through macropores and other soil discontinuities. Akamigbo and Dalrymple (1985) generated illuvial-intrapedal cutans (e.g., clay coatings on soil peds) by applying dilute clay suspensions to undisturbed blocks of soil. That clay could be transported through intact *B* horizon material via natural channels (macropores) associated with ped faces was also demonstrated in this investigation, and was observed by Anderson and Bouma (1977a, b). Such preferential flow can occur within earthworm channels (Ehlers 1975), along ped faces (Anderson and Bouma 1977a, b); and other discontinuities within the unsaturated zone, including particle-size changes in unstructured material (Glass, Steenhusin and Pavlange 1988). The ability of soil macropores and other preferential pathways to conduct significant volumes of water, and the implications of this flow in terms of minimal interaction (e.g., sieving) of dissolved and suspended components by the bulk-soil matrix, has been discussed in detail by Thomas and Phillips (1979) and Beven and Germann (1982).

The transport of colloidal-sized macroorganisms in soils has also been observed. Wollum and Cassel (1978) note that *Streptomycete conidia* were easily transported through sand columns under saturated conditions. Transport of *Escherichia coli* through intact and disturbed soil cores (Smith et al. 1985) and in the field (Rahe et al. 1978), has also been observed. Indications are that soil structure (e.g., macropores) influences the extent of transport, with movement of *coliform* up to 830 m reported by Hagedorn et al. (1981). Additionally, recent studies have provided evidence of in situ transport of bacteria and microspheres through an aquifer, although the processes regulating transport could not be delineated (Harvey et al. 1989).

Soil-humic materials can also facilitate transport of contaminants via a number of mechanisms. Humic materials have been noted to stabilize clay-colloidal suspensions (Jenny

and Smith 1935; Gibbs 1983). Natural organic matter is readily adsorbed by oxide and mineral surfaces, with nearly complete surface-coverage likely for hydrous iron oxides, alumina, and edge sites (faces) of aluminosilicates under typical conditions found in natural waters (Davis 1982). Tessens (1984) found that essentially all topsoil samples from the upland soils of Malaysia had significant amounts of water-dispersible clay, as did a set of Brazilian soils (Camargo and Beinroth 1978), with organic coatings being implicated as the primary controlling factor. Jekel (1986) found that soluble humic materials extracted from surface and ground water stabilized colloidal suspensions of kaolinite and silica, with the degree of stabilization dependent on pH and ionic strength. Based on electrophoretic mobility measurements and the observed high-adsorption affinity at low pH, it was concluded that stabilization was primarily caused by the sorption of higher molecular-weight neutral molecules (Jekel 1986). Additionally, Tipping and Higgins (1982) found adsorbed humic substances stabilized colloidal dispersions of hematite, and that dissolved humics were responsible for stabilizing aluminum-oxide colloidal suspensions, although in contrast to Jekel (1986), their electrophoretic-mobility measurements indicated that the suspended alumina particles were highly charged negatively, as a result of adsorbed organic matter. Beckett and Le (1990) stated that organic coatings were the controlling factors determining the surface-charge behavior of suspended inorganic particles in riverine and estuarine waters from the Tara River system in Australia.

In addition to enhancing the stability and mobility of inorganic colloids, organic coatings greatly facilitate the partitioning of nonionic contaminant organics to their surfaces, since the relative amount of organic matter has been shown to be the most important factor for predicting nonionic organic partitioning to soils and sediments (Chiou 1989).

It has been demonstrated recently that laboratory-modified inorgano–organo clays are efficient sorbents, in many instances as efficient as granulated-activated carbon, for removing a number of organic contaminants, including polychlorinated dibenzo dioxins (PCDDs), polychlorinated biphenyls (PCBs), tetrachloromethane, and polycyclic aromatic hydrocarbons (PAHs) from aqueous solutions and industrial wastewaters (Srinivasan et al. 1989; Lee et al. 1989; Nolan, Srinivasan, and Fogler 1989; Srinivasan and Fogler, 1989, 1990a, b; Smith, Jaff, and Chiou 1990). Many of the modified clays used in these studies are the laboratory cogeners of the hydroxy-interlayered 2:1 clay minerals (HIM), which are important components of the clay and mineral fraction in soils throughout the southeastern and midwest United States. HIM can be an important sink for contaminant organics in organic-poor soils, as well as a potentially mobile phase capable of facilitating colloidal transport.

Colloidal particles are also potentially transported through the solum to underlying strata. Enfield and Bengtsson (1988) found that blue dextran, a model macromolecule, was subject to size-exclusion as it percolated through soil columns, thus flowing through the larger pores and eluting prior to tritiated water. Similarly, the transport of water-soluble organic carbon (WSOC) through soil columns was found to be more rapid than tritiated water; this was also attributed to a size-exclusion mechanism (Bengtsson, Enfield, and Linduvist 1987; Enfield et al. 1989). Such observations have suggested that this mechanism could significantly enhance the transport of contaminant organics to subsequent environments (Enfield and Bengtsson 1988).

An earlier study on facilitated-DDT transport by humic substances (Ballard 1971) and corroborated by recent investigations, has provided evidence that dissolved organic macromolecules enhance the mobility of contaminant organics, that is, naphthalene, phenathrene, and DDT (Kan and Tomason 1990). Few investigations have studied the sorption and transport of actual WSOC through the soil (Jardine, Weber, and McCarthy 1989). The vast majority of investigations in this area have employed either "model" organic macromolecules, or humic materials derived from base-extraction of solid-phase organic matter—both of which can be poor models for naturally-occurring soluble-humic substances. In this

regard, Leenheer and Stuber (1981) found that the hydrophobic neutral-fraction of dissolved organic carbon (OC) from oil-shale process-water was preferentially adsorbed, compared to the more hydrophilic fraction. Transport of the various dissolved organic fractions through soil columns was found to parallel their sorption behavior in batch experiments of the same soil material (Leenheer and Stuber 1981). Likewise, Jardine, Weber, and McCarthy (1989) observed preferential sorption of the hydrophobic, relative to the hydrophillic fractions of WSOC in a number of soils, with the total sorption increasing with increased soil-profile depth.

The preceding discussion illustrates the general concerns regarding colloidal-transport processes in soil, and the potential for colloid-assisted transport of both inorganic and organic contaminants. Contaminants are viewed as being associated with two phases: either dissolved and hence mobile, or matrix-adsorbed and retained. Partition coefficients are often useful for predicting relative mobility of contaminants. Used in conjunction with advection–dispersion models (ADEs), contaminant transport can be simulated and the extent of migration with time estimated. Deviations from model predictions are frequently attributed to preferential pathways. However, such deviations can be partially explained by colloidal transport processes (Jury, Elaboi, and Resketo 1986).

Gschwend and Wu (1985) identified colloidal materials as important components in PCB-adsorption experiments that confounded the determination of partition coefficients. DDT was found to adsorb and concentrate up to 15,800 times its water solubility on colloidal materials, within the highly colored southeastern U.S. streams (Poirria, Bordelon, and Laseter 1972). Enhanced apparent solubility of hydrophobic compounds by humics was also noted by Chiou et al. (1986). Ninety-one percent of the DDT applied to a forested soil was associated with humic acids, while the remaining nine percent was contained within fulvic acid and dissolved fractions (Ballard 1971). Additionally, it was demonstrated that soil-humic material was readily dispersed by urea additions, with a 30-fold increase in DDT mobility noted. Similarly, polycyclic aromatic hydrocarbons also exhibited high affinity for dissolved-humic substances (McCarthy and Jimenez 1985) as did trace metals (Hoffman et al. 1981), and natural estuarine colloids exhibited high affinities for atrazine and linuron (Means and Wijayaratrne 1982). Mineral surfaces can also sorb large amounts of contaminants (e.g., Jenne 1968; Vinten and Nye 1985). Radionuclides were found to be associated principally with 2–3-nm-radius size-class (taken to be humic acids), when equilibrated with soils (Sheppard et al. 1980), while ^{239,240}Pu partitioning was dependent on a number of parameters and not clearly understood (Alberts et al. 1977). The deep (30 m) transport of plutonium and americium at a defense-program site at Los Alamos was also found to be colloid-facilitated, as the transported radiounuclides were shown by ultrafiltration to be present as colloids in the 0.025 to 0.45 m size range (Nylan et al. 1985; Nelson and Orlandini 1986). Similar results have recently been reported for radionuclide transport at the Nevada test site and at Los Alamos National Laboratory (Buddemeir and Hunt 1988; Penrose et al. 1990).

Despite the demonstrated potential for colloidal transport through soils and the viability of contaminant-colloid associations, the role of colloid-assisted, contaminant transport to ground water remains largely conjecture, although a limited number of systems studied provide indication of the significance of the process. Perhaps most notable is the observation of ground water turbidity resulting from application of low-salinity water to a recharge facility in Fresno, California (Nightingale and Bianchi, 1977). Application of water having a lower specific conductivity (from 147 to 100 dS/m) induced dispersion of native inorganic colloidal materials within the surface soils. The dispersed clays were then transported to the aquifer, resulting in high turbidity within monitoring wells. It was estimated that 148 metric tons (3.1 metric tons/hectare) of colloidal material moved out of the surface profiles into the ground water in 1975 (Nightingale and Bianchi 1977), illustrating the possible magnitude of colloidal transport. Gypsum applications were found to destabilize the colloidal suspensions

effectively and clarify the waters (by flocculation). The influence of small-to-modest changes in chemistry upon soil-aggregate stability and the magnitude of mass of the material transported demonstrates the balance of forces operative within many soil/colloid systems.

Release of colloidal particles from sandstone formations during oil-field operations, and the properties and factors serving to generate and stabilize colloidal suspensions has also been reported (Kia, Fogler, and Reed 1987). Particle-release was attributed to an ion-exchange process on the surface of the clay particles, with slow release of fines observed under low pH conditions. More theoretical studies on diffusional-detachment processes (Kallay, Barouch, and Matijevic 1987), kinetics of particle detachment (Barouch, Wright, and Matijevic 1987; Adamczyk and Petlicki 1987), colloidal stability of variable-charge mineral suspensions (Bartoli and Philippy 1987), and precipitation-charge neutralization processes during coagulation (Deutel 1988) have also been provided recently. Gschwend and Reynolds (1987) reported on an aquifer system possessing monodispersed colloids resulting from in situ precipitation. They postulated that phosphate- and carbon-rich wastewaters initially percolated into the shallow aquifer, where oxygen concentrations were sufficiently reduced by respiration such that anoxic conditions were formed. Reduction of the indigeneous iron in the presence of the high-phosphate loadings produced stable monodisperse vivianite particles approximately 100 nm in size. Ryan and Gschwend (1990) found elevated concentrations of predominantly organic-coated inorganic colloids in anoxic (compared to oxic) ground waters (up to 60 mg L^{-1} and < 1 mg L^{-1}, respectively) within an Atlantic Coastal Plain aquifer in the Pine Barrens of southern New Jersey. They suggested that the anoxic conditions resulted in the dissolution of Fe oxyhydroxides that coated the mineral phases, acting as a cementing agent.

Penrose et al. (1990) reported the presence of $^{238,239,240}Pu$ and ^{248}Am in ground water $> 3{,}000$ m down-gradient from the discharge, and these actinides were determined to be associated with colloidal material between 25 to 450 nm in size. Based on the low-water solubility, high-partitioning coefficients, and immobility demonstrated in laboratory experiments, it was predicted that these actinides would migrate only a few meters from the discharge, thus providing strong evidence for a colloid-facilitated transport mechanism within the subsurface environment.

However, many published reports concerning the presence of colloids in ground water have been received with skepticism, resulting from the inability to eliminate unequivocally the possibility that the observed colloids were formed as an artifact of sampling.

A Conceptual Model for Colloid Transport

A general model to conceptualize colloid transport describes two phases: **(1)** detachment and stabilization; and **(2)** transport processes with associated sub-processes (figure 10.9). The initial condition for colloid migration must include the mobilization of colloid-sized particles within the soil. The process is hypothesized to be both physically and chemically controlled. Detachment of colloid particles from the soil matrix (1a in figure 10.9) requires an energy input sufficient to overcome van der Waals forces, coulombic, or other forces binding the particle. These forces could arise from: shear forces of water flowing within individual pores; swelling or repulsive double-layer forces between colloids upon initial wetting, or due to a change in chemical environment; or physical disturbance (e.g., agricultural tillage operations or excavation). Emerson (1967) defined classes of soils that disperse spontaneously with wetting, those that disperse only with mechanical energy input; and those which are nondispersive; the majority of soils seem to fall into the mechanically dispersive category, requiring some form of kinetic energy to initiate the dispersion process (Rengasamy et al. 1984; Miller and Baharuddin 1986). Raindrops or irrigation hitting bare soils disperse large amounts of colloidal clays, some of which enter the soil-surface with infiltrating water; the movement of

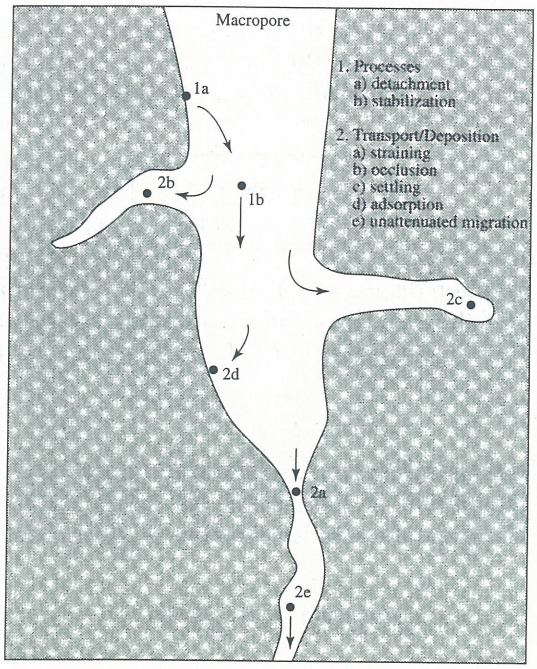

Figure 10.9 A conceptual model for colloidal-facilitated transport via a macropore

low ionic-strength rainwater into soils may also dilute soil solutions and enhance colloid mobility by increasing swelling and particle repulsion (McCarthy and Zachara 1989). Once detached from the matrix, the particle must be stabilized chemically (1b in figure 10.9) in order to avoid immediate redeposition via flocculation with other detached particles. Stabilization is accomplished largely through development of double-layer repulsive forces.

The second phase involved in colloid movement within soil is a transport phase, determined by both physical and chemical forces. Pore sizes must be sufficiently larger than the size of the particle to allow physical passage of the particle, or straining (2a in figure 10.9) occurs. Deposition of particles can also take place under other circumstances: occlusion of particles within micropores (immobile water) within the soil matrix (2b in figure 10.9) via Brownian motion; sedimentation of particles, if flow velocity is sufficiently low compared to settling velocity of the particle (2c in figure 10.9); and adsorption of the particle to the matrix, due to electrostatic or other forces (2d in figure 10.9). The latter process can considered to be largely chemical in nature, as charge characteristics of the soil matrix and particle control adsorption. However, adsorption may occur via van der Waals forces in narrow pores during unsaturated flow, where restricted water-film thickness increases the likelihood of particle approach to surfaces. Quantitative modeling of these processes has been attempted using filtration theory coupled with sub-models of specific processes described above (McDowell-Boyer, Hunt, and Sitar 1986). Straining is often empirically related to the ratio d_m/d_p, where d_m is the average matrix-particle diameter and d_p is the average colloid diameter; ratios < 10 indicate little colloid penetration into the matrix, ratios in the range 10–20 suggest significant straining and reductions in flow rate due to clogging, while ratios > 20 would result in limited straining. In soils with a distribution of particle and pore sizes, such a parameter would obviously need to be modified to be a useful predictor. Diffusion of suspended colloids within the flowing pore water can be described by the Einstein equation for Brownian motion

$$D_p = \frac{kT}{3\pi\eta d_p} \tag{10.131}$$

where the particle diffusivity (D_p) is a function of the fluid viscosity (η) and particle diameter (d_p). At low-flow rates through small pores, this value is large enough to enable colloids to diffuse to the pore wall into connecting micropores, leading to occlusion (2b in figure 10.9), or adsorption (2d in figure 10.9).

Both adsorption of colloids to the soil matrix and settling of colloids (2c in figure 10.9) are highly dependent upon the surface and aqueous chemistry of the system. Particle settling can be predicted as a function of particle size via Stokes Law, as balanced against the flow-velocity of the pore water. Particle size, in turn, is critically dependent upon the chemical environment in terms of flocculation/dispersion of the (initially) colloidal material (Van Olphen 1977). The "thickness" of the electrical field surrounding the colloid (x^{-1}) is determined largely by ionic strength of the aqueous phase (I), as those ions partially balance the internal charge of the colloid

$$x^{-1}\, c\, (\sqrt{I}) \tag{10.132}$$

where c is a constant incorporating the dielectric constant, temperature, and charge of an electron. Surface potential of the particle (ψ_p) and of the soil matrix (ψ_m), along with ion valence z, particle diameter d_p, determine the repulsive energy, σ_{dl}, forces acting between double layers

$$\sigma_{dl} = \left(\frac{\varepsilon d_p}{z}\right)\psi_p\, \psi_m \ln(1 - e^{-xh}) \tag{10.133}$$

where ε is the permittivity ($8.85 \times 10^{-12}\ C^2\ N^{-1}\mathrm{m}^{-2}$) and h is the distance of separation between particle and matrix, assuming surface potentials are roughly equal and < 50 mV. The attractive energy between a spherical colloid and a flat-plate (matrix) can be computed as follows:

$$\sigma_a = \left(\frac{A}{6}\right)\left[\ln\left(\frac{h + d_p}{h}\right) - \left(\frac{d_p}{h}\right)\left\{\frac{\dfrac{h + d_p}{z}}{(h + d_p)}\right\}\right] \tag{10.134}$$

where A is Hamaker's constant and z is ionic valence (see chapter 3). The balance between these attractive and repulsive energies is controlled by variation in the repulsive component, which is highly sensitive to ionic strength of the aqueous phase.

In dealing with colloidal and subcolloidal organic molecules, adsorption to the soil matrix is a major factor retarding movement; adsorption is driven by both enthalpic and eutropic forces, although mechanistic interpretations of adsorption have not proved useful in quantifying sorption behavior. Instead, a number of empirical approaches have been used, particularly the simple approach of assuming a constant partitioning of the solute to the solid phase:

$$K_d = \frac{C_s}{C_f} \tag{10.135}$$

where the distribution coefficient (K_d) is the concentration ratio of adsorbed (C_s) to free (C_f) solute; the well-known Freundlich isotherm is a modification of this relation, adding a curve-fit exponential term to the equation

$$C_s = K_d(C_f)^n \tag{10.136}$$

thus allowing fitting of curvilinear adsorption data. Batch-adsorption experiment data are used to obtain K_d and n, whose values can then be used to account for attenuation during transport.

Approaches for quantifying attenuation and destabilization of migrating colloidal suspensions, such as those given above, can be coupled with basic one-dimensional

advection–dispersion flow equations to yield breakthrough curves under a given set of boundary conditions. Parker and Van Genuchten (1984) offer a derivation of such an approach, and provide a useful integration of adsorption functions into the flow equations to account for partitioning of the solute flow through a one-dimensional soil volume, by the following equation:

$$\left(\frac{\rho_b}{\theta}\right)\left(\frac{\partial s}{\partial t}\right) + \left(\frac{\partial C}{\partial t}\right) = D\left(\frac{\partial^2 C}{\partial x^2}\right) - v\left(\frac{\partial C}{\partial z}\right) - \mu_w C - \left(\frac{\mu_s \rho_b}{\theta}\right)s + \gamma_w + \left(\frac{\gamma_s \rho_b}{\theta}\right) \quad (10.137)$$

where the major measured variables include solute concentration C, adsorbed solute in the solid phase s, vertical distance z, time t, dispersion coefficient D, pore-water velocity v, soil-bulk density ρ_b, and volumetric-water content θ. The μ and γ terms are (empirical) rate-coefficients for adsorption/desorption processes affecting solute concentrations in the liquid phase. The computer program CXTFIT (Toride, Leij, and Van Genuchten 1995) can provide computations for fitting this model to measured concentration-versus-time data. Adsorption parameters can be curve-fit, or varied independently to assess the fitness of the model assumptions with respect to flow conditions. Further refinement of such an approach can include additions of terms to the right-hand side of equation (10.137) to incorporate colloidal stability considerations, that allows a more complete modeling of colloidal transport in soil.

In summary, the most likely scenario for subsurface transport of pollutant-contaminated colloids is that in which colloids are detached and stabilized in surface soils or disturbed subsoils, and are then transported through weathered-underlying-geologic materials by alternate saturated/unsaturated flow to ground water. The initial generation of the colloidal suspension will be highly dependent on the presence of detachment forces (physical shear forces, chemical repulsive forces), and on the chemical environment within that zone, which determines if the suspension can be stabilized and conducted into the underlying material. The variable nature of this subsurface material has a controlling influence on the proportion of colloid conducted to the aquifer below. Layers of weathered rock (saprolite) and/or unconsolidated sediments present varying pore sizes and geometries, as well as different chemical environments (pH, ionic strength, solution-ion composition) that may promote deposition by any of the mechanisms shown in Figure 10.9.

10.15 SOURCES OF CONTAMINATION

Municipal Sewage-Sludge Disposal and Wastewater Irrigation

This section is meant to introduce to the student the environmental impact and importance of various sources of contamination to land surface, surface water, below-surface disposal, and deep-well injections of contaminants. We lack space to treat each area in great detail; however, sufficient references are given that the reader may investigate each area of interest.

The use of manufactured nitrogen fertilizer has increased worldwide since the late 1940s. The application of nitrogen fertilizer in the United States increased from 500,000 metric tons (0.5 Tg) in 1945 to over 10 million metric tons (10 Tg) in 1976 (USDA 1977). Worldwide consumption in 1985 was 70.5 Tg (FAO 1985); Eichner (1990) predicted a consumption of about 94 Tg by 1997, based on World Bank estimates. However, during the past twenty years, the high cost of manufactured fertilizer has generated increased interest in municipal wastewater irrigation and land disposal of nitrogenous animal, municipal, and food-processing wastes.

Numerous studies of water quality in agricultural areas of the United States have documented nitrate concentrations in ground water and surface water greatly in excess of the regulated United States drinking water standard of 10 mg (N) L^{-1} NO_3^- (Mueller and Helsel

1996; Weil, Weismiller, and Turner 1990; Keeney 1982). Nitrate levels in household wells in some agricultural areas have been found to reach acutely toxic concentrations (Keeney 1982). Elevated nitrate concentrations in drinking water can cause methemoglobinemia in some livestock and in human infants under the age of six months. Nitrate consumption has also been circumstantially implicated in a greater incidence of stomach cancer in some localities (Lee and Dahab 1992). The same problems also plague other countries such as the Peoples' Republic of China, but are not as well-documented due to lack of adequate technology (in some cases), and research funds (Jiao Desheng, personal communication).

The application of municipal sewage-sludge to agricultural land can benefit the soil by improving the physicochemical condition and by recycling plant nutrients as well as, by providing a viable alternative to disposal in landfills or by incineration (Sopper and Kerr 1979; Khaleel, Reddy, and Overcash 1981). Investigation of the potential benefits of municipal sewage-sludge application to agricultural lands has been limited, but the practice has been studied extensively for reclamation purposes (Sopper and Kerr 1979). Municipal sewage sludge has been shown to provide substantial amounts of organic matter and plant essential nutrients when applied to soils (Elliott 1986; McCaslin and O'Connor 1982; Knudtsen and O'Connor 1987). However, depending on its source, this sludge may contain metals and other elements that can be harmful to plants and the food chain when applied in excessive amounts (U.S. Environmental Protection Agency 1978; Tindall, Lull, and Gaggiani 1994; Valdares et al. 1983). Sewage sludge can be applied in a variety of forms: dry, wet slurry, or through irrigation systems either to land-surface or tilled into the soil. Occasionally, it is stored in large piles that provide a significant point source for potential contamination. In rural settings, the presence of septic systems, with their associated drain fields, can contribute a significant amount of sewage, which may pose a hazard to ground water, depending on rural population density.

Millions of tons of sewage sludge are produced each year and while there are many benefits to the soil where it is applied, there are also disadvantages. First, sewage sludge contains a multitude of chemical constituents, including metals, organic compounds, and polynuclear aromatic hydrocarbons (PAHs) that are usually significantly higher than the normal range of concentrations found in agricultural soils without municipal-sludge amendments (Jones et al. 1989; Wild, McGrath, and Jones 1990). Second, there is concern that some chemicals have a propensity to transfer from municipal sewage sludge-amended soils into the human food chain, due to plant uptake by food crops grown in these soils (Scheunert and Klein 1985). Third, there is a major concern that, when any municipal sewage-sludge is applied to soil or a sensitive hydrogeologic setting, the ground water could be contaminated by nitrates, metals, organic compounds, or other constituents within the sludge (Berg et al. 1987). Nitrates are present in municipal-sewage sludge and when applied to the soil may reach concentrations greater than 60 mg L^{-1} (Berg, Morse, and Johnson 1987). As greater amounts of sludge are applied, nitrates increase in concentration, and because the nitrate ion is mobile in soil, it is readily leached from the upper soil-profile to deeper depths. In hydrogeologic settings such as fractured rock, karst, and porous soils (such as those with higher sand and rock contents), contamination of ground water and underlying, shallow aquifers is of grave concern (U.S. Environmental Protection Agency 1986).

Few guidelines have been developed for determining acceptable sludge-loading rates to soil in relation to nitrate loading, and the addition of harmful metals associated with sewage sludge. As a result, research has focused on what rates need to be applied with regard to the physical and chemical parameters of the soil (Tindall, Petrusak, and McMahon 1995). Haith (1983) developed a planning model for land-application of sewage sludge. This mathematical model estimated nitrate–nitrogen concentrations in percolation from sludge land-application sites. The model is based on an annual-mass balance of sludge and soil-inorganic

nitrogen, and includes the processes of mineralization, ammonia volatilization, crop uptake, and leaching. The pollution risk of nitrate percolation from sludge land-application sites (Kaufman and Haith 1986) and development of models to evaluate application rates of wastewater sludge to various soils (Haith et al. 1992) are two important areas that are being investigated with regard to application of sludge loading. As the population increases, the need for research in these and other areas becomes a necessity.

Due to competition for valuable water resources, the application of municipal wastewater for irrigation purposes of agricultural crops has increased significantly in China during the past five years (Gao, Sun, and Qu 1991), in the U.S. (Tindall, Lull, and Gaggani 1994), and other countries as well. Irrigation of vegetable crops with wastewater has resulted in increased yields (Osburn and Burkhead 1992) however, Moreno (1981) reported that high levels of detergents in wastewater decreased calf-growth rate and that boron was toxic to both beans and lettuce at concentrations greater than 5 mg L^{-1}. In some instances, plant disease occurs as a result of irrigation with municipal wastewater, the most common diseases being Pythium and Phytophthora root-rots (Epstein and Safir 1982). Other studies have found no major limitations on crop growth by irrigating with wastewater (Neilsen et al. 1989; Lau 1981).

With regards to the application of fertilizers and wastewater, the movement of these chemicals plus associated herbicides and their relation to agricultural mulching practices, is relatively unknown. Lavy (1977) found that the fraction of atrazine free to move in a moist-soil environment is increased by increasing the soil-water content; this could prove to be a management problem where mulches are used for water-conservation purposes. Other research has found that, for advanced stages of redistribution, solute movement became negligible, and that the maximum herbicide concentration was located at the same depth in the soil-profile regardless of irrigation intensity (Selim, Manzell, and Elzeftway 1976b). By applying wastewater as an irrigation source, we are essentially using "chemigation" methodology for nutrient application. Chemigation can have a negative impact on ground water-quality depending on the occurrence of preferential flow (Jennings and Martin 1990). In the presence of preferential flow paths that can occur in all soil types, the ability and likelihood of increased chemical movement is greatly enhanced. For commercial fertilizers, urea added to localized irrigation systems (i.e., trickle, drip, and spray) can be hydrolyzed rapidly in the soil to ammonium, and then oxidized to nitrate (Clothier and Sauer 1988). Also, repeated applications of effluent as wastewater can reduce the assimilative capacity of the soil, leading to increased risk of ground water-contamination.

The effects of irrigation with municipal wastewater on soil components, and subsequent impact on ground water-quality have been varied. It has been found that spray irrigation with municipal wastewater can reduce soil infiltration capacities under certain crops significantly (Sopper and Richenderfer 1978; Sopper and Richenderfer 1979). Kayser (1988) reported no increase in heavy metals in Wolfsburg, Germany, soils, but in Braunschweig, higher levels of heavy metals did accumulate in the upper soil horizon. However, Davis, Grieg, and Kirkham (1988) reported that extractable concentrations of heavy metals (cadmium, copper, iron, lead, manganese, and zinc) were not higher in soils irrigated with wastewater than in soils treated with typical commercial (N-P-K) fertilizer and irrigated with tap water. Page and Chang (1981) reported little or no accumulation of trace metals in the root zone following long-term use of wastewater irrigation, and Schirado et al. (1986) showed that heavy metals may have migrated through the cultivated layer of soil and were distributed throughout the soil profile or leached below the depth of sampling. Lau (1981) showed that, through crop rotation and wastewater dilution, application of wastewater maintained sugarcane yield without polluting the ground water. Additionally, soils irrigated with wastewater exhibited low-denitrification potentials due to a shortage of available organic carbon and

rapid nitrification (Miller, Barr, and Logan 1977; Barr, Miller, and Logan 1978). Present research suggests that transport of chemicals from wastewater is dependent on soil type, application rate, application timing, and on constituent concentrations in the wastewater. The extent to which these waters can be used depends on the nature of the contaminant and the purpose for which the crop is to be used (Abeliuk, Riqueline, and Matthey 1993).

In addition to environmental problems, wastewater irrigation and sewage-sludge application also pose human health hazards. Current research indicates there is strong circumstantial evidence supporting the hypothesis of typhoid and cholera transmission by wastewater-irrigated crops, and demonstrate that wastewater irrigated vegetables are the main mode of transmission (Shuval 1993). In a long-term study of results from Middle East countries, Shuval, Yekutiel, and Fattal (1985) indicated that both *Ascaris* and *Trichuria* infections were actively and massively transmitted to the general public, who consumed vegetables irrigated with raw wastewater. Oron et al. (1991) showed that, in order to reduce the human-health risk associated with fecal coliform contamination of sweet corn, the harvesting schedule should be delayed as long as possible after the last irrigation. The development of a model using empirical evidence, (Shuval, Yekutiel, and Fattal 1986a) suggests that the highest risk of pathogen transmission, infection, and sickness is associated with the helminths, followed in order by bacterial infections, and last by viral infections. Although certain health risks are definitely associated with the use of raw wastewater in agriculture, the epidemiological evidence assembled by Shuval et al. (1986a, b) suggests that the very stringent wastewater-irrigation standards developed in many of the industrialized countries are overly restrictive, and that a guideline for unrestricted wastewater irrigation be based on an effluent with less than one nematode egg (*Ascaris* or *Trichuris*) per liter and a geometric mean fecal coliform concentration of 1,000 per 100 mL. In addition to the threat posed by direct application to land, some researchers have suggested (Shuval et al. 1989; Kowal, Pahren, and Akin 1981) an airborne threat from spray applications of wastewater irrigation; that public access to applied-to areas be limited to a distance of 200 m and humans should have minimal contact with treatment sites them.

Radioactive Waste Disposal

In certain ways, the transport of radionuclides is similar to what we have already discussed. However, the greatest difference is that radionuclides are both nonconservative, and extremely hazardous; because of this, research results are not readily available in this area. The transport of radionuclides is particularly important in the storage of radioactive wastes. Any new radioactive waste disposal site to be established must meet applicable federal and state regulatory criteria to become a licensed site, such as 10 CFR Part 61 under the authority of the Nuclear Regulatory Commission (NRC). This regulation (Part 61.5), contains criteria covering technical requirements for low-level waste (LLW) disposal. For a site to become licensed it must be able to be characterized, modeled, analyzed, and monitored. The disposal zone at such sites must also be well above the water-table fluctuation zone. One of the principal reasons that modeling is required, is to demonstrate that the migration of radionuclides away from the disposed waste, either in liquid or gaseous state, will meet regulatory concentration limits at the boundary of the site or at points of exposure. Current regulations require site-performance criteria to be satisfied for at least 500 years. Due to the hazardous nature of such wastes, it is likely that future regulations will become even more restrictive, especially as our technology for predicting transport improves.

For low-level waste sites, subsurface hydrology is a particularly important aspect of site characterization, because subsurface water and vapor transport are the primary natural pathways for the movement of contaminants from a disposal facility to the accessible environment. Such transport may move in any direction—vertically downward to the water table,

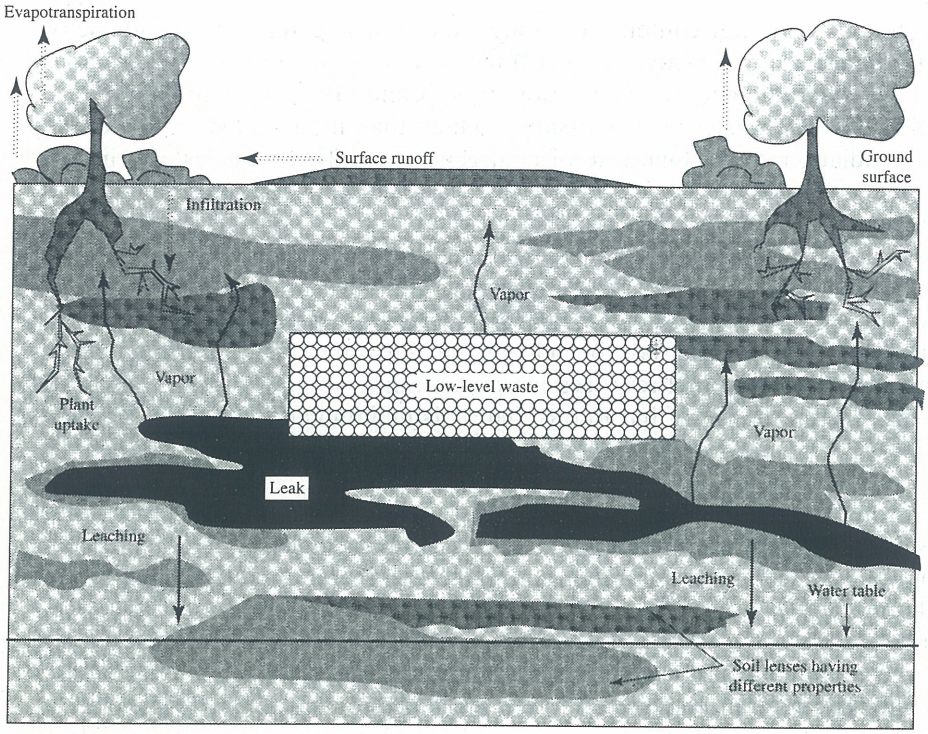

Figure 10.10 Conceptualization of the physical processes that affect contaminant transport at a near-surface, low-level waste site (data from Polmann 1988)

laterally into adjacent soils and root systems, or upward towards the atmosphere; this is illustrated in figure 10.10. The analysis of subsurface contaminant transport is complicated by a number of factors; including the difficulty of observing subsurface processes, the long time-scales required for experiments, and the need to account for soil-water interactions and spatial variability. The situation is particularly complex in the unsaturated zone, where soil properties change dramatically with moisture content; it is even more complicated in the presence of hazardous wastes. Because spatial variability and nonlinear behavior greatly complicate the equation that describes unsaturated flow and transport, performance assessments for unsaturated sites rely heavily on numerical modeling. Also, it is important to note that small-scale fluctuations in soil properties are important because they have large-scale consequences (e.g., anisotropy and macrodispersion). However, small-scale fluctuation in moisture content or concentration is not particularly important, at least from a licensing point-of-view.

Similar conditions are encountered at radioactive-waste disposal sites in comparison to other vadose-zone studies. These conditions include dry media with very low rates of fluid movement, especially for shallow land burial where evapotranspiration losses can have great effects on site hydrology. For arid conditions, evapotranspiration can represent a very large portion of the total water balance. Other conditions include strongly hysteretic and anisotropic conditions, nonlinear sorption, multi-species chain decay, highly variable transient-moisture conditions, dual porosity, and unusual boundary conditions such as wicking schemes, capillary-barrier trench caps, and deep-boring emplacement.

If the unsaturated zone is to be considered as host medium for the emplacement of radioactive wastes, the medium must be an effective barrier to radionuclide transport. The design of suitable repositories depends on the capability to predict the effectiveness of the medium as a barrier. The usefulness of predictive models is limited by the difficulty of analyzing and predicting solute transport as influenced by large reaction-networks. Additionally, there is a general lack of information relating solute-transport mixing parameters and

reaction parameters to the water content of the medium. Typical categories of radioactive waste include: **(1)** high-level radioactive waste, **(2)** transuranic waste, **(3)** low-level radioactive and mixed low-level radioactive and hazardous wastes, and **(4)** uranium mill tailings.

High-level radioactive wastes include fission products that initially have a high level of beta and gamma radiation, and a high rate of heat generation. These wastes also include transuranic elements with long half-lives. Transuranic waste contains long-lived alpha emitters at concentrations greater than 100 nCi g^{-1}, and generate little or no heat. The term "low-level waste" has carried a changing and imprecise definition over the years; currently, it generally means waste that does not fit the definition of high-level waste, and in which the concentration of transuranic elements is less than 100 nCi g^{-1} . In part, these wastes consist of miscellaneous solid materials that have been irradiated and contaminated through use, as well as products of reactors and fuel-reprocessing plants. Some low-level wastes are mixed with materials that are on the list of hazardous materials maintained by the U.S. Environmental Protection Agency, and are thus subject to relevant environmental laws for such substances.

A variety of methods have been developed for storage of various radioactive wastes. Hazardous wastes with lower potential for contamination are often placed in individual containers made out of steel, concrete, and other materials, then stored directly on top of land surface. A similar method involves covering the specially engineered container with soil that generally extends the life-expectancy of the container. Another method is to use the same type of engineered containers and bury them below land surface, then backfill over them or surround the container with an engineered hydro-geological environment to provide enhanced containment for the system. For very deep storage, containers are sometimes placed in boreholes that can be in excess of 30-m deep; they are then either backfilled with the original material, or most often backfilled with bentonite clay. Because bentonite is so adsorptive, and due to its large surface area (750 m^2 g^{-1}) and physical properties, it is a very effective containment material as long as it is not in the presence of a rising and falling water table. The presence of such a water table can destroy the integrity of the bentonite, and cause significant swelling and the possible development of long-term cracks; such cracks can serve as flow paths for deeper movement of the waste material in the event of container leakage.

The preferred climate for burial of wastes is one with an arid environment and a very thick vadose zone. Yucca Mountain, Nevada, 160 km northwest of Las Vegas, meets these basic requirements. The U.S. Department of Energy (DOE) has been conducting a hydrogeological characterization of the soil at the site, as a potential repository for the disposal of commercially generated high-level radioactive wastes and high-level radioactive wastes from DOE defense facilities, as directed by the U.S. Congress. The process and schedule for this program were specified in the Nuclear Waste Policy Act of 1982. In May 1986, the DOE recommended (and the President approved) the Yucca Mountain, Nevada, site as one of three candidate-sites for detailed study. In December 1987, in the Nuclear Waste Policy Amendments Act, the Yucca Mountain site was designated by the Congress for characterization as the single candidate-site for a geological repository (10 CFR Part 60).

It should be made clear that the Yucca Mountain Site has not been selected as a repository; it is at this time the only site designated for study to assess its suitability for containment of high-level radioactive wastes (Nuclear Waste Policy Act, Section 113). Due to the very nature of radioactive wastes, the study of the Yucca Mountain site and its potential as a repository is surrounded by controversy, especially since a 7.5-magnitude earthquake occurred near Landers, California, on June 28, 1992 (O'Brien 1993). Since that time, the State of Nevada and many of its residents have openly expressed criticism of the site and often refer to 10 CFR Part 60 as the "Screw Nevada Bill." While this may sound somewhat humorous, finding a repository for high-level wastes is a necessity, since we continue to produce them.

For a site to be capable of storing radioactive, hazardous wastes, it must be isolated from subsurface-flow regimes and fractured bedrock because of the complexity of delineating flow paths. The flow velocity of the site and therefore of the radionuclides and other wastes, should be low; this indicates a greater residence-time of the chemical within the medium, allowing for physical, chemical, and biological changes such as retardation, degradation, and adsorption. The site should be structurally stable and should lack subsurface flowlines which can lead directly to ground water zones of potable water, or to the atmosphere.

Landfills

Landfills are used for the disposal of solid wastes that are produced by municipalities and local industries. Due to the mass of such wastes (about 3.5 kg of solid waste per capita per day), many cities are seeking disposal in other areas (and states) with more space for disposal, but also with smaller populations. The waste disposed of in landfills may contain many toxic substances, such as liquid industrial wastes, oil, solvents, and other chemicals.

The disposal of such wastes may have a detrimental effect on ground water. In humid regions in the northeastern and southeastern United States, infiltration of water from precipitation events can cause water-table mounding, within or directly below the landfill site; this causes leachates to flow downward and outward from the site. This in turn can induce leachate springs at the edges of the site where chemicals collect, and can then be transported via overland flow during significant-recharge events and potential seepage, into streams or nearby surface waters.

If sites could be ideally selected using the basic criteria described in the section on radioactive wastes, contamination could be minimized. However, due to spatial variability of soils, such sites are extremely difficult to find when considering economical disposal of solid wastes due to the costs of: collection; processing; transportation distances; and dumping. In addition to leachate migration, biochemical decomposition of organic matter (and by-products within the waste) occurs, giving off common gases such as methane, carbon dioxide, and hydrogen sulfide. These common gases can cause extensive damage to vegetation surrounding the site, and can result in odor problems. The generation of methane, while odorless, can also cause hazards due to its explosive potential.

Landfill sites are becoming safer because of better design and technological capabilities; however, many sites are not well-monitored and thus, there is no realistic way to determine how much contamination they cause. Also, without long-term monitoring, conclusions about future contamination by landfills are simply conjecture.

Other Sources of Contamination

There are many other potential sources for contamination of ground- and surface-waters. These include agricultural activities: crop; poultry; swine and cattle production; greenhouses; golf courses; ball fields; and other areas that use high rates of irrigation, along with the significant application of fertilizers and pesticides. In many instances, agricultural activities result in what is termed "non-point source pollution", because they influence water quality some distance away from where actual operations are occurring.

Perhaps the most threatening problem from agricultural activities, other than nitrate leaching, is the potential hazard resulting from transport of herbicides (widely applied in the United States) through the soil profile. Currently, the most threatening of these chemicals may be atrazine. In 1990, about 29 million kilograms of atrazine were applied to soils in the United States to control broad-leaf weeds (Gianessi and Puffer 1991). Such chemicals are commonly sprayed on crops in early spring, when the soil is relatively moist, evapotranspiration

rates are low, and spring rains are prevalent. Because the fate of atrazine is primarily controlled by chemical, biological, and hydraulic properties of soil—as well as by weather conditions—the timing of application of this and other herbicides is extremely important, not only for effective weed control, but also for minimal ground water contamination risks. Research has shown that, for many soils, atrazine and other herbicide transport is directly related to the amount and timing of rain that follows spring application and the occurrence of flooding (Eckhardt and Wagenet 1996; Tindall and Vencill 1995; Kolpin and Thurman 1993). Two other factors were also found to be critical in transport during wet years: **(1)** the variability of herbicide-application rate, and **(2)** degradation rate of the herbicide (Eckhardt and Wagenet 1996). Such research has shown that the coincidence of heavy rain soon after herbicide application can cause the herbicide to move below the rooting-zone depths at which biodegradation rates are assumed to be low, but are often unknown. Once an herbicide has been leached below the rooting zone, it can persist in the underlying soil and can subsequently be transported into ground water as the soil drains, usually after the growing season.

Industry also contributes a large amount of contaminants to the environment. In the U.S., there are about two million underground storage tanks, 90,000 confirmed releases of contaminants, 150 superfund sites, 15,000 annual oil spills, deep-well injections of hazardous wastes, and other contaminants from industrial and urban sources. These can include mine tailings, fly-ash deposits, salts applied to roads during winter months that run off in the spring, both killing vegetation and contaminating surface water, industrial-waste lagoons, and other activities.

Problems arising from these potential sources of contamination will not diminish, but worsen due to increasing population and its encroachment on aquifer recharge areas. It is imperative that scientists carry out well-planned, applied and theoretical research, and develop accurate, predictive models to provide answers that outline proper design and management techniques to deal with these problems.

10.16 CASE STUDY: RADIONUCLIDE DISTRIBUTION AND MIGRATION MECHANISMS AT MAXEY FLATS

The primary purpose of this case study is to help the reader develop an understanding of chemical processes that significantly influence the migration of radionuclides at commercial low-level waste burial sites. The chemical measurements of waste-trench leachate and identification of chemical changes in leachate during migration will provide a basis for geochemical waste-transport models. Two general kinds of radionuclides were determined in the research at Maxey Flats (near Morehead in northeastern Kentucky): endogenous (natural) radionuclides originating from soil parent material; and exogenous (human-induced) radionuclides originating from the nuclear fuel process. Cobalt-60 and ^{137}Cs are exogenous radionuclides and both are constituents of global fallout, as well as being components of low-level radoactive waste stored at Maxey Flats. Potassium-40 and ^{228}Th are endogenous radionuclides originating from the underlying rock strata and soil. In a typical gamma-ray spectrum, most of the peaks that were found at the site were due to endogenous radionuclides, chiefly natural uranium, thorium (and their daughter-products), and ^{40}K.

As with all multidisciplinary large-scale projects, the Maxey Flats study followed a systematic approach. The first part of the study involved an unsaturated-zone hydrology investigation to determine the pathway(s) of water entry into the low-level radioactive waste burial-trenches, and to investigate possible countermeasures for reducing water infiltration into the trenches. A transect across trench 19S (figure 10.11) and the adjacent area was instrumented with electrical soil-moisture sensors to allow measurements of relative porous media matric potential and with mini-porous cups (i.e., suction lysimeters) for extraction of

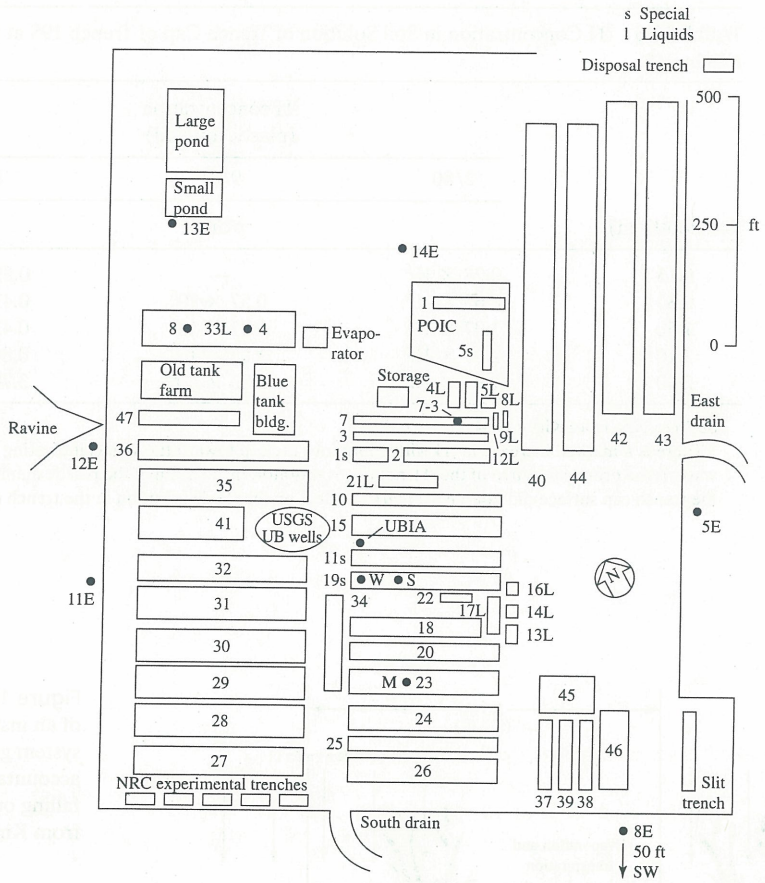

Figure 10.11 Map of Maxey Flats disposal site, showing the location and identification of disposal trenches (data from Kirby 1984)

soil water in the region of the soil-moisture sensors. This type of porous cup allows extraction of soil water under unsaturated conditions down to about −80 kPa and thus are good for sampling in moist unsaturated media. Tritium concentrations in the porous cups in the trench transect indicated that near the trenches, the principal source of tritium was the waste, and not the evaporator located on site (table 10.5). The investigation of transport of tritium to the atmosphere by plant-root uptake (Kentucky fescue grass) of trench water, and leaf transpiration was also part of this investigation. Additionally, a large lysimeter was installed to account for all precipitation at the site, and to investigate the management of countermeasures for reducing water infiltration into the trenches (figure 10.12). Tritium present in the waste was employed as a tracer of fluid movement. It was discovered that the principal mode of water entry into the trench was by percolation through the trench caps, and that lateral movement within the soil profile was very slow; the deep vertical movement of water through the undisturbed soil profile was very slow as well. The Kentucky fescue grass grown and sampled on-site extracted significant amounts of tritium from the trenches and, by transpiration, transported the tritium to the atmosphere (table 10.6). Also, tritium in the plant transpiration stream could have served as a tool for mapping trench boundaries (table 10.7). Data from the measurements conducted on the west side of the restricted area (figure 10.13) indicate that no major tritium sources originated from seepage at the lower elevations leading from the site.

Ethylenediaminetetraacetic acid (EDTA) was found to be the major organic compound in water from various waste trenches at the site and from inert atmosphere wells. Inert atmosphere wells were installed near the experimental trench to help maintain the

TABLE 10.5 ^{3}H Concentration in Soil Solution of Trench Cap of Trench 19S at Station number 4*

	^{3}H concentration (plastic applied)		
	2/80	9/81	8/82
Soil depth (m)	pCi/l		
0.15	0.28×10^{6}	—	0.59×10^{6}
0.30	0.65×10^{6}	0.57×10^{6}	0.43×10^{6}
1.50	1.07×10^{6}	0.97×10^{6}	0.43×10^{6}
2.10	2.07×10^{6}	1.85×10^{6}	0.86×10^{6}
2.40	7.93×10^{6}	5.23×10^{6}	3.70×10^{6}

Source: Data from Kirby 1984

* There is a marked increase in ^{3}H with depth into the cap toward the waste, indicating that the waste is the principal source of the ^{3}H, not the evaporator. Installation of the plastic membrane on the trench cap surface did not have a marked effect on the ^{3}H distribution in the trench cap.

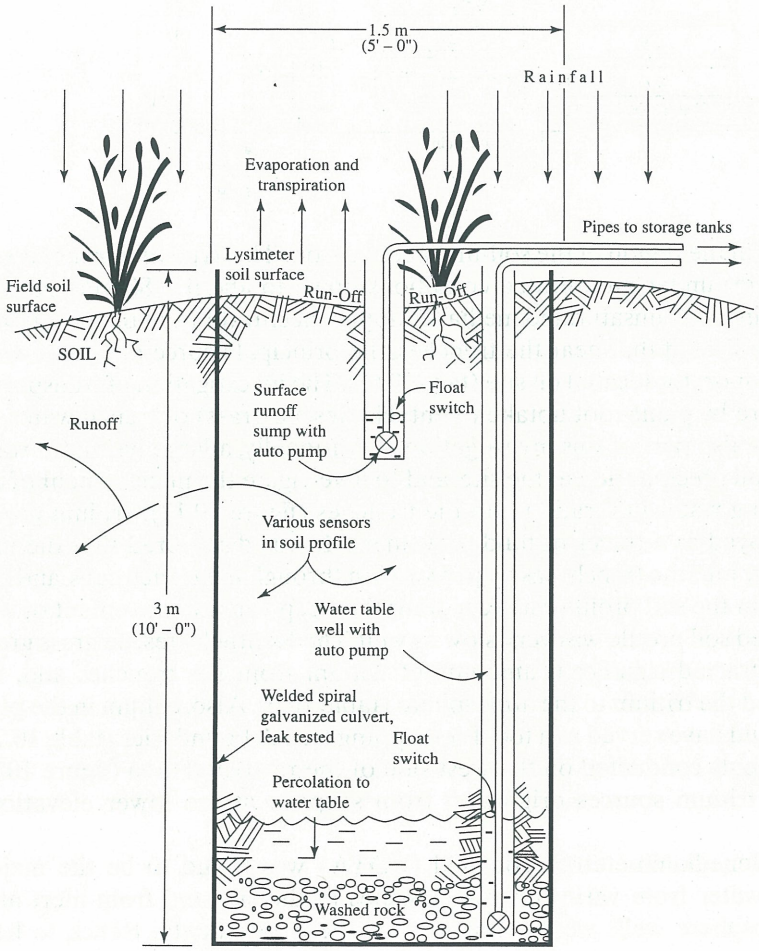

Figure 10.12 Cross-section of an installed lysimeter. The system gives complete accountability of all rain falling on soil surface (data from Kirby 1984).

TABLE 10.6 ^3H Concentration in Leaves of Kentucky Fescue Grass Grown on Trench Caps and Nearby Field (Controls) at the Southeast Corner of the Maxey Flats Site, Sampled February 1982*

Trench number	^3H concentration in plant sap† (^3H_2O)	^3H concentration in trench water (^3H_2O)	^3H concentration in leaf organic material†† (C^3H_2O)
	pCi/l		
37	6.9×10^7	3.7×10^7	9.7×10^4
38	3.5×10^7	3.3×10^7	4.3×10^4
39	10.5×10^7	10.1×10^7	14.0×10^4
control	1.1×10^7	—	2.0×10^4
control	1.0×10^7	—	2.0×10^4
control	0.9×10^7	—	1.0×10^4

Source: Data from Kirby 1984

*This was a preliminary study with one grass sample taken from each trench cap. The ^3H in the transpiration stream was about seven times higher in the plants grown in the trench caps than in that of the controls, but it was only 1/1000 of the trench water. The organic (structural) ^3H was twice as high as it should have been at equilibrium, with the ^3H present in the transpiration stream indicating higher ^3H concentration probable in the soil solution and transpiration stream during the growing season of the past fall.

† Determined by vacuum distillation of fresh leaf material, then liquid scintillation of the ^3H_2O distilled off.

†† Determined by reacting vacuum-dried leaf material with O_2 at 900 °C, then liquid scintillation of the resulting ^3H_2O.

TABLE 10.7 Titrium in Transpiration Stream of Fescue Grass*

Sample no.	Trench no.	^3H pCi/l	Sample no.	Trench no.	3H pCi/l
1N	38	0.12×10^6	7N	39	1.18×10^6
1E	38	0.14×10^6	7E	39	0.91×10^6
1S	38	0.43×10^6	7S	39	6.97×10^6
1W	38	†	7W	39	108.76×10^6
1C	38	0.44×10^6	7C	39	3.79×10^6
2N	38	0.13×10^6	8N	38	0.84×10^6
2E	38	0.65×10^6	8E	38	0.71×10^6
2S	38	†	8S	38	1.05×10^6
2W	38	†	8W	38	2.09×10^6
2C	38	0.40×10^6	8C	38	1.05×10^6
3N	38	0.12×10^6	9N	37	0.25×10^6
3E	38	†	9E	37	0.27×10^6
3S	38	†	9S	37	0.24×10^6
3W	38	†	9W	37	0.28×10^6
3C	38	0.36×10^6	9C	37	0.27×10^6
4	38	0.27×10^6	10N	37	0.67×10^6
4	38	0.50×10^6	10E	37	1.07×10^6
4	38	0.30×10^6	10S	37	1.31×10^6
4	38	0.26×10^6	10W	37	0.18×10^6
4	38	0.27×10^6	10C	37	0.63×10^6
5	38	1.63×10^6	11N	37	0.44×10^6
5	38	†	11E	37	0.67×10^6
5	38	†	11S	37	0.37×10^6
5	38	†	11W	37	0.07×10^6
5	38	0.29×10^6	11C	37	0.46×10^6
6	39	0.30×10^6	12	38	0.12×10^6
6	39	†	12	38	0.12×10^6
6	39	†	12	38	0.18×10^6
6	39	†	12	38	0.13×10^6
6	39	0.43×10^6	12	38	0.14×10^6

Source: Data from Kirby 1984

*Purpose of sampling was to locate a uniform area to use for repeated sampling to determine the annual transport of ^3H to the atmosphere by the transpiration stream of fescue. Location of trench boundaries are not well-known and, evidently, some samples were not taken from over trench. This observation suggests that ^3H concentration in the transpiration stream may serve as an accurate indicator of the location of trench boundaries .

†Samples collected but not yet analyzed.

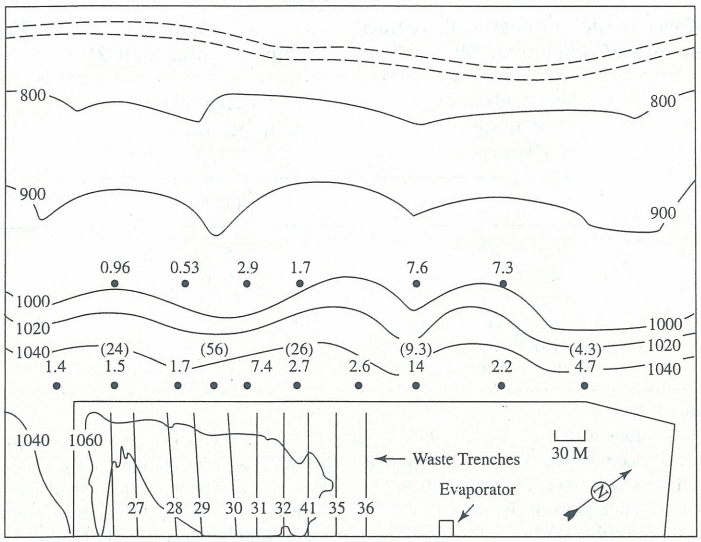

Figure 10.13 Tritium concentrations in systemic water from trees in the west drainage at Maxey Flats in July, 1981 (bracketed numbers) and July, 1982 (unbracketed numbers). Concentration units are 10^4 pCi/L and contour intervals are in feet. The absence of elevated tritium levels at the illustrated elevations demonstrates that there is probably very little subsurface flow from the site (data from Kirby 1984).

initial-oxidation state of the dissolved radionuclides in ground water samples; they were generally filled with inert gases such as nitrogen and argon. EDTA and EDTA-like species coelute with alpha-emitting radionuclides and ^{60}Co. Data collected at Maxey Flats showed that migration of plutonium was as an EDTA complex. Other phases of the study included geochemistry of trench leachates and the influence of soil chemistry on mobility of radionuclides. These studies are not within the scope of this text; the reader is referred to Kirby (1984) for additional information on the Maxey Flats study.

Another phase of the Maxey Flats study was ecological monitoring to develop efficient and statistically valid ecological field-sampling procedures and methods for post-closure monitoring at commercial shallow-land burial sites. The kinds and amounts of radionuclides and trace elements in environmental samples are normally measured with emphasis on biotic uptake, bio-accumulation, biotic transport, and ecological pathways in semi-wild ecosystems. To evaluate potential biotic pathways, forest-floor litter, newly fallen leaves, newly opened leaves and surface soil were sampled in the forest surrounding the restricted area, and then analyzed by high-resolution gamma-ray spectroscopy. Most of the radionuclides in the forest were associated with the soil; relatively small amounts of radionuclides were associated with the litter and leaves. The ^{60}Co content of newly fallen leaves (figure 10.14) was more variable than the other radionuclides, suggesting that the burial site has influenced the ^{60}Co concentrations at a few of the sampling locations and newly opened leaves from one hickory tree suggested that the source of elevated ^{60}Co concentrations was the rooting substrate. The other radionuclide concentrations exhibited little variation between tree species from location to location. Leaf water data indicated that tritium above ambient fallout levels migrated into the edge of the forest at Maxey Flats.

As a potential biomonitor of subsurface-water movement, maple trees (*Acer sacharum*), were also sampled as part of the ecological phase because of their unusual ability to move water through their trunk before new leaves emerge in the spring; if the roots tap tritiated water, tritium will appear in the sap stream. The maple trees were tapped at various locations around the site (figure 10.15) during the most vigorous sap flow of the season. Samples of sap from the maple trees showed concentrations ranging from < 430 pCi L^{-1} at a location about 12 miles south of the site, to a high value of 2.9×10^5 pCi L^{-1} at a location near the west side of the site.

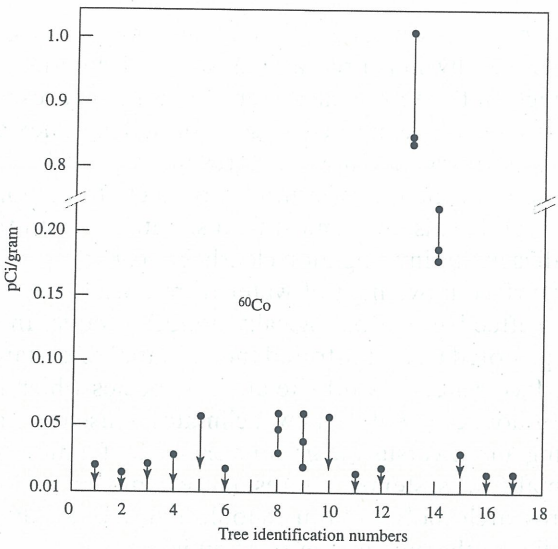

Figure 10.14 Cobalt-60 in newly fallen leaves in the oak–hickory forest at Maxey Flats, Kentucky (data from Kirby 1984)

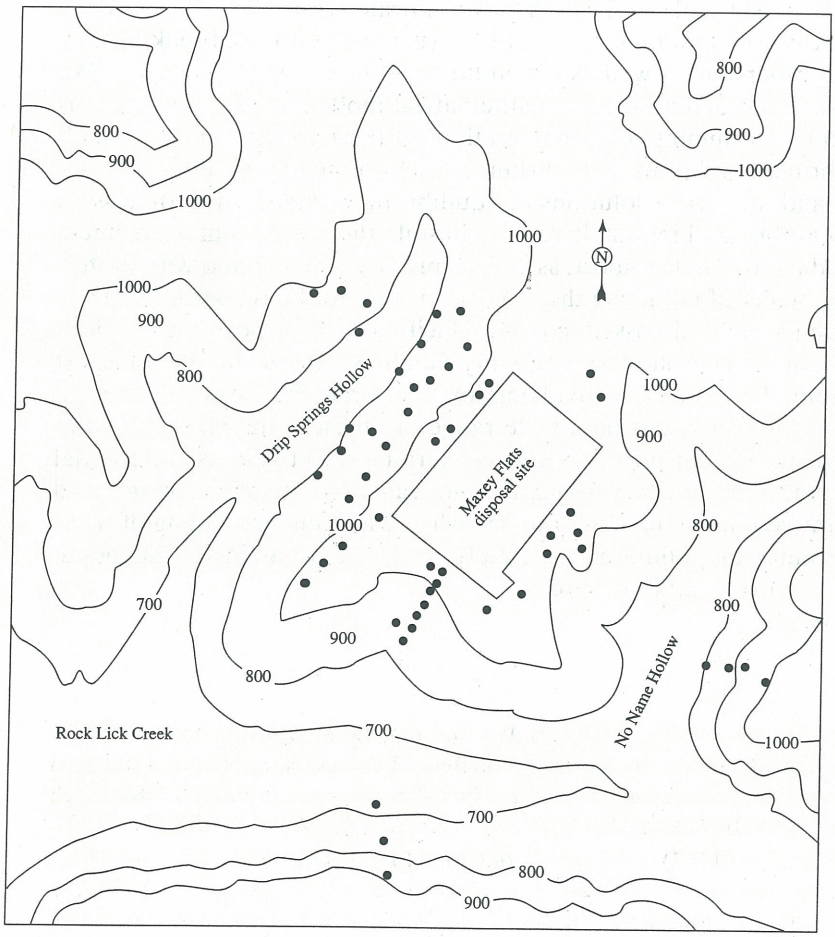

Figure 10.15 Locations of sap sampling trees (•) near the Maxey Flats site, 1983 (data from: Kirby 1984)

From the studies involving the fescue grass, biomass, and maple trees, we hope to illustrate a point to the reader. Generally, much research is accomplished in soil investigations that totally disregard the effects of the ecological system—that is, the presence of plants, microorganisms, and fauna. However, as we have discussed, soil is a complex and dynamic system, especially in the presence of flora and fauna. As a result, most real-world problems are not enhanced, nor is the transport of chemicals accurately predicted by ignoring the presence of living flora and fauna inherently existent in most field situations. Both the studies of fescue grass and ecological studies in this investigation clearly indicate the potential of plants to serve as biomonitors of subsurface movement of water from burial sites, and the ability of such studies to be both cost-effective and biologically nondestructive. In the Maxey Flats study, tritium uptake by deep-rooted trees illustrated the potential of certain plant species to serve as a monitor of subsurface water flow off-site and for species which root in the upper 10–15 m of soil, there is an economic advantage in wet climates to use trees as a tool. The primary reason: the cost of using a tree versus the greater expense of a monitoring well. While the presence of plants may make the system of interest more complex in some instances, they can also serve as valuable research tools and thus, should not necessarily be discounted in favor of purely physical studies of the media (a less-dynamic system).

SUMMARY

This chapter has focused on transport of chemicals in the unsaturated zone. We have discussed the physical processes that cause contaminant transport, types of fluid flow, breakthrough curves and hydrodynamic dispersion, as well as piston flow and mechanical dispersion. We also discussed: nonreactive and reactive solutes; mathematical modeling; general solutions for a displacing-solute front; determining the concentrations of these fronts; various boundary conditions; nonequilibrium conditions; equilibrium chromatography; the effects of ion exchange and dispersion; and numerical solutions of equilibrium exchange. The discussion also focused on aspects of mobile and immobile regions in soils, the effects that aggregated, fractured, and layered-media have on transport, as well as problems associated with preferential pathways and the difficulty of modeling them. We also showed the reader how to calculate dispersion coefficients, and discussed colloidal-facilitated transport and various sources of contamination that affect ground water quality. Finally, we discussed the transport of radionuclides and presented a case study involving low-level, radioactive-waste storage.

Contaminant transport is dependent on a wide range of physical and chemical parameters. Because our knowledge of transport is limited concerning such topics as preferential flow, colloidal-facilitated transport, waste storage, loading rates of municipal wastes and other activities, it is imperative that we increase our knowledge and understanding of these processes to combat environmental pollution successfully in the face of an increasing population and demand on our environmental resources.

ANSWERS TO QUESTIONS

10.1. Determine erf(0.90); erf(0.90) = $2N(1.414)(0.90)$. We find that by multiplying 1.414 * 0.90 = 1.273. This value can be evaluated in the Normal Probability Function Table (from a standard text on statistics); looking up the area for 1.273 we find by extrapolation it is about 0.3985, which we now use in the equation above such that erf(0.90) = $2N(1.414)(0.90)$ = 2(0.3985) = 0.797.

10.2. You will notice that this value (0.797) is the answer obtained for 10.1 thus, when erf z = 0.797, z can be found by the relation erf $z = 2N\sqrt{2z}$. Consequently, $N(\sqrt{2z})$ = erf $z/2$ = 0.797/2 = 0.3985 which matches the area found for question 10.1, thus, z = 0.90. This answer could be

found straight/forward by looking up $z = 0.90$ in the table of complimentary error functions (appendix 3) to find that erf(0.90) = 0.796908.

10.3. The first step is to examine equation 10.24 to see which parameters we need. From the diameter of the column we need to know the area A, to determine q. Thus, $A = 1963.5$ cm^2 and $q = (Q/A)\theta = (280/1963.5)/0.45 = 0.317$ cm hr^{-1}, and the slope $S = 5.0$. Now, using equation 10.24, $D = (0.317 * 125)/(4\pi 5) = 0.631$ cm^2 hr^{-1}.

10.4. This requires taking the upper limit of the integral in equation 10.21, equal to q by using the chain rule to begin with, such that $d[C(x, t)/dp]$ is given by

$$\frac{d\left(\frac{C(x,t)}{C_o}\right)}{dq} = -\sqrt{2\pi}^{-1} \exp\left[-\frac{(1-N_{pv})^2}{\left(\frac{4DN_{pv}}{qL}\right)}\right] \tag{10.138}$$

Because this derivative is a function of $-w^2/2$ raised to the exp and evaluated at $[(1 - N_{pv})/(2DN_{pv}/qL)^{0.5}] \times (2\pi)^{-0.5}$, the derivative of dq/dp is given by equation 10.22.

10.5. Considering equation 10.16 and its relation to the complimentary error function, equation 10.29 can be converted to the normal probability integral such that

$$\frac{C(x,t)}{C_o} = \frac{1}{2}\left(1 - \frac{2}{\sqrt{\pi}}\int_0^{(1-N_{pv})/2\sqrt{DN_{pv}/qL}} \exp(-\beta^2)\, d\beta + \exp\left[\frac{qL}{D}\right]\left[1 - \frac{2}{\sqrt{\pi}}\int_0^{1+N_{pv}/2\sqrt{DN_{pv}/qL}} \exp(-\beta^2)\, d\beta\right]\right) \tag{10.139}$$

Now, by substitution of $w^2/2$ for β^2 as done earlier, we obtain

$$\frac{C(x,t)}{C_o} = \frac{1}{2} - \sqrt{2\pi}^{-1}\int_0^{(1-N_{pv})/\sqrt{2DN_{pv}/qL}} \exp\left[-\frac{w^2}{2}\right] dw + \frac{\exp\left[\frac{qL}{D}\right]}{2} - \frac{\exp\left[\frac{qL}{D}\right]}{\sqrt{2\pi}}\int_0^{(1+N_{pv})/\sqrt{2DN_{pv}/qL}} \exp\left[-\frac{w^2}{2}\right] dw \tag{10.140}$$

This results (skipping several steps) in a derivative of the above equation with respect to N_{pv}, which is evaluated at $N_{pv} = 1$ of

$$\left.\frac{d\left(\frac{C(x,t)}{C_o}\right)}{dp}\right|_{N_{pv}=1} = \left(2\sqrt{\frac{\pi D}{qL}}\right)^{-1} \tag{10.141}$$

A slight manipulation will yield equation 10.24 as previously discussed.

10.6. We can obtain an estimate of K_{oc} by using equation 10.51. First substitute the value for the solubility of dicamba (0.04 mg/L) for S and then calculate to obtain $K_{oc} = 25{,}637$. For K we can use the expression $K = K_{oc}$ (percent oc)/100 to obtain $K = 25{,}637(2)/100 = 512.7$. To obtain S, we may now use equation $S = KC^n$ such that $S = 512.7(10)^{0.87} = 3801$ μg/g.

10.7. For the following derivations of Richard's equation and the ADE, the reader should refer to figure 10.16 to visualize conceptually the mass-change, storage, and flux processes.

Derivation of Richard's equation

$$q = \frac{v}{At} = \frac{\text{cm}^3}{\text{cm}^2/\text{sec}} = \frac{\text{cm}}{\text{sec}} \tag{10.142}$$

flow in	*flow out*	
$q \times \Delta y\, \Delta z$	$\left(q_x + \frac{\partial qx}{\partial x}\Delta x\right)\Delta y\, \Delta z$	(10.143)

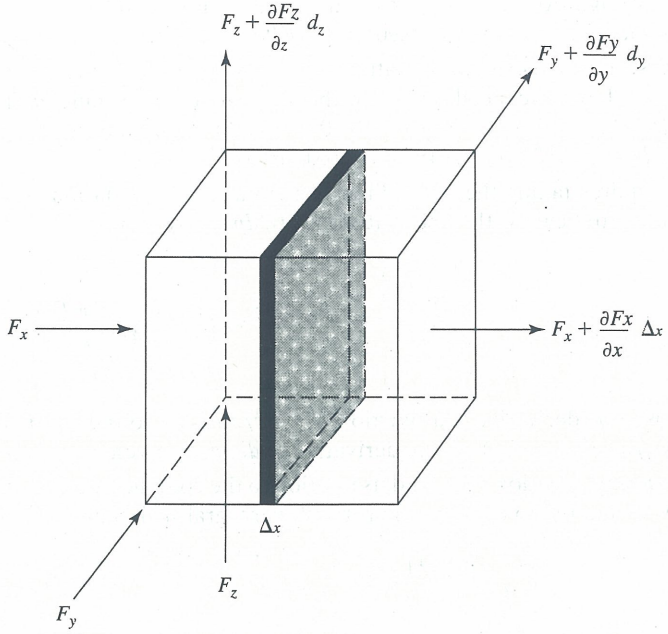

Figure 10.16 Flux across an interval (Δx) within a three-dimensional box

Mass change = flow in − flow out

$$z - \left[qx + \frac{\partial qx}{\partial x}\Delta x\right]\Delta y\,\Delta z = -\frac{\partial qx}{\partial x}\Delta x\,\Delta y\,\Delta z = -\left(\frac{\partial qx}{\partial x} + \frac{\partial qy}{\partial y}\right) \tag{10.144}$$

What is the volume change of H_2O?

$$\frac{\partial}{\partial t}(\theta\,\Delta x\,\Delta y\,\Delta z) = \frac{d\theta}{dt}\Delta x\,\Delta y\,\Delta z \tag{10.145}$$

$$\frac{d\theta}{dt}\Delta x\,\Delta y\,\Delta z = -\left(\frac{\partial qx}{\partial x} + \frac{\partial qy}{\partial y} + \frac{\partial qz}{\partial z}\right)\Delta x\,\Delta y\,\Delta z \tag{10.146}$$

$$\frac{d\theta}{dt} = -\frac{\partial qx}{\partial x} - \frac{\partial qy}{\partial y} - \frac{\partial qz}{\partial z} \tag{10.147}$$

Equation 4 is the three-dimensional continuity equation. In one dimension

$$\frac{d\theta}{dt} = -\frac{\partial qx}{\partial x} \tag{10.148}$$

By Darcy's law

$$q_z = -K\frac{\partial H}{\partial z} \qquad \text{where } H = h + z \tag{10.149}$$

Consequently,

$$\frac{\partial qz}{\partial z} = -\frac{\partial}{\partial z}\left[-K_z\frac{\partial H}{\partial z}\right] \tag{10.150}$$

Thus

$$\frac{\partial\theta}{\partial t} = \frac{\partial}{\partial z}\left[K_z\frac{\partial H}{\partial z}\right] \qquad \text{one dimension (vertical)} \tag{10.151}$$

However, for unsaturated flow $K(\theta)$ and $K(\psi_m)$, then

$$\frac{\partial\theta}{\partial t} = \frac{\partial}{\partial z}\left[K_z(\theta)\frac{\partial H}{\partial z}\right] \tag{10.152}$$

Since $H = h + z$, then

$$\frac{\partial \theta}{\partial t} = \frac{\partial}{\partial z}\left[K_z(\theta)\left(\frac{\partial h}{\partial z} = \frac{\partial z}{\partial z}\right)\right] \tag{10.153}$$

and

$$\frac{\partial \theta}{\partial t} = \frac{\partial}{\partial z}\left[K_z(\theta)\left(\frac{\partial h}{\partial z} + 1\right)\right] \tag{10.154}$$

$$\frac{\partial \theta}{\partial t} = \frac{\partial}{\partial z}\left[K_z(\theta)\frac{\partial h}{\partial z}\right] + \frac{\partial K_z(\theta)}{\partial z} \tag{10.155}$$

Equations 10.153–155 are all one-dimensional forms of Richard's equation to describe water flow under transient conditions. Now, we wish to enter the term D (diffusivity) to describe Darcian flow under unsaturated conditions.

$$D = K_z(\theta)\frac{\partial h}{\partial z} \qquad \text{where } D(\theta) \tag{10.156}$$

By substitution and assuming $\int \theta$ and $\int h(t)$ is continuous, and also by use of the chain rule

$$K(\theta)\frac{dh}{\partial z} = K(\theta)\frac{\partial h}{\partial z}\frac{\partial \theta}{\partial z} \tag{10.157}$$

So

$$\frac{\partial \theta}{\partial t} = \frac{\partial}{\partial z}\left[D(\theta)\frac{\partial \theta}{\partial z}\right] + \frac{\partial K_z(\theta)}{\partial z} \tag{10.158}$$

Equation 15 is the basic form of **Richard's equation** to describe water flow under transient conditions.

Derivation of Solute Transport Equation

Starting with Fick's first law of diffusion

$$J = -D_s\frac{dc}{dx} \tag{10.159}$$

Where hydrodynamic dispersion (D_H) is

$$D_H(V, \theta) = \propto \bar{V} + D_s(\theta) \tag{10.160}$$

By substituting equation 10.159 into equation 10.160

$$J = -D_{S,H}\frac{dC}{dx} \tag{10.161}$$

For mass flow

$$J = qC \tag{10.162}$$

Thus

$$J = \theta D_{S,H}\frac{dC}{dx} - qC \tag{10.163}$$

where

$$q = -K\frac{dH}{dx} \tag{10.164}$$

Now, utilize figure 10.16 for conceptual visualization

$$(J\text{in} - J\text{out})\,\Delta y\,\Delta z = -\frac{\partial J}{\partial x}\Delta x\,\Delta y\,\Delta z \tag{10.165}$$

Written in terms of x, since we are interested in the incremental volume Δx in figure 10.16. Here, the mass change must account for θ and solute concentration (C) with time. Thus

$$\theta\,\Delta x\,\Delta y\,\Delta z \qquad \text{(mass water change)} \tag{10.166}$$

So

$$[C\theta]\,\Delta x\,\Delta y\,\Delta z \tag{10.167}$$

and

$$\frac{\partial(C\theta)}{\partial t}\Delta x\,\Delta y\,\Delta z = -\frac{\partial J}{\partial x}\Delta x\,\Delta y\,\Delta z \tag{10.168}$$

Remembering that

$$J = \theta D_{S,H}\frac{dC}{dx} - qC \tag{10.169}$$

Then

$$\frac{\partial(C\theta)}{\partial t} = \frac{\partial}{\partial x}\left[\theta D_{S,H}\frac{\partial C}{\partial x}\right] - \frac{\partial qC}{\partial x} \tag{10.170}$$

Since $v = q/\theta$, we divide by θ to obtain

$$\frac{\partial C}{\partial t} = \frac{\partial}{\partial x}\left[D_{S,H}\frac{\partial C}{\partial x}\right] - V\frac{\partial C}{\partial x} \tag{10.171}$$

This is the general form of the solute-transport equation (or ADE). However, this is not the final form since we must account for source/sink terms in the soil. Thus,

$$\frac{\partial S}{\partial t}\Delta x\,\Delta y\,\Delta z \tag{10.172}$$

where S is $+$ for source, $-$ for sink, and $S = KC$

$$S = \frac{\mu\text{g}}{\text{g}}\cdot\frac{\text{g}}{\text{cm}^3} = \frac{\mu\text{g}}{\text{cm}^3} \tag{10.173}$$

$$\frac{S\rho_b}{\theta}\Delta x\,\Delta y\,\Delta z = \mu\text{g} \tag{10.174}$$

$$\frac{\rho_b}{\theta}\frac{\partial S}{\partial t}\Delta x\,\Delta y\,\Delta z = \frac{\mu\text{g}}{\text{sec}} \tag{10.175}$$

By substituting equation 10.175 into equation 10.171, we obtain

$$\frac{\rho_b}{\theta}\frac{\partial S}{\partial t} + \frac{\partial C}{\partial t} = D_{S,H}\frac{\partial^2 C}{\partial x^2} - V\frac{qC}{\partial x} \tag{10.176}$$

Using the relation $S = KC$ then

$$\frac{\partial S}{\partial t} = K\frac{\partial C}{\partial t} \tag{10.177}$$

Substituting this into 33, we have

$$\frac{\rho_b}{\theta}K\frac{\partial C}{\partial t} + \frac{\partial C}{\partial t} = D_{S,H}\frac{\partial^2 C}{\partial x^2} - V\frac{qC}{\partial x} \tag{10.178}$$

$$\left(\frac{\rho_b}{\theta}K + 1\right)\frac{\partial C}{\partial t} = D_{S,H}\frac{\partial^2 C}{\partial x^2} - V\frac{qC}{\partial x} \tag{10.179}$$

If we let

$$R = \left(\frac{\rho_b}{\theta}K + 1\right) \tag{10.180}$$

Then

$$R = \frac{\partial C}{\partial t} = D_{S,H}\frac{\partial^2 C}{\partial x^2} - V\frac{qC}{\partial x} \tag{10.181}$$

This is the final form, in one dimensio
ing with radioactive decay, et cetera (
depending on the specific nature of th

10.8. This is an exercise in mathematics to s
tion 10.62 is $C(x_1, t_1) = f(x_1)$ for $t_1 =$
form) using the separation-of-variabl
tion, we shall drop the subscript 1 f
variable technique, we have a solutio
and $G(t)$ is a function of t only. S
$DF''(x)G(t)$. At this time we can d
$F''(x)/F(x)$. Since $F(x)$ and $G(t)$ are f
equal to the same constant, which we
equation as two ordinary differentia
$\alpha^2 DG(t) = 0$. To solve the first ordina
form $F(x) = \exp^{mx}$ which after substit
equal $i\alpha$ where α is an arbitrary const
$F(x) = \cos \alpha x + i \sin \alpha x$. The second
$G(t) = \exp(-\alpha^2 Dt)$. Using a similar
$(-\alpha^2 Dt)(A \sin \alpha x + B \cos \alpha x)$ where t
part is multiplied by constant B. How
series must be used such that the solut

$$C(x, t) = \sum_{n=1}^{\infty} \exp(-$$

for the initial conditions (for which $t =$

$$C(x, 0) = \sum_{n=1}^{\infty}$$

For the evaluation of A_n, B_n, and α_n: a
$-a < x < a$. At this point we shall defi

$$A_n = \frac{1}{a} \int_{-}^{a}$$

and

$$B_n = \frac{1}{a} \int_{-a}^{a}$$

In both equations 10.184 and 10.185, x
is replaced by a dummy variable u and

$$f(u)$$

The results will be substituted into equ
following equation.

$$C(x, t) = \sum_{n=1}^{\infty} \exp\left(\left[-\left(\frac{n\pi}{a}\right)^2 Dt\right.\right.$$

$$\cos \frac{n\pi x}{a} \left[\frac{1}{a} \int_{-a}^{a} f(u)\cos\right.$$

by placing $\sin(n\pi x/a)$ and $\cos(n\pi x/a)$
equation 10.187, we obtain

$$C(x, t) = \sum_{n=1}^{\infty} \exp\left[-\left(\frac{n\pi}{a}\right)^2 Dt\right] \frac{1}{a} \int_{-a}^{a} f(u)$$

By moving the exponential term inside the integral of equation 10.188 and applying the formula (401.04) of Dwight 1961 we obtain

$$C(x,t) = \frac{1}{a}\sum_{n=1}^{\infty}\int_{-a}^{a} f(u)\exp\left[-\left(\frac{n\pi}{a}\right)^2 Dt\right]\cos\frac{n\pi(x-u)}{a}\,du \tag{10.189}$$

Equation 10.189 gives us a solution for u between $-a$ and a—however, we need a solution between minus and plus infinity. Thus, for large values let us write $\Delta\lambda = \pi/a$ and we can express the right side of equation 10.189 as

$$\frac{\Delta\lambda}{\pi}\sum_{n=1}^{\infty}\int_{-a}^{a} f(u)\exp[-(n\,\Delta\lambda)^2 Dt]\cos n\,\Delta\lambda\,(x-u)\,du \tag{10.190}$$

By placing $\Delta\lambda$ after the integral in equation 10.190 we can rewrite it as

$$\frac{1}{\pi}\sum_{n=1}^{\infty}\left[\int_{-a}^{a} f(u)\exp[-(n\,\Delta\lambda)^2 Dt]\cos n\,\Delta\lambda\,(x-u)\,du\right]\Delta\lambda \tag{10.191}$$

For simplification we define the bracketed expression in equation 10.191 as a function like $g(n\,\Delta\lambda)$, and write the expression as

$$\frac{1}{\pi}\sum_{n=1}^{\infty}[g(n\,\Delta\lambda)]\,\Delta\lambda \tag{10.192}$$

The limit (if it exists) of equation 10.192 as $\Delta\lambda$ approaches zero is given by

$$\lim_{\Delta\lambda\to 0}\sum_{n=1}^{\infty}[g(n\,\Delta\lambda)]\,\Delta\lambda = \int_0^{\infty} g(\lambda)\,d\lambda \tag{10.193}$$

To determine when this limit exists we can look at our expression for $g(n\,\Delta\lambda)$ and examine it as $\Delta\lambda$ approaches zero. From equations 10.192 and 10.193, our $g(n\,\Delta\lambda)$ is the integral inside the brackets of equation 10.192. As $\Delta\lambda$ approaches zero it may be seen (from the relation $\Delta\lambda = \pi/a$) that the integral becomes

$$\int_{-\infty}^{\infty} f(u)\,du \tag{10.194}$$

where $f(u)$ is as defined before and we can see that equation 10.193 is valid when $f(u)$ is sectionally continuous, and that equation 10.194 does indeed exist. As a result, we can use equation 10.194 and rewrite equation 10.192 as

$$\frac{1}{\pi}\int_0^{\infty}\left[\int_{-\infty}^{\infty} f(u)\exp(-\lambda^2 Dt)\cos\lambda(x-u)\,du\right]d\lambda \tag{10.195}$$

Since equation 10.195 is the right side of equation 10.189, which has been expanded for $-\infty < x < \infty$, then $C(x,0)$ can be expressed as

$$C(x,0) = \frac{1}{\pi}\int_0^{\infty}\left[\int_{-\infty}^{\infty} f(u)\cos\lambda(x-u)\,du\right]d\lambda \tag{10.196}$$

Equation 10.196 is the Fourier integral formula of $f(x) = C(x,0)$ and upon executing a reverse order of integration, equation 10.195 is written as

$$\frac{1}{\pi}\int_{-\infty}^{\infty} f(u)\left[\int_0^{\infty}\exp(-\lambda^2 Dt)\cos\lambda(x-u)\,d\lambda\right]du \tag{10.197}$$

where the inside integral is given by

$$\int_0^{\infty}\exp(-\lambda^2 Dt)\cos\lambda(x-u)\,d\lambda = \frac{\sqrt{\pi}}{2\sqrt{Dt}}\exp\left[-\frac{(x-u)^2}{4Dt}\right] \tag{10.198}$$

By placing the right side of equation 10.198 in equation 10.197 and also moving the constants outside of the integral, we obtain

$$\frac{1}{2\sqrt{\pi Dt}}\int_{-\infty}^{\infty} f(u)\exp\left[\frac{-(x-u)^2}{4Dt}\right]du \tag{10.199}$$

As one will notice, the right-hand side of equation 10.199 is also the right-hand side of equation 10.189, which is expanded for a near ∞. Thus, for the interval $-\infty < x < \infty$, we rewrite the equation as

$$C(x_1, t_1) = \frac{1}{2\sqrt{\pi Dt_1}}\int_{-\infty}^{\infty} f(u)\exp\left[\frac{-(x_1-u)^2}{4Dt_1}\right]du \tag{10.200}$$

Note that we have now reintroduced the subscript 1 for both x and t. This then is our general solution, which is valid for $-\infty < x_1 < \infty$ and for which the formal boundary condition for our solution is given as $C(x_1, \infty) = 0$ for finite x_1; $C(x_1, 0) =$ the concentration in the medium at time $t_1 = t = 0$ and at $x_1 = x$, where $x_1 = x$ is the starting position in the medium (usually a column or tube) of the slug of fluid that moves with dispersion. The value of $C(x_1, t_1)$ will always depend on the initial concentration, or rather its distribution within the column (i.e., on $C(x_1, 0)$). It is hoped that this problem will help sharpen the reader's calculus skills, help demonstrate the relationship between the ADE and a solution for it, and that one can see where certain parameters are derived from.

10.9. As explained previously, each phase would require its own retardation factor. Thus, the general form would be expressed as

$$\theta_{mo}R_{mo}\frac{\partial C_{mo}}{\partial t} + \theta_{im}R_{im}\frac{\partial C_{im}}{\partial t} = \theta_{mo}D\frac{\partial^2 C_{mo}}{\partial x^2} - \theta_{mo}v\frac{\partial C_{mo}}{\partial x} \tag{10.201}$$

10.10. Using equation 10.130, the wetted fraction is about 0.04.

10.11. A decrease in particle size, assuming the same relative parameters as given in question 10.10, would cause an increase in F. For example a particle size of 500–700 μm would yield an $F = 0.12$ while a particle size of 100–250 μm would yield an $F = 1.0$. What causes this? Is it a linear relationship with one of the other parameters?

ADDITIONAL QUESTIONS

10.12. A colleague has called to obtain your opinion about transport time at a local spill site. He is unsure of the chemical that has been spilled, but wishes to know the worst-case scenario for transport time from soil surface to ground water, 7 m below. The only values he can give are $\theta = 0.08$ and the drainage rate is 0.3 m per year. What is the amount of time it would take, worst-case, for a chemical to reach the water table?

10.13. Assuming the same parameters as above and $\rho_b = 1.35$, how long will be required for dicamba ($K_d = 2.2$) and trifluralin ($K_d = 13{,}700$) to reach ground water?

10.14. Your instructor has assigned you the task of demonstrating the effect of structural voids on contaminant transport. How can you illustrate—visually and mathematically—that structural voids have a greater effect on transport than relatively homogeneous soil profiles?

10.15. As an unsaturated-zone hydrologist, a person will not always work with mobile ions such as nitrate, but will often find it necessary to apply his/her skills to work involving other compounds such as aniline, ethyl acetate, isopropyl iodide, benzene, toluene, radioactive constituents, et cetera. What is the diffusion coefficient of aniline ($C_6H_5NH_2$) in water at 25 °C? *Hint:* use Hayduk and Laudie (1974) method. Assume $\eta = 0.8904$ and the LeBas molal volume is 6(C) = 6(14.8) = 88.8; 7(H) = 7(3.7) = 25.9; 1(N-primary amine) = 10.5; 1 (6-membered ring) = −15.0. Total = V'_B (total molal volume) = 110.2 cm^3 mol^{-1}.

10.16. What is the diffusion coefficient for ethyl acetate ($CH_3CO_2CH_2CH_3$) in water at 25 °C? Assume $\eta = 0.8904$ and the LeBas molal volume is 4(C) = 59.2; 8(H) = 29.6; 2(O) = 19.8. Total = V'_B (total molal volume) = 108.6 cm^3 mol^{-1}.